Sensors & Diagnostics

ROYAL SOCIETY OF CHEMISTRY

TUTORIAL REVIEW

View Article Online
View Journal | View Issue

Cite this: *Sens. Diagn.*, 2022, **1**, 10

Explorations in a galaxy of sialic acids: a review of sensing horizons, motivated by emerging biomedical and nutritional relevance

Saurav K. Guin, *[abc] Trinidad Velasco-Torrijos [ad] and Eithne Dempsey *[ad]

Sialic acid (*Sia*) is widely distributed in free, polymeric and conjugated forms in living creatures and humans. It serves various roles in human physiology including brain development, function of central nervous system, the immune system, lactation and infant cognition. *Sia* is over- or under-expressed in human cells, tissues and fluids during physiological disorders and the onset of cancers. Furthermore, the exploitation of *Sia* by several bacteria and viruses including SARS-CoV-2 to cause human infections has been recently revealed. A special chemical form of *Sia* and 3′- and 6′-sialyllactose have recently received regulatory approval for use in commercial food products as nutrition additives. Therefore, *Sia* production and assay have immense clinical and industrial interests. However, sensing or analytical approaches to *Sia* measurement in complex clinical and food samples are less developed due to lack of a comprehensive review covering both fundamental and perspectives to general readers working at the periphery of *Sia*. This review provides a carefully balanced and comprehensive collation of key aspects of the monosaccharide family of *Sia*, covering their sources, synthesis, biological significance, role in disease and human health and nutrition, culminating in a robust account of their analysis in complex matrices.

Received 21st September 2021,
Accepted 3rd November 2021

DOI: 10.1039/d1sd00023c

rsc.li/sensors

1. Introduction

Sialic acid (*Sia*) having basic D-*glycero*-D-galacto conformational unit belongs to a sub-set of nonulosonic acid monosaccharides with 9-carbon (C) backbone molecular structure. *Sia* is endogenously produced in many living organisms and generally occupies the terminal position of cell surface glycans, glycoconjugates (*i.e.*, glycoproteins and glycolipids), oligosaccharides, lipo-oligosaccharides and polysaccharides. To the best of our knowledge, 94 types of *Sia* have been identified and separated to date from various biological sources. *Sia* has the anomeric position at C-2 atom of the backbone structure and different combinations of the functional groups at C-4, 5, 7, 8 and 9 atoms (Fig. 1[A]). D-Neuraminic acid, *N*-acetyl-D-neuraminic acid (Neu5Ac), *N*-glycolyl-D-neuraminic acid (Neu5Gc) and 2-keto-3-deoxy-D-*glycero*-D-galacto-nononic acid (KDN) are common *Sia* present in many biological sources (Fig. 1[B]). The pK_a of Neu5Ac is reported as 2.6 and thus in the physiological conditions (*i.e.*, at pH 7.4), it exists as an anionic pyranose form (Fig. 1[C]).[1] About 92–95% of free *Sia* at equilibrium exists in the thermodynamically stable β-pyranose form. The anomeric carbon (C-2) is involved in the formation of glycosidic linkages and thus bound *Sia* predominantly exists in the α-pyranose form (Fig. 1[C]). *Sia* is generally part of oligosaccharides bonded to glycoproteins and glycolipids through either α2,3- or α2,6-glycosidic bond. They can also be connected through either α2,9- or α2,8-bond to other *Sia* units *i.e.* oligo-(2–7 units of *Sia*) and poly-(≥8 units of *Sia*) sialic acid (poly*Sia*) as a linear polysaccharide chain.[2]

It is important to mention that several research groups around the world independently identified *Sia* in a range of biological sources and unintentionally named them differently. In 1935, Klenk's research group in Germany extracted and identified a new monosaccharide from human brain glycolipid and named it "*neuraminic acid*".[3–5] In the following year, Blix's research group in Sweden extracted a similar compound from the mucin of submaxillary gland of bovine and named that as "*kohlenhydrat I*".[6,7] Yamakawa's research group in Japan extracted a similar compound from equine blood stroma glycolipid in 1951 and designated it as "*hemataminic acid*".[8] In the same year, Gottschalk in Australia extracted a similar compound from homogeneous mucoproteins by using an influenza virus enzyme and named as "*N-substituted-isoglucosamine*".[9] György's research group, in

[a] *Department of Chemistry, Maynooth University, Maynooth, Co. Kildare, Ireland. E-mail: SauravKumar.Guin@mu.ie, sauravkrguin@yahoo.co.in, Eithne.Dempsey@mu.ie*
[b] *Fuel Chemistry Division, Bhabha Atomic Research Centre, Trombay, Mumbai – 400085, India*
[c] *Homi Bhabha National Institute, Anushaktinagar, Mumbai – 400094, India*
[d] *Kathleen Lonsdale Institute for Human Health, Maynooth University, Maynooth, Co. Kildare, Ireland*

USA in 1953, extracted a similar type of monosaccharide from the nondialyzable fraction of skimmed human milk and called it "*gynaminic acid*".[10,11] A similar type of compound was extracted by Richard *et al.* in Germany in 1954 from the mucoprotein fraction of bovine colostrum and was identified as "*lactaminic acid*".[12] In 1955, Gottschalk identified the structural similarity among the above-mentioned compounds.[13] In order too avoid the global confusion in the identification and reporting of this group of monosaccharides, he in association with Blix and Klenk, provided a unique nomenclature "*sialic acid*" that was unanimously accepted in 1957.[14]

Sia is a "shy" sugar unlike glucose and fructose and is thus relatively less known. *Sia* is endogenously synthesised *de novo via* an anabolic mechanism in the cytosol of eukaryotic cells. The uridine diphosphate-*N*-acetylglucosamine (UDP-GlcNAc), which is a nucleotide sugar, successively undergoes enzymatic reactions with UPD-GlcNAc-2-epimerase (EC: 5.1.3.14), *N*-Acetyl-D-mannosamine (ManNAc) kinase (EC: 2.7.1.60), Neu5Ac-*g*-phosphate synthetase (EC: 2.5.1.57) and Neu5Ac-9-phosphatase (EC: 3.1.3.29) to produce Neu5Ac inside the nucleus where it is activated by cytidine-5′-monophospho (CMP)-Neu5Ac synthetase (EC: 2.7.7.43) as CMP-Neu5Ac. The CMP-Neu5Ac transporter transports CMP-Neu5Ac from the nucleus back to the cytosol for the following catabolic cycle. The bifunctional GNE enzyme (*i.e.*, UPD-GlcNAc-2-epimerase and ManNAc kinase) regulates the anabolic enzymatic reaction through feedback action.[15,16] CMP-*N*-acetylneuraminic acid hydroxylase (EC: 1.14.18.2) hydroxylates CMP-Neu5Ac and produces CMP-Neu5Gc for the catabolic cycle.[17] This enzyme is absent in humans, ferrets and new world monkeys as a result of an independent inactivating mutation and thus Neu5Gc is not endogenously synthesised in their body.[18–20] Recently, it was experimentally observed that the distribution and concentration of Neu5Gc in other mammals depend on the type of species and tissues. For example, the skeletal muscle of goat was found enriched with Neu5Gc (166 ± 48.70 μg g^{-1} of protein), while it was found to be absent in the skeletal muscles of dog and kangaroo. The lung, heart, liver, kidney and spleen of female deer had negligible (in the range 0.31–0.61 μg g^{-1} of protein) amount of Neu5Gc, but it was considerably (36.89 ± 42.60 μg g^{-1} of protein) present in skeletal muscle. Similarly, the large- (851.50 ± 314.20 μg bound Neu5Gc per g of protein; 79.76 ± 57.11 μg free Neu5Gc per g of protein) and small-intestines of sheep (760.52 ± 295.08 μg bound Neu5Gc per g of protein;

Saurav K. Guin

Dr. Saurav K. Guin is an early-career Scientist working in the domain of electrosynthesis, electrocatalysis and electroanalysis for more than 14 years in the Fuel Chemistry Division, Bhabha Atomic Research Centre, Department of Atomic Energy, Government of India. He is an Assistant Professor of Chemical Sciences in Homi Bhabha National Institute, Mumbai, India. At present time, he is working as a Marie Skłodowska-Curie Fellow and Career Fit PLUS Fellow at the Department of Chemistry, National University of Ireland Maynooth (Maynooth University) in Ireland on the development of biosensors for the determination of sialic acids in complex clinical samples, commercial foods and drinks. He worked in the Ulm University, Germany (2016) and National University of Singapore (2009) as visiting research fellow availing international fellowships. He is (co)author of 19 peer-reviewed articles published in international peer-reviewed journals and 44 other scientific publications. He is recipient of several competitive international research-fellowships, travel-grants and presentation-awards in international conferences. He has published a peer-reviewed Special Issue as a Guest Editor in 'Electroanalysis (Wiley)'. He served Indian Society for ElectroAnalytical Chemistry as the Secretary for 6 years. He is also member of reputed academic societies.

Trinidad Velasco-Torrijos

Dr. Trinidad Velasco-Torrijos is currently an Associated Professor and coordinator of BSc in Pharmaceutical and Biomedical Chemistry program at the Department of Chemistry, Maynooth University (Ireland). Trinidad received her PhD in from the University of Bristol (UK) under the supervision of Prof. Tony Davis in the field of carbohydrate recognition and supramolecular Chemistry. She pursued post-doctoral research at Ghent University (Belgium) with Prof. Annemieke Madder. She then joined the group of Prof. Paul Murphy at University College Dublin (Ireland) as a Marie Curie Postdoctoral Fellow (2003–2005). Trinidad's current research interests include the synthesis of glycomimetics and carbohydrate-based soft materials for biomedical applications.

65.96 ± 49.34 μg free Neu5Gc per g of protein) had the highest concentration of Neu5Gc amongst all organs. The concentration of bound Neu5Gc in the commercial cuts of lamb/mutton varied in the range ~31–77 μg g^{-1} of protein.[21] Although KDN is highly abundant in bacteria and lower vertebrates, it is highly expressed on ovarian tumour tissue and in the foetal haemoglobin of humans.[22] *Sia* is also found in some viruses, bacteria, fungi, protozoa, insects, mollusca, sea urchin, and different organs and cells of humans.[23] The edible bird's nest (EBN) of Asian swiftlet showed significantly high concentration of *Sia* due to the involvement of *Sia* rich saliva secreted from the sublingual glands of Asian swiftlets during nest formation.[24–26] The presence of *Sia* in plants and fruits is usually rare and mainly originated from extraneous contaminants.[27–29] However, recently Sun *et al.* reported the presence of a considerable amount of Neu5Ac in pea seedlings.[30] Furthermore, Xia *et al.* extracted *Sia* from the sialylated glycoprotein from the root of a Tibetan plant *Potentilla anserina* L.[31] Hence, the present state of art is not able to confirm that *Sia* is absent in all parts of the plants.

It would be a mistake to ignore the biological importance of *Sia*. Schauer and Kamerling published a book chapter in 2018 exploring the world of *Sia*, covering their discovery, structural analysis and some biological roles.[32] In 2021, Yang *et al.* has published a review article emphasising the biosynthesis, metabolism and various means of production of *Sia*.[33] Furthermore, a couple of interesting reviews have been published in 2020–2021 covering the progress and promises of free *Sia* storage disorder,[34] development of the entry inhibitors for *Sia* targeting viruses,[35] the role of *Sia* as a receptor of various pathogens,[36] role in human immune regulation and therapeutic potentials[37] and utilisation of *Sia* for identifying tumours.[38] In 2010, Lacomba *et al.* published a review emphasising analytical methodologies for *Sia* and gangliosides in the biological and dairy products.[39] In 2021, Cheeseman *et al.* published another review on the identification and quantification of *Sia* covering the traditional colorimetric, fluorometric, enzymatic and chromatographic methods.[40] It is important to mention here, that the European Commission has recently approved inclusion of *Sia* as a supplement in infant and follow-up formula and other food products under regulation EC/258/97.[41] However, the beneficial or inhibiting role of *Sia* in the present pandemic caused by the COVID-19 disease is yet an open question.[42–44] Hence, this serendipitous review has the intriguing ambition to concisely outline the universe of *Sia* to both general and expert readers covering *Sia*'s involvement in human biochemistry; its role in human health, the immune system, pathogenicity and disease; dietary regulations and commercial production and most importantly the evolution of analytical methods from traditional to the latest emerging techniques for assays of *Sia* in complex biological and food matrices.

Eithne Dempsey

Dr. Eithne Dempsey received a PhD in Electroanalytical Chemistry from Dublin City University followed by postdoctoral research at St. Vincent's Hospital, Dublin. She then took up a position as Lecturer in Chemistry at Technological University Dublin – Tallaght Campus where she managed the Centre for Research in Electroanalytical Technologies. She was appointed visiting Professor of Chemistry at the University of the Western Cape, Capetown, South Africa in 2012 and recently (2017) took up a position at Maynooth University, currently as Associate Professor (since 2020) in Dept. Chemistry. Her core research objective is to address electroanalytical challenges using bespoke (nano)materials integrated with biosensing systems suitable for onsite deployment in multiple application scenarios. This includes nanoassembly and characterisation with use of modern electrochemical and surface based techniques, utilisation of electrocatalytic materials in biomedical and environmental science and the design and fabrication of integrated fluidics/sensor microsystems which exploit electrocatalytic/nanomaterials for biomedical diagnostics.

2. Biological relevance of *Sia*

The CMP-sialic acid transporter (*viz.* CMP-Neu5Ac transporter) transports CMP-*Sia* to the lumen of the Golgi body, where *Sia* becomes associated with glycoproteins, glycolipids and oligosaccharides by various silyl transferases. The sialylated glycoproteins/glycolipids/oligosaccharides and poly- or oligo- sialic acids are distributed in the lysosome, cytosol, outer-plasma membrane and intra-cellular cell compartment membrane, where exo-α-sialidase (EC: 3.2.1.18) releases the terminal *Sia* unit in the cell. Sialic acid aldolase (EC: 4.1.3.3) then splits *Sia* into pyruvate and ManNAc in the cell. In this catabolic cycle both free *Sia* and ManNAc may be salvaged to the appropriate stage of the anabolic cycle.[45] The absence of (CMP)-Neu5Ac synthetase and sialic acid aldolase in human milk helps in the accumulation of free Neu5Ac in human milk.

2.1 Diverse biological functions of *Sia* in healthy humans

Sia is generally present on the human cell glycocalyx, which is a sugar-coat or a thick (~500 nm) network of glycans on the surface of human cells. The glycocalyx not only protects the cells, but it also interacts with other cells and outer-cellular environment. Neu5Ac is a major occupant of stroma of human erythrocytes *i.e.*, red blood cell (RBC) and it eventually helps in the dispersion of RBC in blood owing to electrostatic repulsions as shown in Fig. 2[A].[46] Furthermore, the podocalyxin epithelial polyanions consist of negatively

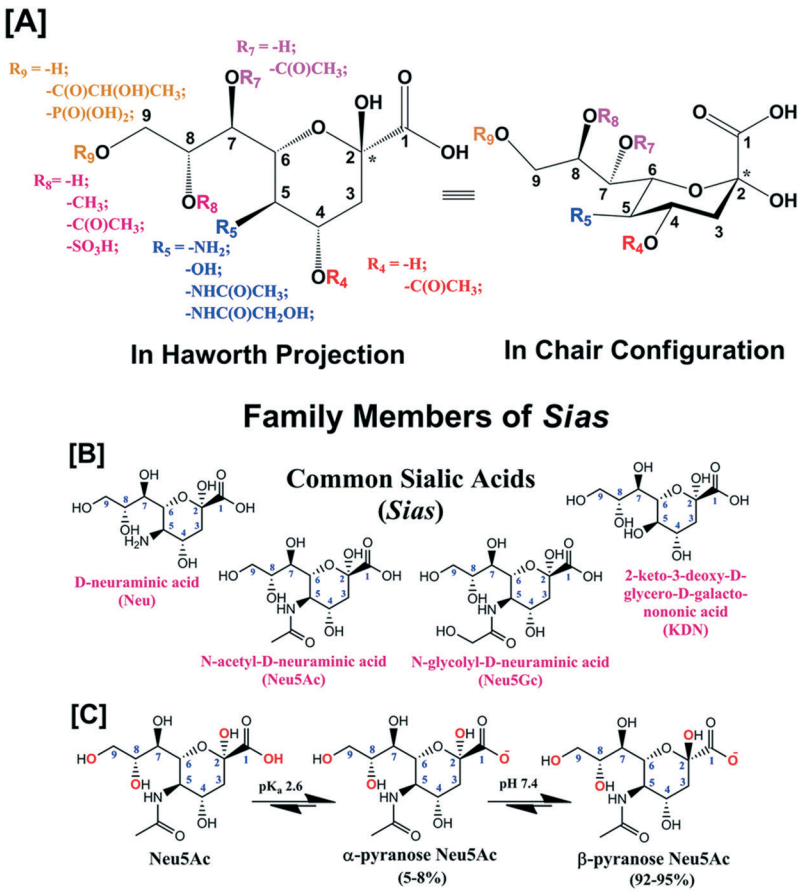

Fig. 1 [A] Generic molecular structure of *Sia*. [B] Molecular structures of common *Sia i.e.* D-neuraminic acid, *N*-acetyl-D-neuraminic acid (Neu5Ac), *N*-glycolyl-D-neuraminic acid (Neu5Gc) and 2-keto-3-deoxy-D-*glycero*-D-galacto-nononic acid (KDN). [C] Anomeric forms of free Neu5Ac at physiological pH (7.4).

charged *Sia* (as shown in Fig. 2[B]), sulphated oligosaccharides and glycopeptides control the glomerular filtration in the kidneys in association with phosphorylated ezrin and Na^+/H^+ exchanger regulatory factor 2.[47] On the other hand, glycans are covalent linear and branched oligosaccharide chains, whose monosaccharide component includes Neu5Ac, glucose, galactose, mannose, fucose, *N*-acetyl-glucosamine (GlcNAc) and *N*-acetyl-galactosamine (GalNAc). Glycans are attached to glycoproteins (by either *N*- or *O*-linkage) and glycolipids on the glycocalyx and extracellular fluids and matrices.

2.1.1 Immune system regulation. The human immune system can identify antigens and cell-damages by different types of molecular patterns known as pathogen- and danger-associated molecular pattern, respectively, by the pattern recognition receptors *viz.* toll-like receptors, C-type lectin receptors, *etc.* Following this, the immune network triggers the release of inflammatory cytokines for consolidated immunological actions to encounter antigens. However, chronic and prolonged inflammation can eventually damage the healthy cells, tissues and organs. Hence, the regulation of inflammation inside the cells is a critical process, where *Sia* plays an important role.

The sialoglycans on the glycocalyx of healthy cells usually form specific self-associated molecular pattern (SAMP).[48] The sialoglycan-SAMP is recognised by sialic acid-binding immunoglobulin type lectin (Siglec) protein receptors on the surface of immune cells (such as monocytes, macrophages, dendritic cells, natural killer cells, B lymphocytes, neutrophils and eosinophils), myelin, myeloid progenitors, trophoblasts and osteoclasts. Siglec discriminates the body's own and foreign antigens and can interact with *Sia* of the same as well as different cells. A total number of 15 human Siglecs (1–12, 14–16) have been identified so far and it is believed that Siglec-13 and -17 genes have been inactivated during the course of human evolution.[49] Siglec-1 (also known as sialoadhesin), -2 (also known as CD22), -4 (also known as myelin-associated glycoprotein) and -15 are found in all mammals and thus are known as conserved classic Siglecs. The other Siglecs have rapidly evolved in humans and are categorised as Siglec-3 (also known as CD-33) related Siglecs. On the other hand, Siglecs are often classified as per their functionality such as inhibitory (2, 3, 5–12), activating (14–16) and non-signalling (1, 4) Siglecs.

The binding of *Sia* by the inhibitory-type Siglecs induces the Src family kinases by the immunoreceptor tyrosine-based

inhibitory motif or its alike tyrosine present in the cytoplasmic domain and eventually it down-regulates the pro-inflammation caused by toll-like receptors (Fig. 2[C]).[50] This phenomenon prevents the pro-inflammatory damage of the self-antigens and healthy cells. On the other hand, the transmembrane DNAX activation protein 12 of the activating-type Siglec electrostatically binds with negatively charged *Sia* and stimulates pro-inflammatory responses through mitogen-activated protein kinase and AKT pathways to destroy the pathogens having specific sialoglycan-SAMPs to circumvent inhibitory Siglecs (Fig. 2[C]).[51] The Siglec-2, -6, -14 and -15 bind α2,6-Neu5Ac, whereas Siglec-5 and -11 bind α2,3-Neu5Ac and α2,8-Neu5Ac, respectively. The Siglec-9 and -10 do not show any preference to α2,3- and α2,6-Neu5Ac; but Siglec-1, -4 and -8 preferentially bind α2,3-Neu5Ac over α2,6-Neu5Ac and the reverse is true for Siglec-3. On the other hand, Siglec-7 preferentially binds to α2,8- over α2,6- and α2,3-Neu5Ac.[52] The α2,3-Neu5Ac-SAMP is recognised by the serum complement factor H of the alternate pathway of innate immune system to identify and protect "self" cells.[53,54]

The selectins are a family of calcium-dependent (C-type) lectins also involved in immune cell adhesion to endothelial cells. They mediate access to lymphoid organs and sites of inflammation. Sialylated tetrasaccharides, *i.e.*, sialyl Lewis^x (sLe^x, Neu5Acα2-3Galβ1-4(Fucα1-3)GlcNAc) and sialyl Lewis^a (sLe^a, Neu5Acα2-3Galβ1-3(Fucα1-4)GlcNAc) are among the best described ligands for the selectins but they can also have high-affinity interactions with sulfatides and non-sialylated glycosphingolipids (Fig. 2[C]).[55] The selectin family can be subdivided in three main groups: P-selectins, expressed on platelets; E-selectins, expressed on endothelial cells and L-selectin, expressed on leukocytes. The biological function and ligand selectivity of these three selectins sub-families are also different. L-selectin is involved in leukocyte trafficking.

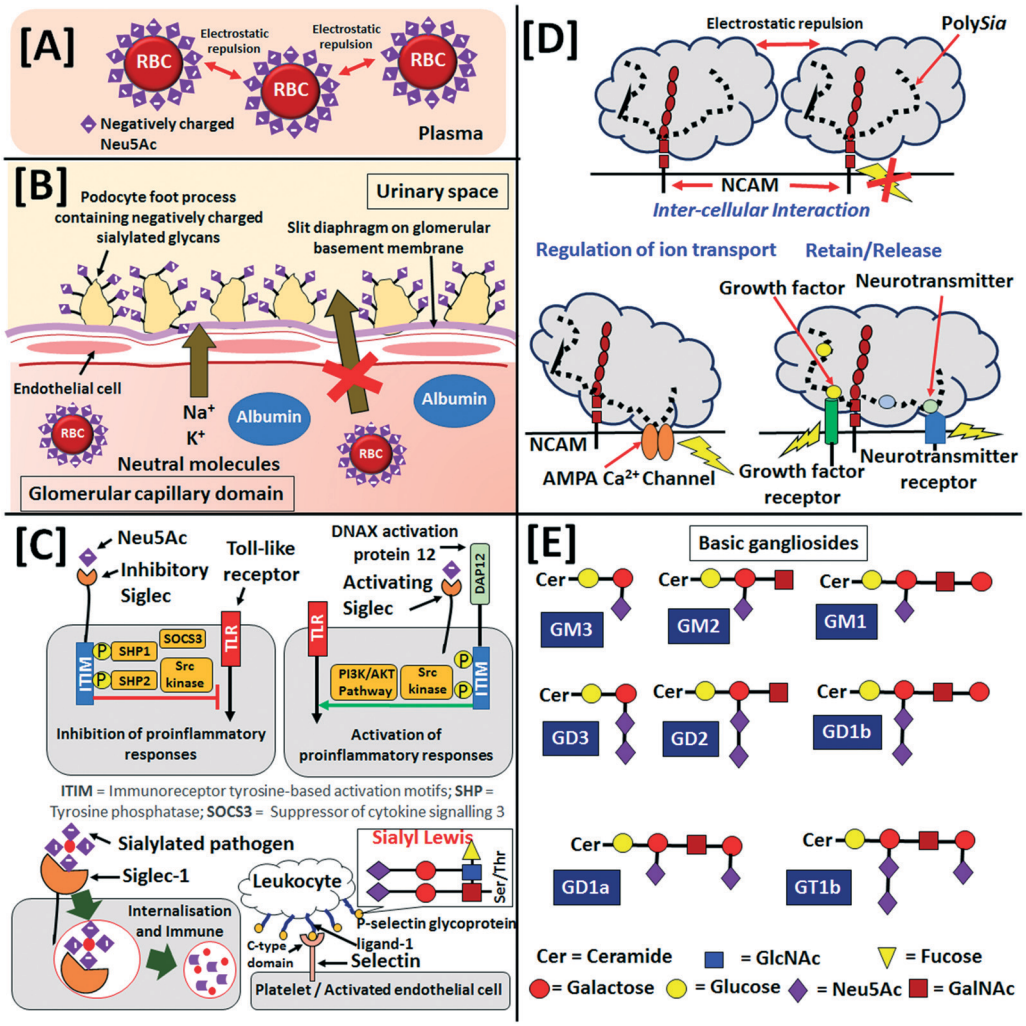

Fig. 2 Negative charge of Neu5Ac in [A] dispersion of RBC in blood and [B] glomerular filtration in kidney. [C] The inhibitory (top left) and activating (top right) siglec actions in immune system, internalisation and immune response of Siglec-1 (bottom left), interaction of C-type domain of selectin with sialyl Lewis of P-selectin glycoprotein ligand-1 of leukocyte (bottom right). [D] Intercellular repulsive interaction of poly*Sia*-NCAM, activation of ion channels and growth factor receptors through attractive interactions. [E] Sequence of saccharides in some of the basic gangliosides (the relative scale of objects of the schemes are not in actual dimensions).

E-selectins are constitutively expressed on endothelial cells in the bone marrow and skin, but exposure to inflammatory cytokines is required for their expression in other organs. P-selectins are found in activated platelets. Sołkiewicz *et al.* recently reported that the specific reactivity of α2,3-Neu5Ac recognising selectin *Maackia amurensis* agglutinin with sialylated serum immunoglobulin G as well as quantitative evaluation of sialylation and agalactosylation factor could be useful to diagnose inflammatory endometriosis disease.[56]

2.1.2 Poly*Sia* in central nervous system. Poly*Sia* in humans is mainly (~90%) linked to the neural cell adhesion molecule (NCAM) (also known as CD56) protein in the brain (studied in rat),[57] human cerebrospinal fluid,[58] α-subunit of type 4 sodium channel protein,[59] *Sia* transfer proteins *viz.* ST8-αN-acetyl-neuraminide-α2,8-sialyltransferase-2 and -4 (*i.e. ST8SiaII* and *ST8SiaIV* (EC: 2.4.99)).[60] Poly*Sia* is also expressed in a large variety of cells and proteins, such as human bone marrow-derived mesenchymal stromal cells,[61] lymphoid cells *viz.* natural killer cell,[62] activated CD4+ T-cells,[63] synaptic cell adhesion molecule-1 mostly found in the subset of NG2 cells,[64] CD36 in human milk,[65] and neuropilin-2 on dendritic cells.[66] Although, human cells have in total six *ST8Sia*, poly*Sia* is synthesised in the human cell's Golgi body by only *ST8SiaII* and *ST8SiaIV* followed by conjugation with NCAM[67–69] and regulation by intercellular Ca(II) catalytic synaptic transmissions.[70] The oligo*Sia* and poly*Sia* are metabolised by the enzyme *endo*-α-sialidase (EC: 3.2.1.129),[71] but it has recently been revealed through an *in vitro* study that although human neuraminidase enzymes NEU3 and NEU4 can degrade oligo*Sia* at pH < 7, no human neuraminidase enzyme can hydrolyse poly*Sia*.[72]

NCAM participates in cytoplasmic signalling, intercellular and extracellular matrix interactions in the central nervous system. The long negatively charged hydrated poly*Sia* on NCAM are responsible for ~20–30 nm intercellular space (-Fig. 2[D]). However, poly*Sia* on NCAM attract neuro- and biologically active molecules *viz.* brain-derived neurotrophic factor, pro-brain-derived neurotrophic factor, neurotrophic factors-3, fibroblast growth factor-2, norepinephrine, dopamine, epinephrine, histone H1, chemokine ligand 21, *etc.* (Fig. 2[D]).[73] It also shows attractive interaction to Ca^{2+} permeable AMPA channel (Fig. 2[D]). Poly*Sia* helps in the migration of neuronal progenitor cells from the subventricular zone of lateral ventricle and rostral migratory stream to the olfactory bulb in the embryonic nervous system. The poly*Sia* on the progenitors in the subventricular zone influences the timing of the differentiation process into interneurons in the olfactory bulb.[74] During the embryonic and neonatal stages, poly*Sia* expressed on the growing axons helps to avoid interference of ectopic synapses projected towards specific targets; then, its under-expression on the developing axons and oligodendrocyte precursors starts at the onset of myelination. Furthermore, during the critical neonatal stage poly*Sia* provides insulation and controls synaptogenesis helping maturation of the central nervous system of the infant. However, the expression of poly*Sia* in the central nervous system is gradually decreased from the embryonic stage to mature infant (~10 years age) and mostly located at very low concentration in adults up to 80 years old in subventricular zone and granule cell layer of the hippocampus to maintain neurogenesis and neural plasticity. Furthermore, trace amounts of poly*Sia* present in the adult thalamus (paratenial, periventricular and anteroventral anterodorsal nuclei), hypothalamus (supraoptic and suprachiasmatic nuclei), habenular nuclei, entorhinal–hippocampal complex, lateral geniculate nucleus, dorsal spinal laminae and mesencephalic central grey control the physiological plasticity. Poly*Sia* is also expressed on some sensory neurons in the spinal cord, optic nerve, tectum (axons of ganglion cells) and piriform cortex. The reintroduction of external poly*Sia* in adults has shown natural neural tissue repair.[75–77] Weisgerber *et al.* reported 15.0 ± 1.5 μg mL^{-1} polyNeu5Ac in the cerebrospinal fluid of new-born and premature infants and its concentration decreased to 0.2 ± 0.02 μg mL^{-1} in children ≥1 year old.[58] Simon *et al.* have recently reported the expression of poly*Sia* in human semen owing to the post-translational modification of NCAM and α2,8-polysialyltransferases *ST8SiaII*.[78] The expression of poly*Sia* to CD36 ratio in human breast milk is initially increased from 0.572 ± 0.225 during 7 days of colostrum to 3.424 ± 0.938 at 1 month and then again decreased to 1.491 ± 0.044 and 1.018 ± 0.478 after 3 and 6 months, respectively, from birth.[65]

Owing to the above-mentioned physiological roles of the poly*Sia* to humans, it is usually recognised as a harmless molecule by the human immune system. This phenomenon is often exploited by some bacteria such as *Escherichia coli*, *Listeria monocytogenes*, *Neisseria meningitidis*, *Haemophilus influenzae* b, *Streptococcus agalactiae* and *Streptococcus pneumoniae* having their own poly*Sia* glycocalyx causing invasive meningococcal diseases *viz.* meningitis, fulminant septicaemia, *etc.*[79] However, Siglec-11 preferentially binds to poly*Sia* and inhibits inflammatory neurotoxicity of phagocytosis.[80] The expression of poly*Sia* on several cancer cells is highly invasive and proliferative, being recognised as onco-developmental antigens. Thus, poly*Sia* is sometimes considered a potential biomarker to diagnose lung carcinoma, neuroblastoma, glioblastoma and pituitary tumours. Cancer therapy sometimes utilises antibodies and inhibitors specific to poly*Sia*-NCAM.[81] Furthermore, the abnormal expression and impairment of poly*Sia* are associated with mental disorders *viz.* schizophrenia, bipolar disorder, autism spectrum disorder.[82] Relapsing–remitting multiple sclerosis is caused by the inflammatory attacks on myelin and nerve fibers. The high activity of immunoglobulin G towards exogenous Neu5Gc and Neu5Ac showed some potential use in immunotherapy of relapsing–remitting multiple sclerosis.[83]

2.1.3 Gangliosides in human brain development and cancer biomarking. Gangliosides comprise a family of complex glycosphingolipids featuring a hydrophobic ceramide moiety bound to a glycan with at least one unit of

Neu5Ac. The ceramide consists of a sphingoid base covalently linked to a fatty acid by an amide bond. The gangliosides are amphiphilic in nature due to the coexistence of hydrophobic ceramide moiety linked on the cell membrane and negatively charged hydrophilic *Sia* in the glycan chain exposed to the extracellular environment. The gangliosides are synthesised at the Golgi apparatus and *trans*-Golgi network through sequential activities of sialyltransferases and glycosyltransferases enzymes, which are regulated by intracellular sphingolipid traffic. The luminal surface of transport vehicles transfers the synthesised gangliosides to the external leaflet of the plasma membranes, where gangliosides in *trans* conformation directly bind membrane proteins such as lectins through either carbohydrate-amino acid or carbohydrate–carbohydrate interactions. Siglecs preferentially bind to the higher sialylated gangliosides, but galectins can bind monosialylated gangliosides. The endocytosis process directs the gangliosides to the surface of intra-lysosomal luminal vesicles, where they are eventually degraded.[84]

In 1978, Svennerholm *et al.* reported the concentration of gangliosides in different human organs.[85,86] The highest concentration (*i.e.*, 3500–3000 nmol g^{-1} of tissue weight) of Neu5Ac was reported for the human brain's cerebral cortex followed by the cells in the cerebral white matter (1250–1000 nmol g^{-1} of tissue weight). The spleen (300–200 nmol g^{-1} of tissue weight), placenta (200–100 nmol g^{-1} of tissue weight) and retina (150–100 nmol g^{-1} of tissue weight) share almost similar concentration of gangliosides. Other organs *viz.* liver (100–50 nmol g^{-1} of tissue weight), thyroid (100–60 nmol g^{-1} of tissue weight), peripheral nerve (80–35 nmol g^{-1} of tissue weight), skeletal muscle and muscular layer of small intestine (80–50 nmol g^{-1} of tissue weight), kidney (60–30 nmol g^{-1} of tissue weight), skin (30–35 nmol g^{-1} of tissue weight), fat tissue (10–15 nmol g^{-1} of tissue weight) and mucosa (5–8 nmol g^{-1} of tissue weight) also showed moderate concentration of gangliosides. In the nomenclature of gangliosides, 'G' refers to the ganglio series of glycosphingolipids, while 'M', 'D', 'T' and 'Q' define 'mono', 'di', 'tri' and 'tetra' Neu5Ac units, respectively. The migration order of gangliosides in thin-layer chromatography is designated by the number 1, 2, 3, *etc.*, whereas 'a', 'b' and 'c' refer to 'one', 'two' and 'three' units of Neu5Ac, respectively, linked to the innermost galactose unit of the glycan chain.[87] Fig. 2[E] shows the arrangement of saccharides in some of the basic gangliosides. Ganglioside distribution and composition in human brain can vary greatly depending on age. The simple gangliosides *viz.* GM3, GD3 and 9*O*Ac-GD3 are predominant in human embryonic brains, but as age increases, comparatively complex gangliosides *viz.* GM1, GD1a, GD1b and GT1b are upregulated with concomitant down-regulation of embryonic gangliosides.[88,89] Ando *et al.* were able to determine the composition of adult white- and grey-matter of human brain by densitometry. They found the ganglioside bound Neu5Ac concentration in the human grey- and white-matter as 875 and 275 μg g^{-1} of the wet tissue, respectively. They also reported that GD1a (21.7%), GD1b (18.2%), GT1b (16.3%) and GM1 (14.9%) are the major components of the grey matter, while GM1 (21.6%), GD1b (16.9%), GT1b (11.1%) and GD1a (8.8%) are major components of white matter. The other gangliosides such as GM2, GM3, GM4, GD2, GD3, GT1a, GQ1b and GD1a-GalNAc are also found in both the grey- and white- matter of the human brain.[90] Sarbu *et al.* recently utilised electrospray-ionization-ion-mobility-mass-spectrometry to study the ganglioside profile of purified normal foetal frontal lobe in the 37th gestation week. They identified a total number of 143 ganglioside species having different glycan structures and ceramide constitutions including 47, 37 and 25 structures of GT, GD and GM, respectively. They also reported the existence of a minimum 12 GQ structures and glycans having Neu5Ac up to 8 units (which was earlier believed to be a maximum 5 units).[91] The same research group later identified more than 140 ganglioside species in the adult human hippocampus by using an ion-mobility-mass-spectrometry hyphenated with the collision-induced-dissociation fragmentation method.[92] They also compared the frontal and the occipital lobes of the brains of the 20 and 82 year-old males by nano-electron-spray-ionisation orbitrap-mass-spectrometry hyphenated with collision-induced-dissociation fragmentation method and reported that the content of sialylated, fucosylated and acetylated gangliosides in the overall human brain could decrease with age. Interestingly, the gangliosides are over-expressed in the frontal lobe compared to the occipital lobe in young ages; while the opposite becomes true in old ages.[93] Through ion-mobility-mass-spectrometry they have recently identified 113 gangliosides including GD2 and GD3 in the human cerebrospinal fluid and confirmed that some of the brain gangliosides could be passed to the cerebrospinal fluid due to immediate proximity to brain.[94]

The gangliosides are expressed along with phospholipids, cholesterol and glycosphingolipids on the plasma membrane's lipid rafts and participate in signal transduction (inhibition, activation, promotion, *etc.*) in cancer cells. This over-/under- expression of gangliosides is often used to diagnose several cancers and other diseases.[95] The malignant brain tumour known as glioblastoma multiforme can be diagnosed from the overexpression of both GD3 and GT1 gangliosides.[96] The high incidence of GD3 and GM3 gangliosides is a signature of human melanoma, a skin cancer.[97] GM1 activates tropomyosin receptor kinase-A and promotes differentiation of the neuroblastoma cells by formation of receptor-GM1 complex on the cell surface.[98] The GM1's expression in the skin increases with aging and senescence. It induces human aortic endothelial cells' insulin resistance.[99] The exogeneous GM1 showed a neuroprotective effect for neurodegeneration, neuronal injury; as well as a beneficial role to patients having Huntington, Alzheimer, Parkinson diseases, epilepsy, stroke and multiple sclerosis.[100] Furthermore, GM1 binds with the platelet-derived growth factor receptors, inhibits the signal to the glycolipid-enriched microdomain and suppresses the cell growth signal.[101] On

the contrary, platelet-derived growth factor B induces GD3 to enhance platelet-derived growth factor signal and promotes the cell proliferation and invasion in the gliomas in the glial cells of brain or spine.[102] GD3 blocks the activation of nuclear factor kappa-light-chain-enhancer of activated B cells in the human hepatoblastoma HepG2 cell-line after ionizing radiation or daunorubicin therapy. Hence, GD3 pre-treatment promotes apoptotic cell death during radiation or chemo therapy in patients having hepatocellular carcinoma.[103] Furthermore, GD3 activates CD95 induced apoptosis of lymphoid and myeloid tumour cells for leukaemia.[104] On the other hand, the overexpression of GD3 on the malignant melanoma and human osteosarcomas cells activates p130Cas and promotes focal adhesion kinase and paxillin pathway.[105–107] GD3 helps in the signalling of epidermal growth factor receptor and its activated form in the breast cancer stem cells and cell line.[108] GM3 showed inhibition in the epidermal growth factor signalling pathway for the human neuroblastoma cell line NBL-W (for neural and brain cancer);[109] human epidermoid carcinoma A431 cell (for skin cancer);[110] PC-3 and LNCaP cell (for prostate cancer);[111] YTS-1, T24, 5637, and KK47 cell (for human bladder cancer);[112] HSC-2 and SAS cell (for squamous carcinoma).[113] GM3 inhibits PI-3K/AKT/MDM2 signalling as well as Wnt/β-catenin signalling pathways,[114,115] but promotes oxidative stress-mediated mitochondrial pathway in HCT116 cell for human colorectal cancer.[116] GM2 has potential in the diagnosis and therapy of pancreatic ductal adenocarcinoma as it is overexpressed in MIA-PaCa-2 cell line and promotes TFG-β1 signalling for invasion.[117] GD2 is expressed on the stem-like cells of triple-negative breast cancer[118] and it is involved in the proliferation of MDA-MB-231 cells by promoting signalling of c-Met receptor.[119] The GD3 and GD2 are overexpressed on glioma cell line U-251MG and promote the signalling of ERK1/2 and AKT pathway.[120] GD2, GD1b, and GT1b are generally expressed on the small cell lung cancer cells[121] and GD2 promotes the activation of focal adhesion kinase pathway for integrin-mediated signal transduction.[122] GD1a targets c-Met receptor and suppresses the metastasis of hepatocellular carcinoma in human hepatoma HepG2 cell by inhibiting the signalling of hepatocyte growth factor.[123] Both exogenous and endogenous GD1b regulate breast cancer apoptosis as evidenced in the MCF-7 human breast cancer cells.[124] The treatment with GT1b induces an early apoptosis in A549 lung cancer cells by modulating both caveolin-1 and p53 to inhibit fibronectin-a5b1-integrin-ERK signalling.[125]

2.1.4 Pregnancy, lactation and infant cognition. Many articles have indirectly indicated the benefits of *Sia* in the human cognitive processes including knowing, remembering, thinking, problem-solving and judgement, however no direct evidence of transferring *Sia* from the mother's placenta to the human foetus is reported to date. Rajan *et al.* reported that the total *Sia* concentration in human plasma increased from 1830 ± 40 μM for women (n = 60) during the menstrual cycle to 2580 ± 50 μM for pregnant women (n = 28) during 3rd trimester (*i.e.*, 26–40 weeks) and further increased to 3460 ± 160 μM in the post-partum period (*i.e.*, 1–14 days post-partum). Similarly, the urine *Sia* concentration increased from 2350 ± 80 μM for women (n = 56) during the menstrual cycle to 5400 ± 330 μM for pregnant women (n = 27) during the 3rd trimester but did not further increase in the post-partum period. However, no statistical correlation was observed in the neuraminidase and sialyltransferase activities during the pregnancy period compared to non-pregnant women.[126] Alvi *et al.* reported an elevation of *Sia* concentration in serum from 1.63 ± 0.3 mM at the onset (*i.e.*, 5–8 weeks of pregnancy) to 2.06 ± 0.49 mM in the last stage (*i.e.*, 37th week) of pregnancy.[127] The concentration of *Sia* in the saliva of women increased from 57.3 ± 10.5 mg L^{-1} (control) to 149.6 ± 62.5 mg L^{-1} at the 21st week of gestation but decreased again to 129.3 ± 16.5 mg L^{-1} at the 40th week of gestation.[128] The progress of pregnancy is also reflected in the *Sia* concentration on RBC membranes, where it increased to 96.30 ± 34.20 mg g^{-1} of protein during 28–32 weeks of pregnancy (n = 25) compared to 42.33 ± 15.85 mg g^{-1} of protein found in non-pregnant women (n = 10).[129] The lectin dotting analysis of sialylation of amniotic fluid glycoconjugates by *Sambucus nigra* agglutinin (which is specific to α2,6-glycosidic link) revealed that α2,6-sialylated glycoconjugates in the amniotic fluid increased from 965 ± 299 pixels at second trimester to 1806 ± 292 pixels in the perinatal period and further increased to 2099 ± 225 pixels in post-date pregnancy.[130] Furthermore, Zhu *et al.* studied the concentration of *Sia* in the serum and breast milk of 133 pregnant women and infant cognitive development of their children over a year. It was reported that the concentration of *Sia* in the serum increased from 2.10 ± 0.92 mM in 10th weeks to 2.59 ± 0.95 mM in the 16th week and 2.95 ± 0.98 mM in the 38th week of pregnancy, while *Sia* in the breast milk decreased from 5.15 ± 0.18 mM after 3 days to 1.99 ± 0.08 mM after 42 days and 0.53 ± 0.04 mM after 90 days of delivery. They evaluated the mental development index and psychomotor development index of infants at 90th day from the date of delivery and found that a high concentration of *Sia* in the serum during the second trimester (*i.e.*, 16th week) of pregnancy promoted both early mental and psychomotor developments of the infants, whereas the high concentration of *Sia* in the serum in the third trimester (*i.e.*, 38th week) of pregnancy and in the breast milk in the first month post-delivery promoted the early mental development of infants.[131] Martín-Sosa *et al.*[132] and Wang *et al.*[133] also reported similar trends of decreasing concentration of total *Sia* in human breast milk from the colostrum to mature stage.

2.1.5 *Sia* in milk oligosaccharides. It is experimentally proven that the constituents of human breast milk are associated with higher cognitive levels of infants.[134,135] Human and bovine milk contain 55–70 and 40–50 g L^{-1} of lactose (*i.e.*, digestible carbohydrate), respectively, but they have vastly different profiles for the neutral and acidic oligosaccharides. The major neutral human milk oligosaccharides (HMOs) are lacto-*N*-tetraose (0.5–1.5 g L^{-1}),

lacto-*N*-fucopentaose I (1.2–1.7 g L^{-1}), II (0.3–1.0 g L^{-1}), III (0.01–0.2 g L^{-1}) and lacto-*N*-difucohexaose (0.1–0.2 g L^{-1}). Although, lacto-*N*-tetraose was found in bovine milk in trace amounts, lacto-*N*-fucopentaose I, II, III and lacto-*N*-difucohexaose could not even be detected in bovine milk. Among the acidic milk oligosaccharides, Neu5Ac(α2,6-) lactose (*i.e.*, 6′-sialyllactose) and Neu5Ac(α2,3-) lactose (*i.e.*, 3′-sialyllactose) are found in the range of concentration 0.3–0.5 and 0.1–0.3 g L^{-1}, respectively in human milk, whereas only 6′-sialyllactose is found in bovine milk in lower concentration (0.03–0.06 g L^{-1}) compared to human milk. Neu5Ac2-lacto-*N*-tetraose, Neu5Ac-lacto-*N*-tetraose-a and -c are other acidic oligosaccharides found in human milk in moderate concentrations (0.2–0.6, 0.03–0.2 and 0.1–0.6 g L^{-1}, respectively), but found in trace levels in bovine milk.[136] It is also reported that most (~70–83%) of the *Sia* in human milk exists in the form of sialylated HMOs, while a small fraction (~2–3%) of *Sia* exists in the casein-bound or free forms. The remaining ~11–25% of *Sia* is generally bound to glycoproteins.[132,133] Martin-Sosa *et al.* reported ~7.7–14.5% *O*-acetylated Neu5Ac in the human milk, but could not find traces of Neu5Gc.[132] The total concentration of *Sia* in commercial infant formulas usually lies in the range 0.05–0.63 mM, which is about 25% less than human breast milk. Furthermore, in contrast to human milk, a major fraction (~70%) of *Sia* in infant formulas is bound to proteins and about 0.9% of *Sia* remains in the free form whereas the oligosaccharide-bound *Sia* is significantly low (~27%).[133] HMOs play a significant role in the nourishment of health-promoting gastrointestinal tract bacteria, pathogen proliferation, brain and neural developments, *etc.*[137] About 247 different HMOs having about 162 different chemical structures have been identified in human milk,[138] however both concentration and profile of HMOs in human milk are highly dependent on the genetics, environment and behaviour.[139] This may be attributed to the systematic evolution of the natural immune system in the population in any particular location.[140] The HMOs help in the development and growth of the infants' guts. A breast-fed infant of <6 month age can consume ~56 g of lactose and 4–12 g non-digestible oligosaccharides from an average consumption of 800 mL human milk per day.[141]

2.2 Involvement of *Sia* in human bacterial and viral infections

Bacteria and viruses often evolve to utilise and exploit *Sia* for evading the human's natural immune system. Hence, *Sia* is responsible for many bacterial and viral infections and eventually a greater number of viruses exploit *Sia* compared to bacterial infections.

2.2.1 Exploitation of *Sia* by bacteria to infect humans. Three main groups of bacteria have been identified to exploit *Sia* or poly*Sia* to cause human infections.

The first group would include bacteria which can *de novo* biosynthesise poly*Sia* or sialylated capsular polysaccharides, lipopolysaccharides, lipooligosaccharides and peptidoglycans by themselves on their own cell surface to mask the host's immune surveillance. *Escherichia coli* bacterial phage receptor displays an endogenous poly*Sia* network similar to poly*Sia* structures of brain microglia.[142] This molecular mimicry helps *E. coli* in the cell-internalisation process as well as conferring protection from the innate immune network by engaging inhibitory Siglec-11. On the other hand, uropathogenic *E. coli* non-specifically binds to *Sia* on the urinary bladder epithelium.[143] However, the interaction of *E. coli* with the activating Siglec-16 enhances proinflammatory cytokine expression. Thus, fortunately the impaired dynamics of Siglecs-11 and -16 leads to the elimination of this pathogen from the human body.[144] Han *et al.* recently used *N*-acetyl-9-azido-9-deoxy-neuraminic acid label in flow cytometry, metagenomic and whole-genome sequencing to identify a new strain of *E. coli* in complex human faecal microbiome.[145] *Neisseria meningitidis* bacteria, which cause meningitis disease, also can synthesise α2,8-(serogroup B) and *O*-acetylated or non-acetylated α2,9-(serogroup C) poly*Sia* on the lipooligosaccharide cell surface.[146] Hence, it inhibits the activation of an alternative pathway of the immune system.[147] However, the preferential binding of *N. meningitidis* with Siglecs-1 and -5 leads to its efficient phagocytosis.[148] *Campylobacter jejuni* bacteria can synthesise α2,3- and α2,8-Neu5Ac themselves on their own lipooligosaccharide cell structures and thus they can easily mimic the human peripheral nerve gangliosides, causing autoimmune neuropathy known as Guillain–Barré syndrome.[149] The sialylated lipooligosaccharide of *C. jejuni* enhances dendritic cell activation and promotes B-cell responses by producing IFN-β and TNF-α cytokines.[150] Furthermore, α2,3- and α2,8- sialylated lipooligosaccharides interact with Siglecs-1 and -7, respectively, on the dendritic cells and polarize naïve T-cells differently to T-helper-2 and -1 cells, respectively.[151] *Staphylococcus agalactiae* bacteria, also known as group B *Streptococcus*, can produce α2,3-Neu5Ac linked capsular polysaccharide themselves, to mimic the human glycocalyx and can cause meningitis in human infant and sepsis. Group B *Streptococcus* blocks the antimicrobial factor derived from the platelets and engages the inhibitory receptor Siglec-9 to block platelet activation.[152] However, genetically or biochemically mediated *O*-acetylation of α2,3-Neu5Ac capsular polysaccharide of group B *Streptococcus* minimises the virulence and neutrophil suppression.[153]

A second group of bacteria cannot synthesise *Sia* by themselves but can exploit host cell's *Sia* as a source of carbon for their own catabolism, colonization and biofilm formation. *Haemophilus influenzae* bacteria use dietary Neu5Gc as well as Neu5Ac from the host cell to sialylate outer membrane glycolipids and lipooligosaccharide and form biofilms.[154] *Streptococcus pneumonia* bacteria, acquire the terminal *Sia* of human nasopharynx sialoglycans as a carbon source for airway colonisation.[155] *Pseudomonas aeruginosa* bacteria which cause chronic infections of lungs, absorb *Sia* on their own surface from the sialylated glycoproteins

present in human body fluids and engage the inhibitory Siglec-9 to attenuate the inflammatory responses of neutrophils.[156,157] *Neisseria gonorrhoeae* bacteria cause the gonococcal infection known as gonorrhea. The bacterial *sialyltransferase* transfers Neu5Ac from host cell's CMP-Neu5Ac to gonococcal lipooligosaccharide and downregulates the alternative complement pathway of innate immune surveillance. However, the use of either a fusion protein (consisting of complement inhibition factor H and fragment crystallizable region of immunoglobulin G) or un-protective analogue of Neu5Ac to interact with the bacterial lipooligosaccharide can be utilised for the immunotherapy of gonorrhoea.[158] *Haemophilus ducreyi* bacteria, responsible for the chancroid disease, and *Pasteurella multocida* pathogen, causing soft-tissue infection, also utilise the host's sialylated glycans to evade human immune surveillance.[159,160]

The third group of bacteria use their own *Sia* or host cell's *Sia* as either receptor or ligand to mediate infection. The erythrocyte binding antigen 175 of *Plasmodium falciparum* pathogen (responsible for malaria) preferentially binds to Neu5Ac available on the RBC membrane.[161] GM1 ganglioside is a known receptor of cholera toxin. The *Vibrio cholerae neuraminidase* enzyme released from *Vibrio cholerae* bacteria cleaves *Sia* from higher order gangliosides to unmask GM1 on the host cell surface.[162] On the other hand, the cluster of genes in the vibrio pathogenicity island 2 of the *Vibrio cholerae* strain indicates that it can utilise the released *Sia* as the sole source of carbon and nitrogen for their own catabolism reactions.[163] The *Sia*-binding adhesin of *Helicobacter pylori* bacteria targets the gangliosides of the host cell surface, stimulating neutrophils to produce reactive oxygen species, which often damage the gastric epithelium.[164] On the other hand, *Sia*-binding adhesin of *Streptococcus gordonii* binds with *Veillonella atypica*; this process is necessary for intergeneric coaggregation, which causes dental biofilm.[165]

2.2.2 Viral exploitation of *Sia* in human infection. *Sia* directly and indirectly participates in the recognition, attachment and internalization of many enveloped and capsid viruses. The envelope glycoprotein-120 (gp120) of human immunodeficiency virus (popular as HIV) has partially sialylated complex oligosaccharides.[166] The gp120 of human immunodeficiency virus envelop thus interacts with Siglecs-1 and -7 of monocyte-derived macrophages and $CD4^{+}$T-cells lymphoid organs.[167,168] The sialylated *O*-glycans of enveloped glycoprotein B of herpes simplex virus have different binding avidity to inhibitory-paired-immunoglobulin-like-type-2 receptor in α- and β-forms expressed on the immune cells. Those sialylated glycans modulate the host immune response and facilitate viral entry to host cells.[169,170] Among the mosquito borne viruses, the sialylated glycoprotein-1 and -2 of the Ebola virus are usually recognised by Siglec-1 of the host cells,[171–173] whereas the envelop protein E of the Zika virus preferentially binds to α2,3-sialylated glycoproteins of host cells.[174] The α2,3-sialylated glycoprotein was found in the saliva of mosquito *Aedes aegypti* and its complex with dengue virus was identified,[175] but its relation to transmission to the host cell is yet not available in the literature. The human picornaviruses *viz.* coxsackievirus A24 and enteroviruses 68, preferentially bind to the unbranched α2,6-Neu5Ac-glycans of the host cell, whereas enteroviruses 70 has preferential affinity to the unbranched α2,3-Neu5Ac-glycans.[176,177] On the other hand, the human Lassa fever virus upon endocytosis engages the endogenous terminal α2,3-Neu5Ac-glycans on the lysosomal-associated membrane protein for further propagation of the infection.[178] The rabies virus can efficiently target the gangliosides of central nervous system.[179]

The human influenza virus A, B, C have two surface glycoproteins *viz.* hemagglutinin and neuraminidase, which interact with the host cells. The globular domain of hemagglutinin trimer in the influenza A and B viruses preferentially binds with α2,6- (in human) and α2,3- (in avian) sialylated glycans, but influenza C virus binds to 9*O*Ac-Neu5Ac. On the other hand, the neuraminidase cleaves the post-infection glycoside bonds and releases the progeny in the cytosol.[180] The human upper respiratory epithelial cells in the nasal mucosa, paranasal sinuses, pharynx, bronchi, *etc.*, are highly susceptible to the influenza infection owing to higher availability of cell surface α2,6-Neu5Ac glycoconjugates in the human upper airway.[181] Human saliva and serum contain a minimum of 116 and 144 glycan binding proteins, which can block the terminal α2,6-Neu5Ac glycoconjugates in competition to the hemagglutinin protein of influenza virus, thus helping to inhibit influenza infection.[182,183] However, the expression of α2,3-Neu5Ac in the salivary glycoprotein MUC5B and immunoglobulin-A of pregnant women decreased drastically, resulting in less screening of avian influenza virus specially in the third trimester.[184] Antiviral agents such as zanamivir, oseltamivir, peramivir, laninamivir are known commercially available neuraminidase inhibitor molecules, while *tert*-butyl hydroquinone, arbidol and their derivatives could restrict the hemagglutinin attachment to the sialylated glycoconjugates of host cells.[185] Human mumps virus and parainfluenza virus use viral hemagglutinin-neuraminidase proteins to target unbranched α2,3-Neu5Ac glycoconjugates, in contrast to the α2,6-Neu5Ac glycoconjugates preferred by the influenza virus.[186–188] The hemagglutinin protein of adeno-associated virus serotype-1, -4, -5 and -6 recognises both α2,3-Neu5Ac and α2,6-Neu5Ac on *N*-linked glycoproteins.[189]

The VP1 of the human capsid protein viruses *viz.* BK polyomavirus and Merkel cell polyomavirus preferentially bind to α2,3-Neu5Ac glycoconjugates of urogenital tissues, astrocytes, oligodendrocytes, lymphocytes, renal cells, *etc.*,[190,191] whereas human JC polyomavirus prefers α2,6-Neu5Ac glycoconjugates of the glial cells.[192] The σ1 protein of reovirus binds GM2 (for type 1 serotype) and α2,3/6/8-Neu5Ac glycans (for type 3 serotype).[193,194] The polypeptide VP8* of the spike protein VP4 of rotavirus interacts with subterminal Neu5Ac residue of the gangliosides GD1a and

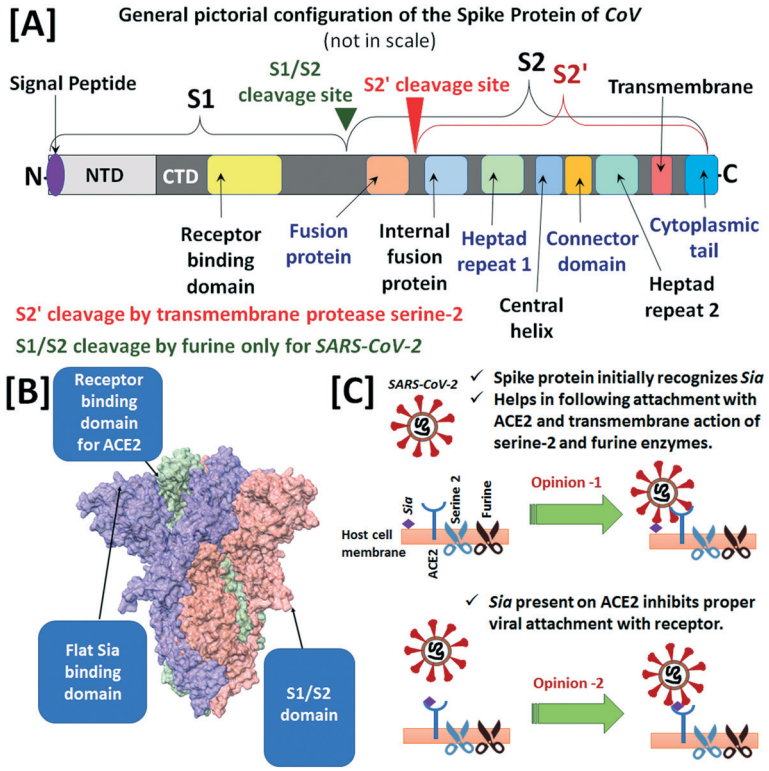

Fig. 3 [A] A pictorial configuration of the main constituents of the spike protein of *SARS-CoV-2* indicating the cleavage sites *viz.* S1/S2 and S2′. [B] The model of unique feature of the spike protein of *SARS-CoV-2* (main figure used with permission from ref. 206) Copyright 2020 John Wiley and Sons. [C] The contradictory opinions about the role of *Sia* in the attachment to human cells (figures are not to scale).

GM1 for key binding of the virus to host cells.[195] The human adenovirus 37, causing severe epidemic keratoconjunctivitis, uses α2,3-Neu5Ac-glycans on GD1a ganglioside for the host cell binding and infectivity.[196,197] On the other hand, the short fibre knob of human adenovirus 52 causing human gastroenteritis, preferentially recognizes poly*Sia* sequence for causing infection.[198]

The glycocalyx of human cells is important in the mechanism of infection of the human corona viruses (CoVs) *viz.* CoV-229E, CoV-NL63, OC43-CoV, HKU1-CoV, severe acute respiratory syndrome coronavirus (SARS-CoV), middle east respiratory syndrome coronavirus (MERS-CoV) and novel corona virus (SARS-CoV-2).[199] Upon attachment of CoV, the transmembrane protease serine-2 of the host cell splits the spike protein S of CoV at site S2′ (in between fusion protein and internal fusion protein of S2) into two subunits *viz.* S1 and S2, responsible for recognition and membrane fusion, respectively (Fig. 3[A]). The N-terminal domain (NTD) of the S1 unit *i.e.*, $S1^A$ identifies the sialylated glycans on the cell surface and facilitates the initial binding of CoV to the host cell, while the C-terminal domain (CTD) of S1 *i.e.*, $S1^B$ binds to the specific host receptors to assist fusion and cell internalization.[200] Among the human CoVs, the CoV-229E and CoV-NL63 do not require *Sia* for host cell adhesion, rather they directly interact with aminopeptidase *N* receptor and angiotensin-converting enzyme 2 (ACE2), respectively.[201,202] The CTD of SARS-CoV binds to ACE2 cell receptor for recognition and host cell entry. On the other hand, OC43-CoV and HKU1-CoV viruses, causing common cold, pneumonia and bronchiolitis, have homodimeric hemagglutinin-esterase in $S1^A$ and that recognises 9*O*Ac-Neu5Ac glycans as host cell receptors.[203] The $S1^A$ of MERS-CoV preferentially interacts with α2,3-Neu5Ac glycans compared to α2,6-Neu5Ac glycans, while $S1^B$ is involved in adherence to the specific cell surface entry receptor dipeptidyl peptidase 4.[204]

The novel corona virus SARS-CoV-2 which is responsible for the COVID 19 disease, is now considered most infectious among the group of human CoVs. The spike protein of SARS-CoV-2 has another cleavage motif at the boundary of S1–S2 subunits for furin-like enzymes of the host cell in addition to the transmembrane protease serine-2 unit, which is less expressed in the human lungs (Fig. 3[A]). The specific amino-acid sequence of the furin-like cleavage site is not present in other types of human CoVs. Hence, more efficient cleavage of the spike protein sub-units by both transmembrane protease serine-2 and furin of the host cell may be one of the possible reasons for higher pathogenicity of SARS-CoV-2 compared to SARS-CoV and MERS-CoV.[205] On the other hand, the presence of a flat and non-sunken sialic acid-binding unit at NTD of S1 subunit of the spike protein has theoretically been proposed in a recent article (Fig. 3[B]).[206] The recent *in silico* (performed through molecular docking simulations and electron density mapping) and computational studies, in line

with the cryogenic microscopic evidence, have suggested the involvement of a flat *Sia* binding domain in the NTD of the spike protein in the establishment of initial contact with the sialylated glycoconjugates and GM1 of the host epithelium. This initial interaction is proposed to provide higher affinity binding between the spike protein and ACE2 receptor (opinion 1 in Fig. 3[C]).[42,207,208] Furthermore, the *in silico* computational representation of the molecular isoelectronic density surface in terms of 2D Zernike polynomials also suggested the interaction of spike protein of SARS-CoV-2 with *Sia* receptors of the cells in the upper airways.[209] Recently, a computational study in synchronization with mass-spectrometric and surface plasmon resonance (SPR) experiments on the interaction between Neu5Ac and SARS-CoV-2 spike protein reported that both up and down states of receptor-bonding-domain (known as RBD) of the spike protein moderately bind with Neu5Ac.[210] Furthermore, an exploration in the Human Protein Atlas repository revealed high expression of Neu5Ac biosynthesis enzymes *viz.* glucosamine (UDP-*N*-acetyl)-2-epimerase/*N*-acetylmannosamine kinase, Neu5Ac-9-phosphate synthase and Neu5Ac-9-phosphate phosphatase in the salivary glands and hence, proposed about a possible role of Neu5Ac in SARS-CoV-2 infection.[211] On the other hand, the participation of other co-receptors *viz.* CD147,[212] heparan sulfate,[213] *etc.* is also proposed for the initial recognition of the virus by the host cell. Moreover, complex sialylated *N*- and *O*-glycans have recently been evident on human ACE2,[214] but those glycans have shown indication of resistance in the viral recognition by the host cells.[215] Furthermore, the studies of SARS-CoV-2 infection on human epithelial lung cells and *ex vivo* human lung tissues revealed that heparan sulfate is an important co-receptor of this virus, while the sialylated glycans present on ACE2 can prevent protein spike and ACE2 interaction, which is most needed for viral attachment to the host cell (opinion 2 in Fig. 3[C]).[216] A study of the binding of soluble form of SARS-CoV-2 spike protein (in which entire external domain was stabilised by six proline residues and secondary antibody StrepMAB Classic, anti-twin-Strep-tag MoAb) to a sialoglycan microarray presenting 139 glycans representative of common terminal structures on vertebrate glycans showed the preferential affinity order as α2,3-Neu5Ac > 4*O*Ac-Neu5Ac > α2,6-Neu5Ac ~ 9*O*Ac-Neu5Ac ~ 9*N*Ac-Neu5Ac > α2,3-Neu5Gc ~ α2,6-Neu5Gc. This multivalent *Sia*-affinity of the spike protein may be responsible for the formation of small and long-lived aerosol particle production from human upper airways.[217] Recently published work by Nguyen *et al.* (during the proof-reading period of this review and included here for completion), revealed that the receptor-binding domain of the spike protein of SARS-CoV-2 has good binding affinity towards the gangliosides (GM1 and GM2), acidic (sialylated) HMOs and ABH blood group antigens (particularly A and H types 2, 3, 4).[218] The authors used catch-and-release ESI-MS and hydrophilic-interaction-ultra HPLC to scan the affinity of both receptor-binding domain and S protein of SARS-CoV-2 over 132 mammalian and 7 non-mammalian glycans. The work provides an insight into aspects of COVID 19 disease 1) glycolipids of the host cell, especially gangliosides GM1 and GM2 in competition with cell surface heparan sulfate, bind to a common site of receptor-binding domain and S protein of SARS-CoV-2 and facilitate viral entry by the action of ACE2. The human brain and central nervous system share a higher fraction of gangliosides compared to other human organs (see Section 2.1.2), and this work aids understanding of the spread of SARS-CoV-2 infection to the central nervous system.[219] 2) Human milk has the lowest fraction (~12–14%) of acidic (sialylated) HMOs which can bind to the receptor-binding domain and the S protein of SARS-CoV-2. In this study, none of the 72 neonates breastfed for 14 days by COVID 19 positive mothers tested COVID 19 positive.[220] 3) Antigen A of human blood cells predominantly stimulates (compared to other antigens B and AB) the formation of sialoside clusters in target cells through *cis*-carbohydrate–carbohydrate interactions. Therefore, humans having blood group A are more susceptible to SARS-CoV-2 infection.[221] Furthermore, Nguyen *et al.* showed that decreasing cell surface *Sia* by either sialyltransferase inhibition, genetic knockout of biosynthesis of *Sia* or neuraminidase treatment decreased the SARS-CoV-2 infectivity by 30–40% and this information is now very useful for the development of COVID 19 therapy.[218] However, several questions on *Sia*-SARS-CoV-2 interactions including the influence on the human immune response and change of viral affinity with new variants of SARS-CoV-2 are yet to be explored.[222] Overall, the role of *Sia* for SARS-CoV-2 infection is still an open question.[44]

The infection of SARS-CoV, MERS-CoV and SARS-CoV-2 to human organs leads to the release of high levels of pro-inflammatory cytokines and chemokines, which is known as a "cytokine storm". It is proposed that the cross reactivity of *Sia* with the host immune lectins might be responsible for this cytokine storm.[43] Gas and water phase quantum mechanical calculations revealed that the monoprotonated form of anti-malarial drugs chloroquine and hydroxychloroquine, having anti-inflammatory properties, can form stable complexes with Neu5Ac. This may interfere with the ACE2 receptor and spike protein interaction and subsequently inhibit SARS-CoV-2 infection.[223] Thus, in the uncertain therapeutic trials against COVID-19, these two drugs are being administrated to COVID-19 patients to fight against SARS-CoV-2 infection.[224–226] However, more clinical studies are recommended for the prolonged use of chloroquine and hydroxychloroquine solely or in combination with other drugs for COVID-19 treatment.[227] Another drug *viz.* remdesivir, which showed reliable clinical performance for MERS-CoV and SARS-CoV in the past pandemics, is also being used for clinical treatment of COVID-19.[228,229] Interestingly, owing to the preferential affinity of Neu5Ac towards the spike protein glycoprotein of SARS-CoV-2 compared to SARS-CoV, a paper-based lateral flow point-of-care diagnostic sensor is prepared with Neu5Ac modified poly(*N*-hydroxyethyl acrylamide) coated gold nanoparticles to detect SARS-CoV-2 spike protein down to 5

Table 1 Concentration of *Sia* in human body fluids and organs at occurrence of some diseases, cancers and addictions

Human organ/system affected	Patients having addiction/cancer/disease and healthy controls	Type of samples	Number of individuals (age group)	Concentration of *Sia* [probability (*P*) value]			Ref.
				Total *Sia*	Bound *Sia*	Free *Sia*	
Addictions							
Oral	Smokeless tobacco (Paan) consumers	Saliva	44 (27.52 ± 9.9 years)	39.57 ± 26.58 mg L^{-1} (*P* 0.63)	NR	23.21 ± 18.98 mg L^{-1} (*P* 0.001)	239
	Non Paan consumers		50 (29.5 ± 10.3 years)	38.39 ± 28.55 mg L^{-1}	NR	18.11 ± 16.5 mg L^{-1}	
	Smokers		33 (23.80 ± 3.43 years)	62.60 ± 3.91 mg L^{-1} ($P < 0.001$)	NR	NR	240
	Maras powder users		37 (29.03 ± 6.46 years)	75.52 ± 6.86 mg L^{-1} ($P < 0.001$)	NR	NR	
	Healthy control		30 (22.23 ± 2.45 years)	51.60 ± 3.51 mg L^{-1}	NR	NR	
Liver	Alcoholics	Serum	51 (mean 49 years)	1.449 ± 0.3019 mM (NR)	NR	NR	242
	Alcoholics with liver disease		32	1.421 ± 0.3082 mM (NR)	NR	NR	
	Alcoholic without liver disease		19	1.497 ± 0.2927 mM (NR)	NR	NR	
	Non-alcoholics		20 (mean 51 years)	1.154 ± 0.1702 mM	NR	NR	
	Alcoholics		106 (20–71 years)	76.8 ± 14.9 mg dL^{-1} ($P < 0.001$)	13.67 ± 3.55 mg dL^{-1} (lipid bound) (*P* 0.003)	NR	245
	Non-alcoholics		50 (21–76 years)	63.1 ± 8.2 mg dL^{-1}	11.67 ± 2.08 mg dL^{-1} (lipid bound)	NR	
	Alcoholics		49 (24–70 years)	82 ± 13.5 mg dL^{-1} (female); 85 ± 19.8 mg dL^{-1} (male); $P < 0.001$	NR	NR	246
	Non-alcoholics		38 (40 years)	60 ± 10.4 mg dL^{-1} (female); 64 ± 16.0 mg dL^{-1} (male)	NR	NR	
Diseases							
Central nervous system and brain	Pyogenic meningitis	Cerebrospinal fluid	5 (NR)	NR	38–1450 μM (NR)	80–620 μM (NR)	247
	Tuberculous meningitis		5 (NR)	NR	32–220 μM (NR)	13–26 μM (NR)	
	Healthy control		9 (NR)	NR	12–40 μM (NR)	6–32 μM (NR)	
	Alzheimer		39 (47–86 years)	NR	NR	16.75 ± 3.89 μM ($P = 0.001$)	248
	Idiopathic normal pressure hydrocephalus		19 (70–86 years)	NR	NR	13.35 ± 3.2 μM ($P = 0.001$)	
	Patients having cerebellar ataxia with free sialic acid		5 (19–37 years)	NR	NR	43.4 ± 11.0 μM	250
	Patients having neurological symptoms including psychomotor retardation, cerebellar ataxia, paraplegia, parkinsonism or other extrapyramidal manifestations, neuropathy, psychiatric symptoms and leukodystrophy		144 (1–80 years)	NR	NR	8.2 ± 4.2 μM ($P < 0.001$)	
	Patients having other well-defined metabolic diseases		88 (1–80 years)	NR	NR	9.9 ± 5.6 μM ($P < 0.001$)	

Table 1 *(continued)*

Diseases							
	Salla		3 (1–80 years)	NR	NR	31.3 ± 4.9 μM	
	Alzheimer	Plasma	60 (74.13 ± 1.683 years)	0.7133 ± 0.0201 ng L^{-1} ($P < 0.0001$)	NR	NR	249
	Healthy control		60 (70.00 ± 1.255 years)	0.5972 ± 0.01866 ng L^{-1}	NR	NR	
	Autism spectrum disorder		82 (4.22 ± 1.01 years)	3.27 ± 0.90 mM ($P < 0.01$)	NR	NR	252
	Healthy control		60 (4.52 ± 0.84 years)	5.32 ± 1.85 mM	NR	NR	
	Autism spectrum disorder with medication (risperidone, 0.32 ± 0.013 mg per day; 2–6 months)	Saliva	28 (5.50 ± 2.05 years)	0.102 ± 0.062 mM (P 0.027)	NR	NR	251
	Autism spectrum disorder without medication		18 (5.50 ± 2.05 years)	0.100 ± 0.099 mM (P 0.027)	NR	NR	
	Healthy control		30 (5.35 ± 2.15 years)	0.160 ± 0.097 mM	NR	NR	
Blood and related organs (diabetes mellitus and associated diseases)	Type 1 diabetes mellitus	Serum	20 (22–79 years)	2.00 ± 0.37 mM ($P < 0.02$)	NR	NR	253
	Healthy non-diabetes		20 (19–66 years)	1.98 ± 0.67 mM	NR	NR	
	Type 2 diabetes mellitus (T2DM)		16 (36–67 years)	2.32 ± 0.41 mM	NR	NR	
	Type 1 diabetes mellitus		16 (34–71 years)	1.84 ± 0.24 mM ($P < 0.001$)	NR	NR	
	Healthy non-diabetes		16 (22–64 years)	1.92 ± 0.35 mM ($P < 0.001$)	NR	NR	
	Type 1 diabetes mellitus with retinopathy		6 (NR)	2.38 ± 0.33 mM ($P < 0.01$)	NR	NR	
	Type 1 diabetes mellitus without retinopathy		6 (NR)	1.85 ± 0.26 mM	NR	NR	
	T2DM normoalbuminuria (albumin excretion rate 16.5 ± 6.6 μg min^{-1})	Serum (urine)	26 (54.2 ± 9.9 years)	1.9 ± 0.4 mM (0.08 ± 0.01 mol% *Sia*/creatinine) ($P < 0.001$)	0.5 ± 0.2 mM (lipid bound)	NR	254
	T2DM microalbuminuria (albumin excretion rate 78.1 ± 23.2 μg min^{-1})		52 (54.2 ± 9.9 years)	2.0 ± 0.4 mM (0.08 ± 0.01 mol% *Sia*/creatinine) ($P < 0.001$)	0.6 ± 0.2 mM (lipid bound)	NR	
	Healthy nondiabetic control (albumin excretion rate 1.1 ± 0.8 μg min^{-1})		28 (NR)	1.6 ± 0.1 mM (0.04 ± 0.01 mol% *Sia*/creatinine)	0.5 ± 0.1 mM (lipid bound)	NR	
	T2DM and nephropathy comorbidity		190 (26–79 years)	93.2 ± 3.6 mg dL^{-1} (17.7 ± 1.4 mg dL^{-1}) ($P < 0.05$)	NR	NR	255
	Nephropathy		36 (30–73	84.0 ± 2.7 mg dL^{-1} (14.3 ± 0.7 mg dL^{-1})	NR	NR	

Table 1 *(continued)*

Diseases							
			years)	($P < 0.05$)			
	T2DM		30 (38–70 years)	82.6 ± 1.3 mg dL^{-1} (12.5 ± 0.9 mg dL^{-1}) ($P < 0.05$)	NR	NR	
	Healthy control without T2DM and nephropathy		240 (20–79 years)	59.1 ± 3.6 mg dL^{-1} (9.2 ± 1.0 mg dL^{-1})	NR	NR	
	T2DM	Plasma (RBC membrane)	146 (22–80 years)	175.00 ± 68.89 μM (4.20 ± 2.14 mmol per mg protein) ($P < 0.05$)	NR	NR	256
	T2DM and nephropathy comorbidity			174.13 ± 23.20 μM (4.00 ± 2.51 mmol per mg protein) ($P < 0.05$)	NR	NR	
	T2DM and hypertension comorbidity			176.00 ± 54.82 μM (4.14 ± 2.00 mmol per mg protein) ($P < 0.05$)	NR	NR	
	T2DM and hyperlipidemia comorbidity			160.80 ± 48.61 μM (3.93 ± 2.10 mmol per mg protein) ($P < 0.05$)	NR	NR	
	Healthy control		15 (22–80 years)	149.9 ± 47.30 μM (5.84 ± 1.43 mmol per mg protein)	NR	NR	
	Gestational diabetes mellitus	RBC membrane	16 (29 ± 6 years)	81.29 ± 41.80 mg per g protein ($P < 0.001$)	NR	NR	129
	Healthy pregnant women		25 (28 ± 5 years)	96.30 ± 34.20 mg per g protein ($P < 0.001$)	NR	NR	
	Healthy nonpregnant women		10 (30 ± 4 years)	42.33 ± 15.85 mg per g protein	NR	NR	
	High in 50 g glucose challenge test (1 h; glucose > 140 mg dL^{-1}) and 100 g oral glucose tolerance test (3 h; glucose > 176 mg dL^{-1})	Serum	8 (20–38 years)	3.05 (2.67–3.49) mM ($P < 0.001$)	NR	NR	258
	High in 50 g glucose challenge test (1 h; glucose > 140 mg dL^{-1}); but low in 100 g oral glucose tolerance test (3 h; glucose ≤ 176 mg dL^{-1})		36 (19–38 years)	3.22 (2.34–5.04) mM ($P < 0.001$)	NR	NR	
	Normal in 50 g glucose challenge test (1 h; glucose ≤ 140 mg dL^{-1})		61 (18–38 years)	2.66 (1.2–4.59) mM	NR	NR	
	Behcet's syndrome		16 (NR)	95.6 ± 15.3 (76–129) mg dL^{-1} ($P < 0.01$)	29.8 ± 7.4 (17.2–45.6) mg dL^{-1} ($P > 0.05$)	NR	259
	Uveitis disease		12 (NR)	75.8 ± 8.1 (64–91.8) mg dL^{-1} ($P < 0.01$)	26.6 ± 3.0 (21.4–32.4) mg dL^{-1} ($P > 0.05$)	NR	
	Healthy control		22 (NR)	59.5 ± 7.5 (47–75.5) mg dL^{-1}	19.2 ± 3.2 (15–24.5) mg dL^{-1}	NR	
Gum	Periodontitis	Saliva	5 (NR)	NR	NR	0.0040% (whole saliva) 0.0019% (parotis saliva)	260
	Rheumatoid arthritis		5 (NR)	NR	NR	0.0053% (whole saliva) 0.0035%	

Table 1 *(continued)*

Diseases							
	Healthy control		8 (NR)	NR	NR	(parotis saliva) 0.0047% (whole saliva) 0.0024% (parotis saliva)	
	Gingivitis		30 (46.70 ± 13.59 years)	12.98 ± 18.06 mg dL^{-1}	NR	NR	262
	Periodontitis		33 (45.18 ± 8.98 years)	19.81 ± 16.45 mg dL^{-1}	NR	NR	
	Healthy control		30 (44.67 ± 9.51 years)	5.79 ± 2.49 mg dL^{-1}	NR	NR	
	Chronic gingivitis	Saliva (serum)	30 (27.73 ± 7.51 years)	68.23 ± 2.71 mg dL^{-1} (65.65 ± 3.56 mg dL^{-1}) $P < 0.0001$	NR	NR	261
	Chronic periodontitis		30 (31.23 ± 6.74 years)	81.33 ± 3.94 mg dL^{-1} (75.98 ± 3.58 mg dL^{-1}) $P < 0.0001$	NR	NR	
	Healthy control		30 (27.37 ± 9.69 years)	39.05 ± 6.35 mg dL^{-1} (49.75 ± 4.87 mg dL^{-1})	NR	NR	
	Aggressive periodontitis		10 (35.16 ± 6.81 years)	5.83 ± 0.74 mg dL^{-1} (parotis); 10.01 ± 1.92 mg dL^{-1} (whole) (134.28 ± 27.84 mg dL^{-1}); $P < 0.001$	NR	NR	263
	Chronic periodontitis		10 (35.16 ± 6.81 years)	4.16 ± 1.10 mg dL^{-1} (parotis); 8.87 ± 1.57 mg dL^{-1} (whole) (108.65 ± 17.71 mg dL^{-1}); $P < 0.001$	NR	NR	
	Chronic gingivitis		10 (35.16 ± 6.81 years)	3.72 ± 0.84 mg dL^{-1} (parotis); 4.72 ± 1.08 mg dL^{-1} (whole) (80.69 ± 9.09 mg dL^{-1}); $P < 0.001$	NR	NR	
	Healthy control		10 (22.20 ± 1.55 years)	3.01 ± 0.57 mg dL^{-1} (parotis); 3.54 ± 0.93 mg dL^{-1} (whole) (60.03 ± 10.62 mg dL^{-1})	NR	NR	
Heart and arteries	Patient had myocardial infarction before 1 day	Plasma	19 (64.8 ± 11 years)	0.88 ± 0.29 g L^{-1} ($P < 0.05$)	0.28 ± 0.13 g L^{-1} ($P < 0.05$)	NR	264
	Patient had myocardial infarction before 2 days			0.89 ± 0.30 g L^{-1} ($P < 0.05$)	0.20 ± 0.12 g L^{-1} ($P < 0.05$)	NR	
	Patient had myocardial infarction before 5 days			0.75 ± 0.19 g L^{-1} ($P < 0.05$)	0.27 ± 0.13 g L^{-1} ($P < 0.05$)	NR	
	Healthy control		19 (50.6 ± 18.6 years)	0.62 ± 0.13 g L^{-1}	0.24 ± 0.08 g L^{-1}	NR	

Table 1 *(continued)*

Diseases							
	Myocardial infarction	Serum	100 (63.44 ± 10.51 years)	297 (220–374) μg L^{-1} ($P < 0.001$)	NR	NR	265
	Unstable angina pectoris		537 (64.96 ± 10.13 years)	227 (114–312) μg L^{-1} ($P < 0.001$)	NR	NR	
	Healthy control		129 (57.43 ± 9.67 years)	207 (114–276) μg L^{-1}	NR	NR	
	Normal coronary artery	Plasma	235 (58.6 ± 9.0 years)	147.20 (123.42–186.79) μg L^{-1}	NR	NR	267
	Nonobstructive coronary atherosclerosis		496 (62.5 ± 8.8 years)	148.43 (123.88–181.57) μg L^{-1}	NR	NR	
	Stable angina		135 (64.3 ± 8.1 years)	143.70 (128.30–177.97) μg L^{-1}	NR	NR	
	Unstable angina		587 (64.9 ± 9.0 years)	178.25 (135.46–212.38)	NR	NR	
	Acute myocardial infarction		566 (63.1 ± 10.8 years)	182.34 (147.16–234.70) μg L^{-1}	NR	NR	
	Coronary artery disease	Serum	16 (63.6 ± 10.3 years)	71.91 (68.33–75.60) mg dL^{-1}	NR	NR	268
	Healthy control		25 (56.9 ± 13.3 years)	60.76 (57.04–65.92) mg dL^{-1}	NR	NR	
	Periodontitis in comorbidity with cardiovascular disease	Serum (saliva)	26 (40–85 years)	86.87 ± 15.61 mg dL^{-1} (9.48 ± 4.55 mg dL^{-1}) ($P < 0.0001$)	NR	NR	269
	Periodontitis only		26 (45–75 years)	53.2 ± 7.89 mg dL^{-1} (5.05 ± 1.49 mg dL^{-1})	NR	NR	
	Carotid atherosclerosis	Serum	322 (59.9 ± 5.2 years)	75.0 ± 9.7 mg dL^{-1} ($P < 0.0001$)	NR	NR	270
	Healthy control		323 (58.7 ± 5.4 years)	70.7 ± 8.9 mg dL^{-1}	NR	NR	
	Hypertriglyceridaemia		15 (59 ± 9 years)	84.9 ± 21.5 mg dL^{-1} ($P < 0.03$)	23.0 ± 4.3 mg dL^{-1} ($P < 0.001$)	NR	271
	Cholesterolemia		15 (53 ± 11 years)	58.4 ± 11.7 mg dL^{-1} ($P < 0.03$)	14.9 ± 4.7 mg dL^{-1} ($P < 0.001$)	NR	
	Healthy control		15 (52 ± 14 years)	64.9 ± 20.8 mg dL^{-1}	12.0 ± 3.2 mg dL^{-1}	NR	
Eye	Sympathetic ophthalmia		16 (13–43 years)	120.2 ± 12.6 (99–142) mg dL^{-1} ($P < 0.001$)	NR	NR	272
	Traumatic uveitis		36	71.3 ± 8.4 (60–86)	NR	NR	

Table 1 *(continued)*

Diseases							
			(12–46 years)	mg dL^{-1} ($P > 0.1$)			
	Healthy control		40 (16–40 years)	67.8 ± 7.9 (56–83) mg dL^{-1}	NR	NR	
Thyroid	Sub-clinical hypothyroidism		35 (34.4 ± 10.3 years)	37.1 ± 15.5 mg L^{-1} (*P* 0.775)	NR	NR	273
	Overt hypothyroidism		25 (33 ± 9.3 years)	58.2 ± 18.9 mg L^{-1} ($P < 0.001$)	NR	NR	
	Healthy control		30 (32.5 ± 7.5 years)	38.1 ± 12.0 mg L^{-1}	NR	NR	
Bowl	Active ulcerations		6 (24.3 ± 3.8 years)	69.7 ± 9.4 mg dL^{-1} ($P < 0.01$)	NR	NR	274
	No active ulcerations (post-surgery)		6 (35.5 ± 12.8 years)	54.7 ± 5.5 mg dL^{-1} ($P < 0.01$)	NR	NR	
	Healthy control		6 (32.3 ± 4.7 years)	50.3 ± 4.4 mg dL^{-1}	NR	NR	
Liver	Hepatitis B		50 (19–71 years)	1.32 (0.06–1.84) mM (*P* 0.047)	NR	NR	275
	Hepatitis C		40 (19–67 years)	1.67 (1.18–2.96) mM (*P* 0.025)	NR	NR	
	Healthy control		30 (21–54 years)	1.43 (0.96–2.16 mM)	NR	NR	
	Malignant jaundice		55 (35–87 years)	7.95 mg L^{-1} (median); *Sia*/protein 1.20	NR	NR	276
	Jaundice		30 (35–87 years)	6.86 mg L^{-1} (median); *Sia*/protein 1.03 ($P < 0.001$)	NR	NR	
	Healthy control		24 (24–56 years)	5.97 mg L^{-1} (median); *Sia*/protein 0.79 (*P* 0.041)	NR	NR	
	Alcoholic patients having cirrhosis		31 (27–52 years)	5.81 (3.89–10.06) mg L^{-1} ($P < 0.001$)	NR	0.55 (0.34–0.94) mg L^{-1} (*P* 0.017)	277
	Non-alcoholic patients having cirrhosis		24 (27–52 years)	5.43 (3.79–7.88) mg L^{-1} ($P < 0.001$)	NR	0.49 (0.34–0.82) mg L^{-1} (*P* 0.035)	
	Patients having chronic viral hepatitis C		24 (27–52 years)	5.76 (4.42–8.11) mg L^{-1} ($P < 0.001$)	NR	0.48 (0.34–0.63) mg L^{-1} (*P* 0.016)	
	Healthy control		49 (21–79 years)	6.22 (5.4–8.0) mg L^{-1}	NR	0.49 (0.36–0.61) mg L^{-1}	
Kidney	Chronic glomerulonephritis	Serum (urine)	35 (25–60 years)	82.3 ± 6.5 mg dL^{-1} (0.150 ± 0.03 mg mL^{-1}) ($P < 0.001$)	19.7 ± 0.9 mg dL^{-1} lipid bound (NR) ($P < 0.001$)	NR	278
	Chronic renal failure		27 (19–54 years)	70.7 ± 5.5 mg dL^{-1} (pre-dialysis)	17.7 ± 0.8 mg dL^{-1} lipid bound (pre-dialysis)	NR	
				71.2 ± 6.8 mg dL^{-1} (post-dialysis) (0.147 ± 0.04 mg mL^{-1}) ($P < 0.001$)	20.6 ± 1.1 mg dL^{-1} lipid bound (post-dialysis) (NR) ($P < 0.001$)		
	Healthy control		60 (16–64	59.8 ± 7.9 mg dL^{-1} (0.098 ± 0.04 mg mL^{-1})	15.9 ± 0.8 mg dL^{-1} lipid bound	NR	

Table 1 *(continued)*

Diseases							
			years)				
	Low glomerular filtration rate (8–82 mL min^{-1} per 1.73 m^2)	Plasma	16 (27–74 years)	NR	NR	310–1260 μg L^{-1} (NR)	279
	GNE myopathy (glomerular filtration rate 85–155 mL min^{-1} per 1.73 m^2)		19 (30–65 years)	NR	NR	151 ± 29 (109–206) μg L^{-1} (NR)	
	Healthy control (glomerular filtration rate > 90 mL min^{-1} per 1.73 m^2)		6 (NR)	NR	NR	100–200 μg L^{-1} (NR)	
Multiorgans	Hyperemesis gravidarum	Serum	30 (27.17 ± 5.63 years)	28.370 ± 8.69 mg L^{-1} ($P < 0.05$)	NR	NR	280
	Healthy control		30 (28.63 ± 6.21 years)	20.978 ± 9.96 mg L^{-1}	NR	NR	
	Preeclampsia	Plasma	47 (27.1 ± 5.5 years)	103.9 (91.3–111.0) mg dL^{-1} ($P < 0.05$)	NR	NR	281
	Transient hypertension in pregnancy		50 (24.7 ± 7.1 years)	102.2 (96.7–108.9) mg dL^{-1} ($P < 0.05$)	NR	NR	
	Uncomplicated pregnant women		40 (23.8 ± 5.8 years)	104.4 (91.2–106.9) mg dL^{-1} ($P < 0.05$)	NR	NR	
	Non pregnant women		20 (22.2 ± 4.0 years)	72.0 (62.7–78.8) mg dL^{-1}	NR	NR	
	Brucellosis	Serum	29 (NR)	2386 ± 82 μM ($P < 0.01$)	NR	NR	282
	Healthy control		64 (NR)	1821 ± 44 μM	NR	NR	
Cancers							
Oral	Oral squamous cell carcinoma	Saliva	30 (26–73 years)	NR	3.02 ± 0.01 mg dL^{-1} ($P < 0.001$)	4.30 ± 0.01 mg dL^{-1} ($P < 0.001$)	295
	Healthy control		30 (26–46 years)	NR	2.06 ± 0.01 mg dL^{-1}	3.40 ± 0.02 mg dL^{-1}	
	Oral cancer	Serum	26 (23–50 years)	94.69 ± 7.26 mg dL^{-1} ($P < 0.001$)	NR	NR	296
	Leukoplakia (pre-cancer)		27 (23–50 years)	60.30 ± 7.96 mg dL^{-1} ($P < 0.001$)	NR	NR	
	Oral sub mucous fibrosis (pre-cancer)		27 (23–50 years)	59.97 ± 6.03 mg dL^{-1} ($P < 0.001$)	NR	NR	
	Healthy tobacco consumers		40 (23–50 years)	48.52 ± 6.49 mg dL^{-1} ($P > 0.05$)	NR	NR	
	Healthy tobacco non-consumers		40 (23–50 years)	48.77 ± 5.88 mg dL^{-1}	NR	NR	
	Gingival cancer, palatal cancer, buccal cancer		37 (16–80 years)	69.46 ± 11.23 mg dL^{-1} ($P < 0.01$)	NR	NR	297

Table 1 *(continued)*

Cancers							
	Salivary gland tumours		23 (16–80 years)	70.58 ± 12.07 mg dL^{-1} ($P < 0.01$)	NR	NR	
	Lip and skin cancer		22 (16–80 years)	59.24 ± 12.10 mg dL^{-1} ($P < 0.01$)	NR	NR	
	Tongue and floor cancer		20 (16–80 years)	75.01 ± 12.00 mg dL^{-1} ($P < 0.01$)	NR	NR	
	Malignant fibrous histiocytoma		4 (16–80 years)	85.63 ± 5.45 mg dL^{-1} ($P < 0.01$)	NR	NR	
	Sarcoma		3 (16–80 years)	64.06 ± 5.01 mg dL^{-1} ($P < 0.01$)	NR	NR	
	Mandibular cancer		1 (NR)	69.72 mg dL^{-1} ($P < 0.01$)	NR	NR	
	Benign tumours in oral and maxillofacial region		60 (23–54 years)	58.28 ± 8.34 mg dL^{-1} ($P > 0.05$)	NR	NR	
	Healthy control		80 (22–44 years)	55.02 ± 7.2 mg dL^{-1}	NR	NR	
Bile duct	Cholangiocarcinoma		89 (55 ± 10 years)	2.75 ± 0.67 mM ($P < 0.001$)	NR	NR	298
	Benign hepatobiliary diseases		38 (55 ± 14 years)	2.33 ± 0.69 mM ($P < 0.002$)	NR	NR	
	Healthy control		43 (44 ± 14 years)	1.89 ± 0.46 mM	NR	NR	
Colon/rectum	Colorectal cancer		123 (34–88 years)	3.27 ± 1.12 mM; 49.01 ± 16.52 μmol g^{-1} of total protein ($P < 0.001$)	3.24 ± 1.11 mM; 48.59 ± 16.43 μmol g^{-1} of total protein ($P < 0.001$)	0.03 ± 0.01 mM	299
	Healthy control		72 (34–88 years)	2.14 ± 0.41 mM; 23.90 ± 4.81 μmol g^{-1} of total protein	2.12 ± 0.41 mM; 23.59 ± 4.78 μmol g^{-1} of total protein	0.03 ± 0.01 mM	
Ovary	Endometrial neoplasia		45 (37–81 years)	2.38 ± 0.72 mM; 27.91 ± 8.00 μmol g^{-1} of protein ($P < 0.001$)	NR	NR	300
	Other neoplasia		7 (37–81 years)	2.53 ± 1.29 mM; 28.45 ± 11.80 μmol g^{-1} of protein (P 0.0086)	NR	NR	
	Healthy women		20 (20–36 years)	1.52 ± 0.25 mM; 19.28 ± 2.24 μmol g^{-1} of protein	NR	NR	
	Ascites cells	Tissue	6 (adults), 7 (cords)	1.46 μg g^{-1} (KDN); 91.2 μg g^{-1} (Neu5Ac) (NR)	0.16 μg g^{-1} (KDN); 82 μg g^{-1} (Neu5Ac) (NR)	1.3 μg g^{-1} (KDN); 9.2 μg g^{-1} (Neu5Ac) (NR)	301
	Tumour ovary			0.87 μg g^{-1} (KDN); 244 μg g^{-1} (Neu5Ac)	0.10 μg g^{-1} (KDN); 230 μg g^{-1} (Neu5Ac)	0.77 μg g^{-1} (KDN); 14 μg g^{-1} (Neu5Ac)	
	Healthy ovarian tissue			0.56 μg g^{-1} (KDN); 170 μg g^{-1} (Neu5Ac)	0.11 μg g^{-1} (KDN); 135 μg g^{-1} (Neu5Ac)	0.45 μg g^{-1} (KDN); 35 μg g^{-1} (Neu5Ac)	
Throat	Tumour		49 (mean 62.2)	1.8 ± 0.2 μg g^{-1} (KDN); 85.2 ± 7.6 μg g^{-1} (Neu5Ac); 0.03 ± 0.01 μg g^{-1} (Neu5Gc) ($P < 0.01$)	0.1 ± 0.01 μg g^{-1} (KDN); 79.7 ± 7.5 μg g^{-1} (Neu5Ac); 0.02 ± 0.01 μg g^{-1} (Neu5Gc) ($P < 0.01$)	1.7 ± 0.2 μg g^{-1} (KDN); 5.5 ± 0.7 μg g^{-1} (Neu5Ac); 0.01 ± 0.003 μg g^{-1} (Neu5Gc) ($P < 0.01$)	302
	Regional lymph nodes		10 (mean 62.2)	1.2 ± 0.2 μg g^{-1} (KDN); 70.8 ± 7.9 μg g^{-1} (Neu5Ac); 0.015 ± 0.005 μg g^{-1} (Neu5Gc)	0.1 ± 0.01 μg g^{-1} (KDN); 67.2 ± 7.8 μg g^{-1} (Neu5Ac); 0.01 ± 0.004 μg g^{-1} (Neu5Gc)	1.1 ± 0.2 μg g^{-1} (KDN); 3.6 ± 0.5 μg g^{-1} (Neu5Ac); 0.005 ± 0.003 μg g^{-1} (Neu5Gc)	
Lung	Advanced level of lung cancer	Serum	3 (NR)	4839 ± 443 μM	NR	NR	282
	Healthy control		64 (NR)	1821 ± 44 μM	NR	NR	
Breast	Breast cancer with secondary growth		36 (NR)	1773 ± 58 μM (not differentiable)	NR	NR	

Table 1 *(continued)*

Cancers							
	Breast cancer		6 (NR)	2034 ± 135 μM (not differentiable)	NR	NR	
	Healthy women		64 (NR)	1821 ± 44 μM	NR	NR	
Blood forming tissue	Leukemia	Serum (plasma)	16 (NR) (9 (NR))	2780 ± 110 μM (2769 ± 142 μM) ($P < 0.01$)	NR	NR	
	Healthy women		64 (NR) (13 (NR))	1821 ± 44 μM (1715 ± 42 μM)	NR	NR	
Bladder	Freshly diagnosed tumour at bladder	Serum (urine)	5 (NR)	2400 ± 141 μM ($P < 0.01$) (327 ± 6 μM; $0.05 > P > 0.02$)	NR	NR	
	Healthy control		64 (NR, serum) 18 (NR, urine)	1821 ± 44 μM (176 ± 17 μM)	NR	NR	
	Bladder tumour	Urine	60 (50 ± 15 years)	99.80 ± 35.80 μg g^{-1} (*Sia*/creatinine) ($P < 0.001$)	NR	NR	303
	Healthy control		34 (15 ± 8 years)	52.57±15.60 μg g^{-1} (*Sia*/creatinine)	NR	NR	
	Bladder tumour		73 (NR)	92.37 ± 42.55 μg g^{-1} ($P < 0.001$)	NR	NR	304
	Healthy control		34 (NR)	52.57 ± 15.6 μg g^{-1}	NR	NR	

NR: not reported.

mg L^{-1} concentration within 30 min through a biolayer interferometry analysis.[230]

2.3 *Sia* as potential biomarker for human diseases

2.3.1 Metabolic diseases of *Sia*. The metabolic diseases of *Sia* are generally rare in humans. The impaired transport of free Neu5Ac across the lysosomal membrane causes an autosomal recessive lysosomal storage disorder known as Salla disease, which is diagnosed from the high concentration of free Neu5Ac in urine and tissues of the patients compared to the healthy control. The mean concentrations of total and free *Sia* were evident as 163.3 and 90.0 mg g^{-1} of creatinine, respectively, in the urine of the Salla patients (n = 13; 16–61 years old) compared to 52.1 and 5.5 mg g^{-1} of creatinine, respectively, in the urine of healthy control (n = 24; 25–40 years old).[231] Similarly, the impaired transport of free Neu5Ac and gluconic acid across the lysosomal membrane causes infantile sialic acid storage disease to infants. It was reported that even in the normal activities of the lysosomal enzymes, the concentration of free Neu5Ac in the pathogenic fibroblast of a male infant having infantile sialic acid storage disease was elevated to 3.5 ± 0.7 μmol g^{-1} of fresh weight compared to 0.2 ± 0.04 μmol g^{-1} of fresh weight found in the healthy control fibroblast.[232,233] Sialuria is another metabolic disease of *Sia*, when the feed-back mechanism for biosynthesis of *Sia* by the rate-limiting enzyme UDP-*N*-acetylglucosamine-2-epimerase is inhibited, the *Sia* gets stored in the cytoplasm resulting into elevated urinary excretion in the concentration range 5.8–7.2 g Neu5Ac per day and ~40 times higher concentration of free Neu5Ac in the skin fibroblasts.[234] The sialidosis disease is a result of a deficiency of α-neuraminidase enzyme and it leads to an accumulation of sialylated oligosaccharides and glycoproteins in human tissues and urine.[235] The lysosomal protective protein cathepsin-A is essential for the activity of α-neuraminidase enzyme and it delays the proteolysis of β-galactosidase. The defect in the lysosomal protective protein cathepsin-A enzyme complex results into the galactosialidosis disease.[236] The reduced activity of the enzymes *N*-acetylmannosamine kinase and UDP-*N*-acetylglucosamine-2-epimerase leads to impaired biosynthesis of Neu5Ac causing congo-red-positive and rimmed vacuoles depositions in the fibres of the muscles. This is known as hereditary inclusion body myopathy.[237] The blocking of endogenous synthesis of NeuNAc because of a rare genetic disorder stops the production of Neu5Ac in cells. Hence, the concentration of ManNAc increases in urine and plasma resulting in Neu5Ac synthase deficiency disorder. A recent clinical study on oral administration (@150 mg kg^{-1} day^{-1}) of exogenous free Neu5Ac to six Neu5Ac-synthase-deficiency disorder patients (4 adults and 2 children) for 3 days has showed no decrease in the ManNAc concentration in urine, although an increase in the concentration of Neu5Ac was evident in urine. It was attributed to the fact of rapid excretion of Neu5Ac in urine following a rapid adsorption of the same in human body.[238]

2.3.2 The potential of *Sia* as a biomarker of addiction, disease and cancer. Given the critical roles *Sia* plays in many

biological processes, as described in section 2.1, *Sia* and their bioconjugates have received much attention as biomarkers for several diseases. The concentration of *Sia* in human body fluids and organs alters due to occurrence of some diseases, cancers and addiction to tobacco, alcohols, maras and paan. Related case studies are outlined in Table 1 and discussed below. In order to avoid any statistical propagation of errors, we have listed the units and figures as reported by the original authors.

2.3.2.1. Sia as biomarker of harmful addictions. The tobacco specific nitrosamines are metabolites of nicotine formed during the growth, curing, aging and processing of tobaccos. Smoking of burned tobaccos and chewing of smokeless tobaccos *viz.* paan (tobaccos and other ingredients wrapped with betel quid) and Maras powder (extracted from *Nicotiana rustica* Linn tobacco) increase chronic inflammation and concentration of reactive oxygen species in human body. The free *Sia* concentration in the saliva of addicted paan consumers (@1.41 ± 0.65 pack per day for 4.23 ± 3.42 years) was found higher (23.21 ± 18.98 mg L^{-1}; $P < 0.001$) compared to non-consumer controls (18.11 ± 16.5 mg L^{-1}), but the total *Sia* concentration in saliva did not statistically differ upon consumption of paan.[239] On the other hand, the saliva of young group of regular Maras powder consumers (@~20 g per day) showed presence of higher (75.52 ± 6.86 mg L^{-1}; $P < 0.001$) concentration of total *Sia* compared to that of young group of regular tobacco smokers (@~20 cigarettes per day) (62.60 ± 3.91 mg L^{-1}; $P < 0.001$) and unaddicted controls (51.60 ± 3.51 mg L^{-1}).[240]

The activity of sialidase increases in the presence of ethanol and its metabolites such as acetaldehydes, reactive oxygen species and fatty-acid ethyl esters, whereas the activity of sialyltransferases in the Golgi body decreases. Hence, the concentration of total *Sia* in human serum is generally elevated for chronic alcoholics (~1000 g ethanol per week) due to desialylation of apolipoprotein J, cholesteryl ester transfer protein and transferrin.[241] The concentration of total *Sia* in serum of 51 chronic alcoholics was found specifically higher (1.449 ± 0.3019 mM) compared that of 20 non-alcoholics (1.154 ± 0.1702 mM). However, those with or without liver disease could not be statistically differentiated from the measured concentration of total *Sia* in serum.[242] Apolipoprotein J is highly sialylated (~26–28 *Sia* per molecule) glycoprotein found in human plasma and serum and long-term alcohol intake inhibits the hepatic glycolization process of apolipoprotein J. About 28 moles of *Sia* per mole of apolipoprotein J (known as *Sia* index) was found in the blood of non-alcoholic healthy human (n = 20), while the *Sia* index decreased to 12–14 moles of *Sia* per mole of apolipoprotein J in the plasma of alcoholics (n = 15) consuming alcohol @85–90 g per day ($P < 0.001$)[243] and interestingly *Sia* index started partially recovering slowly after stopping alcohol consumption.[244] Although, the concentration of total *Sia* was found to be distinctly elevated in heavy alcoholics, a noticeable difference was observed in the concentration of lipid bound *Sia*, which was not much influenced by the status of the liver cells.[245] The *Sia* index or elevated total *Sia* concentration in the serum of both male and female alcoholics can be used for biomarking alcohol abuse as an alternative or a supplement to the existing laboratory biomarkers *viz.* carbohydrate-deficient transferrin, γ-glutamyltransferase, mean corpuscular volume, aspartate aminotransferase and alanine aminotransferase. *Sia* is highly specific (95.5%) and sensitive (57.7%) as an alcohol abuse biomarker for female alcoholics, where its sensitivity is slightly inferior to γ-glutamyltransferase, comparable to carbohydrate-deficient transferrin and superior to other alcohol biomarkers. However, *Sia* (81.3%) and γ-glutamyltransferase (87.5%) have low specificity to identify male alcoholics compared to carbohydrate-deficient transferrin (100%).[246]

2.3.2.2. Sia as biomarker of disease. The concentration of total Neu5Ac in the cerebrospinal fluid significantly increased to 38–1450 μM for pyogenic meningitis and 32–220 μM for tuberculous meningitis compared to 12–40 μM for healthy controls. The high concentration of free Neu5Ac in the range 80–620 μM is much distinctive for pyogenic meningitis patients compared to healthy control (6–32 μM), which entirely covers the range of free Neu5Ac concentrations found in tuberculous meningitis patients (13–26 μM).[247] The dementia disease *viz.* Alzheimer is difficult to be diagnosed from the neurodegenerative disease *viz.* idiopathic normal pressure hydrocephalus. The elevated concentrations of free Neu5Ac and glycerate simultaneously with demoted concentration of serine and 2-hydroxybutyrate in the cerebrospinal fluid could easily discriminate Alzheimer disease from idiopathic normal pressure hydrocephalus disease. The concentrations of free Neu5Ac in the cerebrospinal fluid of Alzheimer and idiopathic normal pressure hydrocephalus patients were found to be 16.75 ± 3.89 and 13.35 ± 3.2 μM, respectively.[248] *Sia* has antioxidant properties and thus defends oxidative stress in brain cells. The concentration of total *Sia* in the plasma of Alzheimer patients were found to be higher (0.7133 ± 0.0201 ng L^{-1}) compared to that of healthy control (0.5972 ± 0.01866 ng L^{-1}). The total *Sia* concentrations in the plasma of 38 female and 22 male Alzheimer patients were found to be 0.6814 ± 0.14022 and 0.6755 ± 0.1985 ng L^{-1}, respectively.[249] A rare *Sia* syndrome known as cerebellar ataxia is difficult to be diagnosed with free *Sia* as its patients usually have similar free *Sia* concentration in urine, plasma and peripheral nerves compared to healthy controls. However, the free *Sia* concentration in the cerebrospinal fluid of cerebellar ataxia patients were found to be much higher (43.4 ± 11.0 μM) compared to other patients having well-defined neurological symptoms (8.2 ± 4.2 μM) and other diseases (9.9 ± 5.6 μM) including Salla disease (31.3 ± 4.9 μM).[250] In-cell polymerization of *Sia* forms poly*Sia* glycans, which are associated with NCAM and control the molecular interactions during neural development, synaptic plasticity, *etc.* Thus, the concentration of *Sia* in the saliva of children having autism spectrum disorder is significantly less (0.100 ± 0.099 mM)

compared to healthy children (0.160 ± 0.097 mM). The medication of risperidone @0.32 ± 0.013 mg per day to a group of children for 2–6 months slightly increased the *Sia* concentration in saliva to 0.102 ± 0.062 mM.[251] Similar trends are also observed in the concentration of *Sia* in the plasma of children having autism spectrum disorder compared to the healthy control.[252]

Crook *et al.* reported that the total *Sia* concentration in the serum of 20 type-1 diabetic mellitus patients (having 10.6 ± 4.5 mM plasma glucose concentration and taking daily insulin dose of 54.6 ± 21.2 unit) was 2.00 ± 0.37 mM, which was not statistically significant ($P < 0.02$) compared to that of 20 non-diabetic healthy humans (1.98 ± 0.67 mM). The comorbidity of retinopathy to type-1 diabetes mellitus further increased the total *Sia* concentration in serum to 2.38 ± 0.33 mM ($P < 0.01$). The total serum *Sia* concentration of 16 age-gender matched type-1 diabetic mellitus patients, type-2 diabetic mellitus (T2DM) patients and non-diabetic patients were found to be 1.92 ± 0.35 mM ($P < 0.001$), 2.32 ± 0.41 mM and 1.85 ± 0.26 mM ($P < 0.001$), respectively.[253] Nephropathy is a disease which interrupts the usual activity of kidney due to the damage of its cell membrane. The neuraminidase activity increases in the blood of nephropathic patients compared to the healthy individual and it further increases with the comorbidity of T2DM. Diabetic normoalbuminuria and diabetic microalbuminuria are two pre-stages of diabetic nephropathy and those are identified by the daily urinary albumin excretion rate ≤30 and 31–299 mg, respectively. Although total *Sia* concentration in both serum and urine of T2DM patients having either normoalbuminuria or microalbuminuria distinguishably increased compared to the non-diabetic healthy controls, while no correlation in the concentration of lipid bound *Sia* concentration in serum was observed.[254] Furthermore, the higher neuraminidase activity in both serum and urine increased independently due to T2DM and nephropathy diseases compared to healthy controls and therefore, the comorbidity of these two diseases further increased the neuraminidase activity in serum and urine. Hence, the total concentration of *Sia* in serum and urine of T2DM-nephropathic patients, nephropathic patients, T2DM patients and healthy control follow the same decreasing order.[255]

The lipid membrane of RBC becomes damaged due to the oxidative stress in the blood of T2DM patients. Therefore, the lipid peroxidation of RBC increases the concentration of *Sia* in plasma but decreases that on RBC. This effect becomes more pronounced in T2DM patients having nephropathy. Therefore, simultaneous monitoring of lipid peroxidation of RBC and *Sia* level on RBC could be able to predict the appearance of nephropathy in T2DM patients.[256] A large cohort study including 40 years of follow-up on 6718 T2DM patients (3445 men and 3273 women) in the age-group of 47.2 ± 13.0 years showed that the median of *Sia* concentration in blood is 680 mg L^{-1} for both men and women. After adjusting the covariates such as age, body mass index, systolic blood pressure, cholesterol, aspartate aminotransferase and alanine aminotransferase activities and socioeconomic status, it was found that the elevated *Sia* concentration in the blood of T2DM patients was statistically correlated to a higher chance of incidence responsible for diabetes-related hospitalizations and the risk-factor ($P < 0.0001$) was more to women compared to men.[257] The gestational diabetes mellitus disease is associated with higher whole blood viscosity and reduced erythrocyte deformability in the 26th week of pregnancy. Gestational diabetic mellitus patients have blood glucose concentration more than 140 mg dL^{-1} in the '1 h–50 g glucose tolerance test' and having the same exceeding 176 mg dL^{-1} in the next '3 h–100 g oral glucose tolerance test'. The amount of *Sia* in RBC protein increases during the development of the pregnancy, but due to the irregularities in the microcirculation of the blood in gestational diabetic mellitus patients, there exists an imbalance in the amount of *Sia* in the RBC.[129,258] The blood vessel inflammation happened due to Behcet's syndrome and thus because of that the total *Sia* concentration in serum increased to 95.6 ± 15.3 mg dL^{-1} compared to that of patients having uveitis disease (75.8 ± 8.1 mg dL^{-1}) and healthy humans (59.5 ± 7.5 mg dL^{-1}). However, the resolution in the lipid bound *Sia* concentration for diagnosis of Behcet's syndrome and uveitis disease was very poor.[259]

Periodontal disease happens due to the attack of oral bacteria at the gum tissue around the teeth. The recoverable early stage of periodontal disease is known as gingivitis, whereas the destructive acute stage of this disease is known as periodontitis. Zipkin *et al.* reported that the free *Sia* concentration in the parotid and whole saliva of young patients having periodontal disease decreased to 0.0019% and 0.0040%, respectively, compared to those of healthy control (0.0024% and 0.0047%, respectively) owing to its utilization in the bacterial plaque formation. However, the opposite phenomenon was observed for patients having autoimmune rheumatoid arthritis (0.0035% and 0.0053%, respectively).[260] The inflammatory periodontal disease increases the oxidative stress in human body and to defend that oxidative stress, the total *Sia* concentration in human saliva and serum increases owing to higher sialidase activity. Therefore, the total *Sia* concentration in both saliva and serum progressively increases from gingivitis to periodontitis diseases compared to healthy controls.[261–263]

The concentration of *Sia* in plasma increases during and immediately after the event of myocardial infraction. Hence, the total plasma *Sia* concentration, but not the lipid bound *Sia*, was statistically correlated to the event of the myocardial infraction compared to the healthy control. The total plasma *Sia* concentration increased continuously after 1, 2 and 5 day(s) to 0.88 ± 0.29 g L^{-1} ($P < 0.05$), 0.89 ± 0.30 g L^{-1} ($P < 0.05$) and 0.75 ± 0.19 g L^{-1} ($P < 0.05$) compared to that in the plasma of healthy humans (0.62 ± 0.13 g L^{-1}) not encountered the event of myocardial infraction. However, no difference and correlation were observed in the concentration of total serum *Sia* between patients and survivors.[264]

Recently, it was observed that Neu5Ac concentration in serum has similar diagnostic efficacy compared to the common biomarkers *viz.* creatine kinase-MB and troponin I for acute coronary syndrome. Patients having myocardial infarction have higher concentration (median 297 μg L^{-1}) of Neu5Ac in the serum compared to the that of patients having unstable angina pectoris (median 227 μg L^{-1}) and healthy control (median 207 μg L^{-1}), however it cannot statistically differentiate between the ST-elevation and non-ST-elevation myocardial infarction. The cut-off value of Neu5Ac in serum was reposted as 330.5 μg L^{-1} (optimal) and 351.5 μg L^{-1} (high-risk) acute coronary syndrome.[265] A cohort study on 18 429 men and 19 414 women of age 59.5 ± 6.5 years along with 40 years of follow-up revealed that the elevated blood *Sia* concentration (>median 700 mg L^{-1}) and pulse pressure (>median 70 mm Hg) could both independently predict the risk of cardiovascular incident for patients of cardiovascular diseases ($P < 0.0001$).[266] It has recently been reported that Neu5Ac fits well in the cavity of the protein RhoA and Cdc42 in human plasma and activates Rho/Rho-associated coiled-coil containing protein kinase (both 1 and 2), c-Jun *N*-terminal kinase and extracellular signal-regulated kinase signalling pathways in cardiomyocytes, but it does not fit with Rac1 protein and thus it does not follow p38 signalling pathway. Hence, the elevated concentration of Neu5Ac in the serum of patients having normal coronary artery, nonobstructive coronary atherosclerosis, stable angina found in the range 143.70–147.20 μg L^{-1} and it increased to 178.25 μg L^{-1} ($P = 9.3 \times 10^{-3}$) in patients having unstable angina and 182.34 μg L^{-1} ($P = 1.7 \times 10^{-4}$) in patients having acute myocardial infarction.[267] The coronary artery disease also caused desialylation of low-density lipoprotein and increased the total *Sia* concentration in serum of the patients (mean 71.91 (68.33–75.60) mg dL^{-1}; $P < 0.001$) compared to the healthy control (60.76 (57.04–65.92) mg dL^{-1}).[268] Furthermore, total *Sia* concentration in the serum and saliva of periodontitis patients increased in the comorbidity of cardiovascular diseases.[269] The total *Sia* concentration in the serum can also statistically identify ($P < 0.0001$) the induction of carotid atherosclerosis in humans caused by plaque deposition in the brain arteries.[270] Crook *et al.* studied the total and lipid bound serum *Sia* concentrations in the patients having lipoprotein patterns of Fredrickson phenotypes IIa (cholesterolemic) and IIb (hypertriglyceridaemic). The total *Sia* concentration of healthy controls was found to be higher compared to the cholesterolemic patients, but lower compared to the hypertriglyceridaemic patients. However, the lipid bound *Sia* concentration was highest in hypertriglyceridaemic patients (23.0 ± 4.3 mg dL^{-1}) compared to cholesterolemic patients (14.9 ± 4.7 mg dL^{-1}) and healthy controls (12.0 ± 3.2 mg dL^{-1}).[271]

A perforating injury to the eyes after surgical or accidental trauma causes a bilateral granulomatous uveitis known as sympathetic ophthalmitis. The concentration of total *Sia* in the serum of sympathetic ophthalmia patients was significantly higher (120.2 ± 12.6 mg/100 mL; $P < 0.001$) compared to that of the healthy control (67.8 ± 7.9 mg/100 mL). However, the symptoms of traumatic uveitis (71.3 ± 8.4 mg/100 mL; $P > 0.1$) in humans could not be statistically diagnosed compared to healthy controls.[272] The concentration of *Sia* in the serum of patients having overt hypothyroidism (58.2 ± 18.9 mg L^{-1}) was statistically distinctively elevated compared to that observed in the patients having sub-clinical hypothyroidism (37.1 ± 15.5 mg L^{-1}) and healthy individual (38.1 ± 12.0 mg L^{-1}) might be due to the influence of atherogenesis.[273] The inflammation due to the formation of ulcerations in the digestive tract happens in Crohn's disease. The total *Sia* concentration in the serum of patients having active ulcerations was significantly increased to 69.7 ± 9.4 mg dL^{-1} compared to that of the healthy humans (50.3 ± 4.4 mg dL^{-1}). The successful surgery of the ulcerations could decrease it to 54.7 ± 5.5 mg dL^{-1}, which was close to the normal levels.[274]

Sialylation of glycoproteins and glycolipids happens in the liver and thus chronic liver disease *viz.* hepatitis B and C alters the total *Sia* concentration in the serum. The median of *Sia* concentration in serum decreases to 1.32 mM in hepatitis B patients from 1.43 mM in healthy human due to reduced sialyltransferase activity by hepatitis B viral infection. In contrast, the median of *Sia* concentration in serum increases to 1.67 mM in hepatitis C patients due to elevated sialyltransferase activity by hepatitis C viral infection, but it cannot provide any indication about the progress of either hepatitis B or C.[275] The total *Sia* concentration in serum of patients having jaundice with malignant tumours of ampulla of Vater, pancreas, liver, cholecystitis and bile ducts was found 7.95 mg L^{-1} (median) with the *Sia* to total protein ratio 1.20 compared to those of healthy individual (5.97 mg L^{-1} (median); 0.79; $P < 0.001$). The total *Sia* concentration (6.86 mg L^{-1}) and *Sia* to total protein ratio (1.03) are statistically different ($P = 0.041$) for patience having non-malignant jaundice *viz.* choledocholithiasis, cholecystolithiasis, calculous or non-calculous chronic cholecystitis, exacerbation of chronic cholangitis, stricture of the common bile duct.[276] The free *Sia* concentration in serum was reported as a potential biomarker for chronic liver diseases *viz.* alcoholic cirrhosis, although it could not statistically differentiate non-alcoholic patients having cirrhosis and other liver diseases *viz.* hepatitis C, *etc.*[277]

The concentration of pyruvate increases in chronic renal failure and chronic glomerulonephritis. Thus, the biosynthesis of Neu5Ac becomes predominant in renal disease. The total *Sia* concentrations in serum and urine of patients having chronic renal failure and glomerulonephritis are statistically differentiable compared to the healthy control, however the concentration of lipid bound *Sia* does not meet this trend.[278] The kidney can filter free *Sia*, which cannot be reabsorbed there. The concentration of free *Sia* in the plasma of patients having GNE myopathy (glomerular filtration rate 85–155 mL min^{-1} per 1.73 m^2) was not differentiable compared to healthy controls, but the

concentration of free *Sia* in plasma of patients having very low glomerular filtration rate increased drastically to 310–1260 μg L^{-1} due to the glomerular dysfunction.[279]

Pregnant women sometimes suffer from hyperemesis gravidarum disease during the 22nd week of pregnancy and it can be predicted and diagnosed from the elevation of the concentration of total *Sia* in the serum of pregnant patients having hyperemesis gravidarum (28.370 ± 8.69 mg L^{-1}) compared to that in the healthy control group (20.978 ± 9.96 mg L^{-1}) with statistical significance $P < 0.05$.[280] Pregnancy syndrome preeclampsia is another pregnancy related disease resulting to high blood pressure, damage of liver and kidney extending even to neonatal and maternal morbidity and mortality. Owing to high inflammation in preeclampsia patients, *Sia* was thought to be a potential biomarker for this disease. However, studies showed that plasma concentration of *Sia* could not be considered as suitable biomarker compared to neopterin for diagnosing preeclampsia during pregnancy.[281]

The bacterial infection brucellosis caused by the consumption of raw and unpasteurized dairy products increased the total serum *Sia* concentration to 2386 ± 82 μM compared to the healthy controls (1821 ± 44 μM).[282] Oxidative stress in the cell produces reactive oxygen species including hydrogen peroxide, which can be arrested by Neu5Ac and polysia to form a decarboxylation product 4-(acetylamino)-2,4-dideoxy-D-*glycero*-D-galacto-octonic acid (ADOA) at neutral pH ~ 7.5.[283]

It is also observed that long exposure (21.00 ± 11.75 years) of pesticides to non-alcoholic and non-smoker field workers increased the total *Sia* concentration in serum to 44.854 ± 36.48 mg L^{-1} compared to the healthy control (581.95 ± 134.36 mg L^{-1}) due to induction of several diseases originated from the pesticides.[284] Similarly, workers exposed to cadmium in nonferrous smelter for about 8 years had lower *Sia* in RBC membrane (22.6 ± 1.8 mg g^{-1} of protein; $P < 0.01$) compared to the healthy controls (25.8 ± 3.0 mg g^{-1} of protein), however they had elevated concentration of total *Sia* in plasma (761.8 ± 83.5 mg L^{-1}; $P < 0.01$) and urine (276.7 ± 132.3 μg g^{-1} of creatinine; $P < 0.05$) compared to the control group (640.4 ± 70.7 mg L^{-1}; 174.5 ± 70.9 μg g^{-1} of creatinine).[285] Synovial fibroblasts are stromal cells present in synovium joint and they maintain the lubrication and cartilage integrity of the joints. Local inflammation stimulates tumour necrosis factor, which inhibits the activity of glycosyltransferase ST6Gal1 and diminished α2,6-sialylation on synovial fibroblasts leading to rheumatoid arthritis.[286]

The Neu5Gc is not synthesised in the human body, but it is eventually released in human cells mainly through diets of dairy products and animal meats. Interestingly, the human natural immune system does not identify it as fatal "*xeno* (foreign)-antigen", but automatically produces anti-Neu5Gc antibody even during the first year of human life.[287] The concentration of anti-Neu5Gc antibody in the blood of healthy human (n = 120; 20–80 years) is reported as 2.7 ± 0.3 ng μL^{-1}.[288] However, excessive consumption of Neu5Gc rich diets (lamb, pork and beef meats, goat and sheep milks)[289–292] increases the interaction of anti-Neu5Gc antibody with *xeno* Neu5Gc antigen and thus eventually may promote inflammations leading to cancers.[28,293,294]

2.3.2.3. Sia as cancer biomarkers. The oral squamous cell carcinoma is an oral cancer that happens due to excessive smoking of tobacco and drinking alcohol. Sanjay *et al.* reported that the concentrations of both lipid bound and free *Sia* in the saliva of 30 oral squamous cell carcinoma patients were higher (3.02 ± 0.01 and 4.30 ± 0.01 mg dL^{-1}, respectively) compared to 30 healthy humans (2.06 ± 0.01 and 3.40 ± 0.02 mg dL^{-1}, respectively).[295] Other oral cancers, pre-cancers and tumours can be diagnosed from the total serum *Sia* concentrations. Bose *et al.* did not find any statistically significant difference in total *Sia* serum concentration between healthy tobacco consumers (48.52 ± 6.49 mg dL^{-1}) and non-consumers (48.77 ± 5.88 mg dL^{-1}). However, the total serum *Sia* concentration increased to 60.30 ± 7.96 and 59.97 ± 6.03 mg dL^{-1} for pre-cancers leukoplakia and oral sub mucous fibrosis, respectively. It further increased to 94.69 ± 7.26 mg dL^{-1} for patients having oral cancers.[296] The total serum *Sia* concentration also increased in patients having malignant fibrous histiocytoma (85.63 ± 5.45 mg dL^{-1}), tongue and floor cancer (75.01 ± 12.00 mg dL^{-1}), salivary gland tumours (70.58 ± 12.07 mg dL^{-1}), mandibular cancer (69.72 mg dL^{-1}), gingival, palatal and buccal cancer (69.46 ± 11.23 mg dL^{-1}), sarcoma (64.06 ± 5.01 mg dL^{-1}), lip and skin cancer (59.24 ± 12.10 mg dL^{-1}) and benign tumours in oral and maxillofacial region (58.28 ± 8.34 mg dL^{-1}) compared to healthy controls (55.02 ± 7.2 mg dL^{-1}).[298]

The serum concentration of total *Sia* increased to 2.75 ± 0.67 mM ($P < 0.001$) in the case of cholangiocarcinoma patients compared to the healthy controls (1.89 ± 0.46 mM) and further it remained statistically different (2.33 ± 0.69 mM; $P < 0.002$) from the serum concentration of *Sia* for patients having benign hepatobiliary diseases *viz.* liver abscesses, liver cirrhosis, cholecystitis, cholangitis, bile duct stricture and stones, pancreatic stones, gallstones, intrahepatic stones, *etc.*[298] The concentration of bound as well as total *Sia* in the serum of patients having colorectal cancer affecting the colon and rectum significantly increased compared to the healthy control. Therefore, the total *Sia* concentration in serum and *Sia* to total protein ratio can be used to diagnose the induction of colorectal cancer and Dukes' stage.[299]

The monoclonal premalignant endometrial glandular lesion, which is known as endometrial intraepithelial neoplasia, is a pre-stage of endometrial adenocarcinoma. The patients having intraepithelial neoplasia had higher (2.38 ± 0.72 mM and 27.91 ± 8.00 μmol g^{-1} of serum protein) total *Sia* concentration in serum compared to healthy women (1.52 ± 0.25 mM and 19.28 ± 2.24 μmol g^{-1} of protein). However, it could not statistically discriminate endometrial intraepithelial neoplasia from other neoplasia.[300] Inoue *et al.*

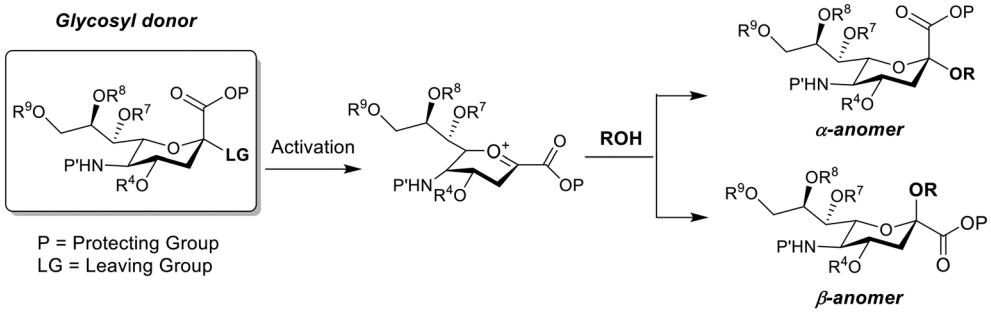

Fig. 4 Schematic representation of a generic sialylation reaction.

first reported by using HPLC-FLD that the ratio of free KDN to free Neu5Ac increased to 6.3% in the ovarian cancerous RBC compared to 1.5% in RBC of healthy human ovarian tissue and it further increased to 16% in the RBC of ascites cells. A positive correlation of the ratio of KDN/Neu5Ac (both in free form) was observed in different types and stages of ovarian cancers. This ratio was found as 18% in a young woman having ovarian mature cystic teratoma, while it was found as 5.3% in the ovarian cyst of a patient having mucinous adenocarcinoma. The ratio significantly changed in the ascites cell having mucinous adenocarcinoma from 0.55% at incidence to 33% in stage IIIa. Further, it was proposed that free KDN in the RBC of ovarian cancer patients might act as oncofetal antigen and thus it overexpressed (1.6 μg free KDN per mL RBC; 0.7 μg free Neu5Ac per mL RBC) in the foetal cord RBC of neonates compared to the maternal RBC of mothers having malignant ovarian cancer (0.9 μg free KDN per mL RBC; 0.4 μg free Neu5Ac per mL RBC).[301] Wang *et al.*, in 2015, by LC-MS/MS found that the overexpression of KDN in human cells was not limited to only ovarian cancer, rather it was also overexpressed in the human body for many types of cancers. They further identified the presence of Neu5Gc in cancer cells. They reported a higher amount of free KDN in throat tumours compared to lymph nodes and furthermore, the overexpression of free KDN in throat cancers even occurred in the absence of lymphatic metastasis. The amount of total KDN also varied upon the tumour sites in the order of hypopharynx (2.4 ± 0.8 μg g^{-1}) > glottis (1.9 ± 0.3 μg g^{-1}) > supraglottic region (1.7 ± 0.3 μg g^{-1}) > sub-glottic region (0.8 ± 0.11 μg g^{-1}).[302] However, the mechanism of synthesis of KDN in the cancerous cells is still unconvinced to date.

The total serum *Sia* concentration of 3 patients having active level of lung cancer was found to be sufficiently high (4839 ± 443 μM) compared to that of healthy controls (1821 ± 44 μM). Thus, total serum *Sia* can be considered as a potential biomarker for lung cancer, but not for breast cancer as the total serum *Sia* concentration of 3 patients having breast cancer and 36 patients having secondary growth were found to be 2034 ± 135 and 1773 ± 58 μM, respectively.[282] On the other hand, the total *Sia* concentrations in both serum and plasma of leukemia patients (2780 ± 110 and 2769 ± 142 μM, respectively) were found to be sufficiently higher compared to healthy humans (1821 ± 44 and 1715 ± 42 μM, respectively).[282] The ratio of total *Sia* to creatinine concentration in the urine was a good marker for bladder tumours as this ratio significantly increased to 99.80 ± 35.80 μg g^{-1} (ref. 303) and 92.37 ± 42.55 μg g^{-1} (ref. 304) for the tumour patients compared to the healthy human (52.57 ± 15.60 μg g^{-1}; $P < 0.001$) and interestingly with the progress of the treatment/therapy this ratio decreased and became closer to the control value indicating the disappearance of the tumour from the bladder.[303,304] Further, a recent study on human glial cell line (1321N1) revealed that *Sia* assisted in the upregulation of interleukine-4,10 gene expressions resulting into metastasis of glioblastoma (an aggressive brain cancer), but in contrast lipopolysaccharide retarded the same.[305]

3. Commercial production of *Sia*

3.1 Extraction of *Sia* from natural resources

The EBN is one of the largest commercial resources of free Neu5Ac. Owing to high content *i.e.*, ~2–5% w/w of extractable Neu5Ac in boiling water, stew of EBN is very popular in eastern countries. In 1977, Martin *et al.* developed a facile method to extract 6.5 g of Neu5Ac from 300 g of EBN simply by refluxing the pulverized EBN in boiling water for 5 h followed by partial-freeze drying pre-concentration and subsequently ultra-filtration through Diaflo XM-50 and Diaflo UM-10 filters. The filtrate was again passed through Dowex 1 × 4 ion-exchange column for further purification and crude Neu5Ac was obtained by lyophilization of the purified filtrate. The crude Neu5Ac was then dissolved in water, passed through Dowex 1 × 4 and lyophilized to achieve pure Neu5Ac.[306] In 2018, Wong *et al.* reported that 48 h of digestion of EBN in a simulated gastric fluid at pH 2 and 37 °C could completely release free Neu5Ac digestible by humans.[307] Nowadays EBN has been used in foods, cosmetics and pharmaceuticals as one of the ingredients. It is being commercially produced and exported worldwide from Thailand, Indonesia, Malaysia and China generating a good revenue. However, commercially produced EBN in swiftlet farms generally contains nitrite, minerals, heavy metals, fungi, mites and bacteria contaminants originating from the farm, packing materials and adulterants such as egg white,

swim bladder, porcine skin, white fungus. Thus direct consumption of commercial EBN has associated risk.[308–311]

κ-Caseinoglycomacropeptide (cGMP) is a C-terminal sialylated phosphorylated glycopeptide having 64 amino acid residues and it is another recognised natural source of *Sia*.[312] Chymosin enzyme releases cGMP during cheese making and then cGMP is isolated from the caseinate hydrolysate. The regular cGMP contains ~81% (w/w) protein and 42–52 mg *Sia* per g of protein, however pre-treatment of bovines with exogenic *Sia* may enrich the *Sia* concentration in cGMP to 190–230 mg *Sia* per g of protein and reduce the protein content to 50–60% (w/w) in cGMP. Hence, mixing of normal or enriched cGMP in infant formula is a means to bring the bovine based infant formula closer to human breast milk.[313]

Sialex,[314] which is a *Sia* concentrate production of Ecological Formulas,[315] is commercial dietary supplement available in the market and it is derived from mucin extract. The commercially available Lacprodan® CGMP-10/20 consisting of ≥95% cGMP, >81% protein concentrate and a very low level of phenylalanine is a good source of protein for people suffering from phenylketonuria.[316]

3.2 Chemical, chemoenzymatic and whole cell biocatalytic synthesis of Neu5Ac

Danishefsky *et al.* reported the stereoselective method for chemical synthesis of Neu5Ac starting from lactic ester by using furan surrogate and boron trifluoride etherate catalyst. However, the yield of Neu5Ac was not encouraging for large scale production.[317] The chemical synthesis of *Sia* glycoconjugates remains a challenging task despite impressive developments in this field which have allowed for very precise control of the stereochemical outcome in *Sia*'s glycosylation reactions with α-anomers typically being the targets with biological relevance (Fig. 4).[318] This often requires the multi-step synthesis of complex Neu5Ac and other *Sia* glycosyl donors.[319,320] Some of these difficulties are related to the unusual structure of the 9-carbon backbone of *Sia*, the hindered tertiary anomeric centre, the presence of an electron-withdrawing carboxyl group directly linked to the anomeric carbon and the lack of neighbouring participating group in *Sia*.[321]

For these reasons, chemoenzymatic strategies have been found to be efficient approaches for the preparation of *Sia* and their derivatives.[322–324] Neu5Ac can be produced in large scale in a two-step enzymatic process, where GlcNAc is initially converted to ManNAc by *N*-acetylglucosamine-2-epimerase (EC 5.1.3.8) under alkaline condition and then ManNAc produces Neu5Ac in the presence of excess pyruvate and sialic acid aldolase. Here, the aqueous alkaline solution (*i.e.*, pH > 11) of GlcNAc mixed with a catalytic amount of epimerase (cloned and developed from porcine kidney[325]) is kept at 25–35 °C for 12–20 h to reach the equilibrium ratio 4 : 1 of GlcNAc : ManNAc followed by neutralisation with acetic acid. The neutralised mixture is diluted with 6 times volume of isopropanol at 20–25 °C for precipitating out GlcNAc and enriching supernatant with ManNAc. This step is usually repeated several times to reach the ratio 1 : 4 (for large scale) or 1 : 10 (for lab scale) of GlcNAc : ManNAc. The ManNAc enriched mixture is incubated at pH 7–8, 20–30 °C for 48 h with sodium pyruvate in the presence of aldolase cloned from TG1[pMexAld] and TG1[pPLAld] strains of *E. coli*. Here, the ratio of ManNAc : pyruvate should be maintained as 1 : 2.5 to get ~95% conversion of ManNAc to Neu5Ac, which is separated from the equilibrium mixture by ion-exchange chromatography.[326] The isolation and purification of Neu5Ac from the equilibrium mixture is indeed a difficult step and thus a membrane reactor containing two embedded enzymes could be an economic way to produce large quantities of Neu5Ac, but it often encounters low production yield.[327]

Table 2 The recommended level of Neu5Ac·2H_2O as an ingredient in commercial food products as per regulation EU/2017/2375 dated on 15/12/2017 (ref. 41)

Category of Food where	Recommended level of Neu5Ac·2H_2O
Infant and follow-on formulae	50 mg L^{-1} of reconstituted formula
Baby foods for infants; processed cereal-based foods; foods for young children	50 mg kg^{-1} of solid food
Special medical purpose food for infants and young children	Should be considered case to case; but in any case, not exceeding the specified level for the category mentioned in this table
Dietary intakes for weight control	200 mg L^{-1} (for liquid); 1.7 g kg^{-1} (for solid)
Foods suitable for people having intolerance to gluten	1.25 g kg^{-1}
Unflavoured pasteurised and sterilised milk; flavoured drinks; fruit juices and nectars; vegetable juices and nectars	50 mg L^{-1}
Table-top sweeteners	8.3 g kg^{-1}
Coffee, tea, herbal and fruit infusions; chicory and its extracts	200 mg kg^{-1}
Cereal bars	500 mg kg^{-1}
Unflavoured and flavoured fermented milk-based products including heat treated products after fermentation	50 mg L^{-1} (for liquid); 400 mg kg^{-1} (for solid)
Dairy analogues including beverage whiteners	50 mg L^{-1} (for liquid); 250 mg kg^{-1} (for solid)
Food supplements in any form for infants (≤1 year old)	55 mg per day
Food supplements in any form for young children (1–2 year(s) old)	130 mg per day
Food supplements in any form for children (3–10 years old)	250 mg per day
Food supplements in any form for general population (>10 years old)	300 mg per day

Furthermore, the use of rhRnBp, which is a recombinant human renin binding protein, in the reaction mixture enhances the activity of both enzymes.[328] The epimerase, which is cloned and developed from porcine kidney, has limited solubility in the aqueous solution. This issue is recently overcome by the strain BT0453 cloned and isolated from *Bacteroides thetaiotaomicron*, which is a human gut symbiont.[329] Bloemendal *et al.* prepared a continuous flow reactor by immobilising aldolase on immobead-150P to increase the process efficiency and conversion factor (up to 82%) of Neu5Ac.[330]

The company Glycom A/S,[331] Denmark, which was acquired by the Royal DSM[332] in 2020, developed (in 2013) a two-step chemical and chemicoenzymatic method to prepare Neu5Ac·2H_2O by avoiding the epimerization reaction. In the first step, *N*-substituted-D-mannosamine was prepared from a chemical reaction of D-fructose with 3–4 equivalent excess of benzylamine *via* Heyns-rearrangement reaction followed by hydrogenation on palladium black catalyst. Then ManNAc was prepared by acetylation of *N*-substituted-D-mannosamine. The second step of this method was the usual chemicoenzymatic aldolase reaction between purified ManNAc and sodium pyruvate. The product Neu5Ac·2H_2O was washed, purified and crystallized several times with acetic acid and acetone.[333]

Whole cell biocatalysis is another prospective means to prepare Neu5Ac on a large scale. This concept was developed with an objective to avoid the tedious extraction of aldolase and epimerase enzymes as well as excessive use of exogeneous pyruvate. Whole cell biocatalysis directly uses a culture medium having an engineered strain of microorganism, which is unable to decompose Neu5Ac compared to natural strain but capable of *in situ* production of both enzymes necessary for the synthesis of Neu5Ac from a precursor (such as GlcNAc) and a carbon source (such as glucose or fructose or glycerol) in the culture medium. The engineered strain *E. coli* NAN8-71/pLT4 (ref. 334) and *E. coli* SA-05/pDTrc-AB/pCDF-pck-ppsA[335] could successfully produce 35 and 18.17 ± 0.27 g L^{-1} Neu5Ac, respectively, by whole cell biocatalysis.

4. Timeline of regulatory affairs relevant to *Sia* in food and nutritional products

Neu5Ac is the most abundant *Sia* in healthy humans and it is biosynthesised endogenously *de novo* in cytosol through an anabolic physiological process. It participates directly and indirectly in many physiological processes especially in the growth and development of neonatal and infants as discussed in Section 2. Either compromised biosynthesis or heavy loss of Neu5Ac at any stage of life can induce harmful effects to humans especially in their early stages of life. In this direction, a strong hypothesis exists to compensate the deficiency of Neu5Ac by an external dietary input, where the dietary *Sia* could be adsorbed in the human body by an action of neuraminidase in the small intestine and colon.[336,337] The European Parliament and Council of European Union issued regulation EC/258/97 in January, 1997 on novel foods and food ingredients.[338] Although, the presence of Neu5Ac in human breast milk and bovine milk derived infant formula was evident by several research groups, the Scientific Committee on Food of the Health and Consumer Protection Directorate-General, European Commission, in May 2003, did not find adequate scientific data to consider Neu5Ac as an essential component for infant and follow-on formula.[339] Thus, Neu5Ac was not included in the global standard for infant formula composition recommended by the international expert group coordinated by the European Society for Paediatric Gastroenterology, Hepatology and Nutrition in 2005.[340] In December 2006, the European Parliament and Council of European Union issued another regulation EC/1924/2006 on the nutrition and health

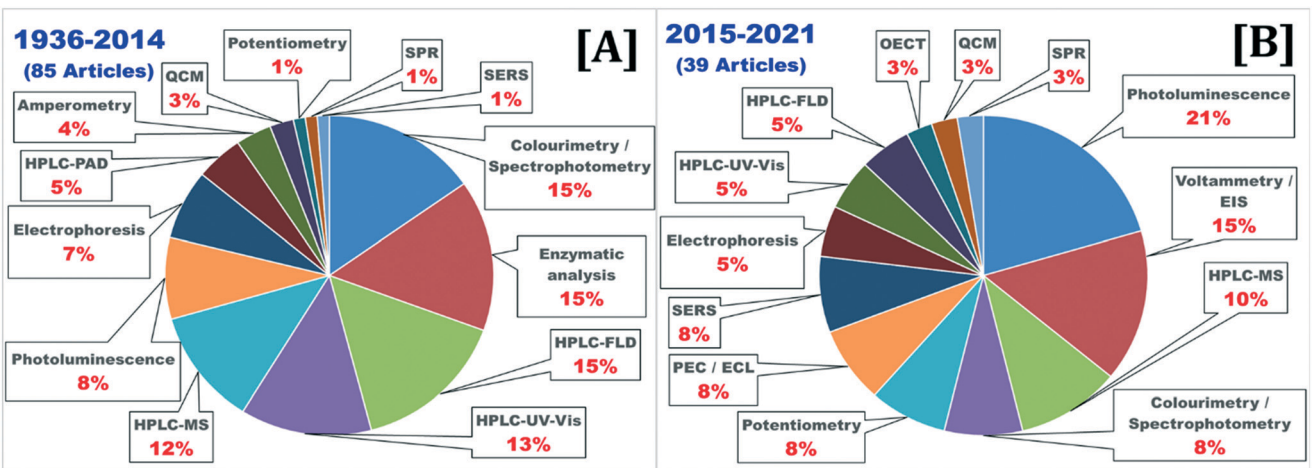

Fig. 5 Statistical analysis of different analytical methods for assay of *Sia* in biological and commercial food samples reported during [A] 1936–2014 and [B] 2015–2021 (September).

claims on foods. Article 13 of this regulation deals with inclusion of compounds adding nutritional value to growth, development and other functions of the body, psychological benefits, slimming effects, *etc.*[341] Following this, the European Commission requested the European Food Safety Authority (EFSA) panel on dietetic products, nutrition and allergies to provide an opinion addressing scientific substantiation of claims for including *Sia* in food products under Article 13 of the regulation EC/1924/2006 owing to its positive role in learning and memory developments (Question No. EFSA-Q-2008-2330 dated on 02/07/2009). The panel evaluated the contemporary relevant information provided by the Member States, but did not find any conclusive evidence of benefits by the dietary intake of *Sia* in relation to learning and memory.[342] Hence, scientific opinion in 2014 on the essential composition of infant and follow-on formula was that although *Sia* was recognised as a source of energy and macronutrients originating from milk, it was not recommended for deliberate addition for uncertainty probability of sub-chronic dietary toxicity effects.[141]

Later in 2014, the sub-chronic dietary toxicity effect of Neu5Ac·2H_2O as prepared by Glycom A/S (briefly mentioned in Section 4.2) was tested on both male and female Sprague–Dawley rats for 13 weeks. No observed adverse effect level for the oral toxicity of Neu5Ac·2H_2O was determined as 974 (for male rats) and 1246 (for female rats) mg kg(body weight)$^{-1}$ day^{-1}. It was also found safe to use up to 2% level (*i.e.*, 1895 mg kg(body weight)$^{-1}$ day^{-1}) of maternal dietary intake. Furthermore, this compound was assessed as non-mutagenic and non-genotoxic through the bacterial-reverse-mutation and *in vitro* mammalian cell micronucleus tests with samples taken from a 23 year old adult male.[343] It was experimentally proven in 2014 that the supplement of *Sia* in the form of either free *Sia*, gangliosides, 3′-sialyllactose, cGMP or their combination during at least one stage of preconception, pregnancy and lactation could improve the health and development of the foetus and/or child.[344]

The progress of research on the health benefits of *Sia*, results on the lack of mutagenic, genotoxic and sub-chronic toxicity effect of *Sia* up to 2% dietary level and industrially viable production of *Sia* could set the scene for its industrial application. Hence, on September 24, 2015, Glycom A/S applied for the pre-market "Generally Recognized as Safe Exemption" approval for Neu5Ac·2H_2O (off-white crystalline powder; purity ≥97%, stable for 36 months without any special package), which was structurally identical to the human milk's free Neu5Ac, to the office of Food Additive Safety in the Food and Drug Administration.[345] The Food Safety Authority of Ireland made an initial assessment on that application in March 2016 and they did not identify any

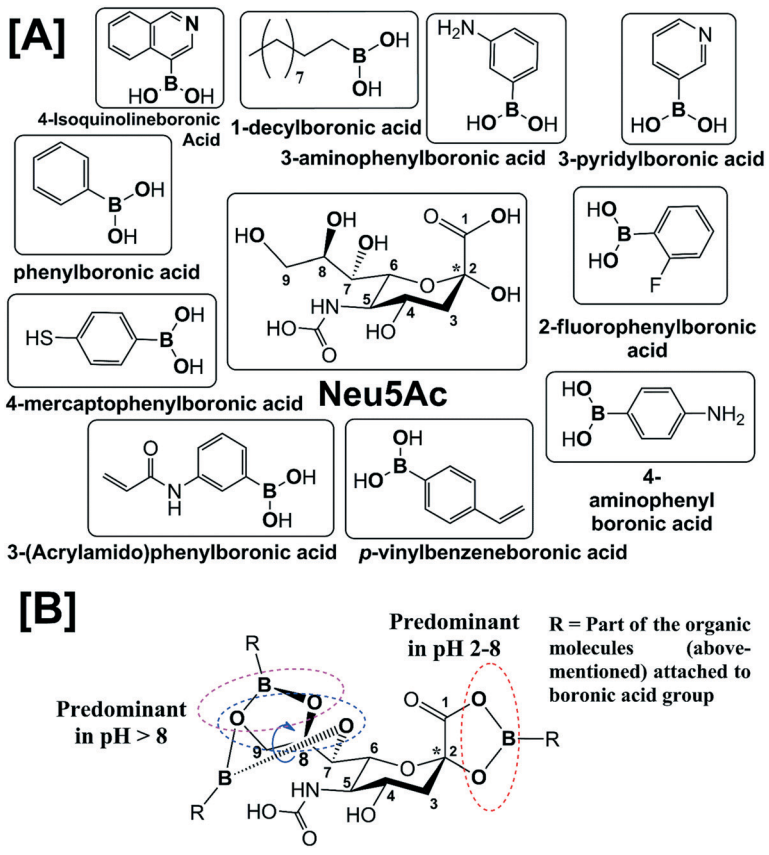

Fig. 6 [A] Types of boronic acid molecules used in different assays of Neu5Ac as discussed in Section 5. [B] Change of binding sites of boronic acid functional group at Neu5Ac in different pH ranges.

safety concern in using of Neu5Ac·2H_2O in food products.[346] Hence, Dossier 187 was issued in April 2016 by the advisory Committee for Novel Foods and Processes on the initial assessment.[347] The EFSA Panel on dietetic products, nutrition and allergies (NDA) in June 2017 published a scientific opinion on the safety of synthetic Neu5Ac·2H_2O as a novel food pursuant to EC regulation 258/97. They found it a safe additive for foods and food supplements at proposed levels suitable for general population above 10 years of age.[348] Following that opinion, the European Commission published a decision EU/2017/2375 on December 15, 2017 authorising use of Neu5Ac·2H_2O in the market as a food ingredient at recommended levels (Table 2) under regulation EC/258/97.[41]

As mentioned in Section 2.2.1, *Sia*-binding adhesin of *Helicobacter pylori* bacteria often targets cell surface gangliosides causing gastric adenocarcinoma. Hence, food ingredients/supplements having anti-adhesive agents have good commercial importance in terms of prevention and therapy of *H. pylori* related diseases. Although, bovine milk and chicken egg white are promising dietary sources of anti-adhesive agents against *H. pylori*, commercial preventive and therapeutic supplements having lactoferrin, fat globule membrane fractions and 3′-sialyllactose sodium salt have high prospect in the food industry.[349–351] In April 2019, Phipps *et al.* reported the toxicological safety studies of 3′-sialyllactose sodium salt[352] and 6′-sialyllactose sodium salt,[353] which were manufactured by Glycom A/S through microbial fermentation process with a genetically engineered strain *E. coli* K-12-DH1-MDO. They performed *in vitro* genotoxicity studies in addition to a 90 day-oral (gavage) toxicity study initiating test doses from 7th day from birth of neonatal rats, which can equivalently represent the development of the reproductive system and central nervous system of new-born human infants. New-born infants consume ~600 mL human milk per day and thus they can consume up to <360 mg per day of 3′-sialyllactose and ~72–324 mg per day of 6′-sialyllactose only from human milk. Therefore, it was proposed to be safer to include 0.2 g L^{-1} of 3′-sialyllactose[352] and 0.4 g L^{-1} of 6′-sialyllactose in reconstituted products.[353] On August 21, 2019, Glycom A/S again applied for the pre-market "Generally Recognized as Safe Exemption" approval for 3′-sialyllactose sodium salt (GRAS Notice No. 880)[354] and 6′-sialyllactose sodium salt (GRAS Notice No. 881)[355] to the office of Food Additive Safety in the Food and Drug Administration. The European Food Safety Authority has recently reviewed both the applications and concluded these materials as safe according to the novel food pursuant regulation EU/2015/2283 for using as food supplements, consumption of which should be avoided on the same day of consuming human and bovine milks, fermented milk-based products, curd cheese, *etc.* so as not to exceed daily intake limits of 3′-sialyllactose and 6′-sialyllactose from other natural sources.[356,357] As per the latest update available on DSM's website, GlyCare™ 3SL (ref. 358) and GlyCare™ 6SL (ref. 359) will be commercially available soon in the market.

Herrmann *et al.* recently reported a COGNIS study (a neurocognitive and immunological study of a new formula for healthy infants) on 220 healthy infants by feeding breast milk (n = 50), standard infant formula (n = 75) and nutrient enriched infant formula (n = 75) for 18 initial months since their birth. The enriched infant formula had a different composition of arachidonic acid (10.2–15.8 mg dL^{-1}), docosahexaenoic acid (10.2–11.2 mg dL^{-1}); gangliosides (9 mg L^{-1}); nucleotides (2.92–2.94 mg dL^{-1}) and sialic acid (105 mg L^{-1}) compared to the standard infant formula. This study revealed that the risk of respiratory tract and gastrointestinal infections was reduced by 30.2% and 32.5%, respectively, in the infants consumed enriched formula compared to the infants consumed standard formula. The enriched infant formula showed almost similar benefits compared to human breast milk.[360] Ma *et al.* have recently published an article stating that oral administration of Neu5Ac @ 0.1–0.3 mg per day to mice for 3 weeks increased the liver weight, gut villus volume, number of goblet cell; decreased activity of *aspartate aminotransferase* and changed the microbial composition and activity in gastrointestinal tract of mice.[361] However, the effect of oral administration of *Sia* in human gastrointestinal tract is yet unreported.

5. Analytical approaches to the assay of *Sia* in biological and commercial food samples

The sections above demonstrate the commercial and biological relevance of *Sia* in relation to the immune system, the central nervous system, pregnancy and lactation, their role in bacterial and viral infections in addition to disease biomarkers. This clearly conveys the medical and commercial importance of accurate determination of *Sia* in human plasma, serum, urine, brain-fluid; commercial dairy products, infant formula; plants tissues and animal organs. It can be seen from Fig. 5[A] that a majority of assays of *Sia* up to 2014 was based on colourimetry-spectrophotometry (15%), enzymatic analysis (15%), high-performance liquid chromatography (HPLC) coupled with fluorescence detection (FLD) (15%), UV-visible detection (UV-vis) (13%) and mass-spectrometry (MS) (12%). Assays with photoluminescence (8%) and electrophoresis (7%) were moderately studied and HPLC coupled with pulse amperometric detection (PAD), amperometry (4%), quartz crystal microbalance (QCM) (3%), potentiometry (1%), SPR (1%) and surface enhanced Raman spectroscopy (SERS) (1%) were introduced in late 90s and early 2000s. In the last 7 years (*i.e.*, 2015–2021), a significant thrust is evident in the development of photoluminescence (21%) and electrochemical assay of *Sia* including voltammetry and electrochemical impedance spectroscopy (EIS) (15%), potentiometry (8%), photoelectrochemistry (PEC) and electrochemiluminescence (ECL) (8%) and organic electrochemical transistor (OECT) (3%) (Fig. 5[B]). The development of colourimetry–spectrophotometry (8%), HPLC-

UV-vis (5%), HPLC-FLD (5%) is significantly decreased, whereas shares of HPLC-MS (10%), electrophoresis (5%) and QCM (3%) remain almost similar. A slight increase in interest of SPR (3%) and SERS (8%) assay methods has been observed in the last 7 years. Citing key observations of 124 landmark publications, this section will briefly discuss the evolution of different assays for *Sia* accounting for the limitations of preceding methods.

5.1 Exploitation of preferential interaction between *Sia* and boronic acid for *Sia*'s assay

The boronic acid functional group, present in compounds known as "*boronlectins*", chemically mimics the action of lectins for high affinity towards the diol of saccharides such as glucose at high pH.[362] It is important to mention that many analytical methods exploited the preferential interactions of boronic acid functional group with *Sia* compared to other sugar molecules. Fig. 6[A] shows the molecules *viz.* 4-isoquinolineboronic acid, phenylboronic acid, 3-aminophenylboronic acid, 4-aminophenylboronic acid, 4-mercaptophenylboronic acid, *p*-vinylbenzeneboronic acid, 2-fluorophenylboronic acid, 1-decylboronic acid, 3-pyridylboronic acid, 3-(acrylamido)phenylboronic acid, *etc.* as mentioned in this review. The insights into specific interaction between Neu5Ac and phenylboronic acids (PBAs) are briefly discussed here. Otsuka *et al.* studied the complexes of free Neu5Ac and 3-(propionamido)-phenylboronic acid in the pH range 4–10 by ^{1}H, ^{11}B, ^{13}C and ^{15}N nuclear magnetic resonance (NMR) spectroscopies. The binding constant (at physiological pH *i.e.*, 7.4) of 3-(propionamido)phenylboronic acid complex with free Neu5Ac (37.6 ± 3.1 M^{-1}) was found to be exceptionally high compared to that of galactose (15.0 ± 2.2 M^{-1}), mannose (8.5 ± 0.9 M^{-1}) and glucose (5.1 ± 1.2 M^{-1}). They proposed that Neu5Ac possessed favourable intramolecular hydrogen bonding interaction between the glycerol moiety (involving –OH groups of C-7, C-8 and C-9) and amide group at C-5 (Fig. 6[A]). The $-B(OH)_2$ functional group of the compound was proposed to interact with the glycerol side chain (C-7, C-8) of Neu5Ac.[363] Later, Djanashvili *et al.*, performed ^{11}B, ^{13}C and ^{17}O NMR spectroscopy of phenylboronic acid (pK_a 10.05 ± 0.03) complexes of glycolic acid, erythronic acid, threonic acid, Neu5Ac and 2α-methyl derivative of Neu5Ac in the pH range 2–12 and found that the stability constant of phenylboronic acid complex (at 25 °C and pH 7.4) of Neu5Ac (11.6 ± 1.9 M^{-1}) is higher compared to that of glycolic acid (1.6 ± 0.2 M^{-1}), erythronic acid (4.4 ± 0.5 M^{-1}) and threonic acid (11.4 ± 1.5 M^{-1}). They proposed, in contradiction to Otsuka *et al.*'s report,[363] that phenylboronic acid interaction should be formed with the α-hydroxycarboxylate unit (*i.e.*, C-1 and C-2) of Neu5Ac in the pH range 2–8 and with the glycerol tail (*i.e.*, C-7/C-8 and C-9) of the side chain at pH > 8, but the involvement of C-7, C-8 glycerol tail was unfavourable due to the *erythro* configuration (Fig. 6[B]).[364] Since then, the actual mechanism of boronic acid and Neu5Ac complexation was unresolved for a long period. Meanwhile it was also reported that this complexation might not occur for bound Neu5Ac in physiological conditions. Recently, Nishitani *et al.* performed ^{11}B, ^{13}C NMR spectroscopy and density functional theory simulations of phenylboronic acid complex with both α- and β-pyranoid structures of Neu5Ac and concluded that phenylboronic acid could bind with α-hydroxycarboxylate unit (*i.e.*, C-1 and C-2)

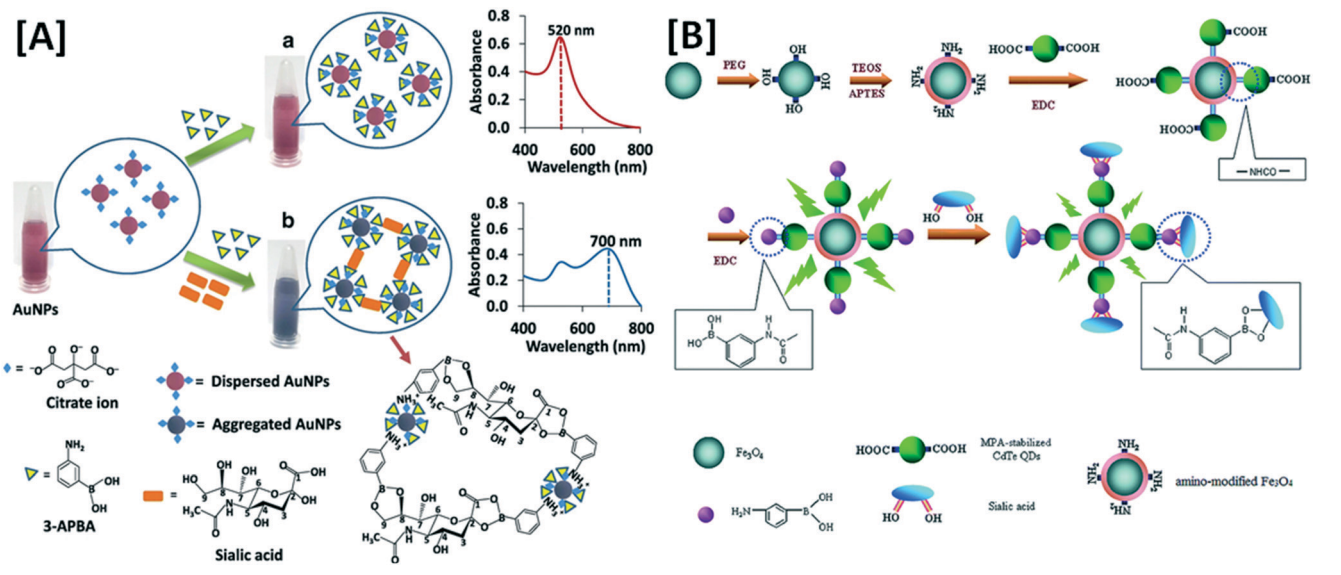

Fig. 7 [A] Ratio-metric spectrophotometric assay of Neu5Ac by using relative absorbances at 520 and 700 nm of the aqueous dispersion of citrate capped-gold nanoparticles (AuNPs) modified with 3-aminophenylboronic acid (3-APBA) before and after incubation with *Sia* (figures reproduced with permission from ref. 379) Copyright 2018 Springer Nature. [B] Fluorometric assay of Neu5Ac by covalently linking both 3-APBA and Fe_3O_4 nanoparticles with CdTe fluorophores through 1-ethyl-3-(3-dimethylaminopropyl)carbodiimide (EDC) (figures reproduced with permission from ref. 388) Copyright 2016 The Royal Society of Chemistry.

of β-pyranoid Neu5Ac, but could not interact with α-pyranoid Neu5Ac, which predominantly exists in membrane bound glycans. Furthermore, the C-2 position is also not available for the phenylboronic acid complexation due to blockage by glycoside bond. Therefore, phenylboronic acid or similar compounds although preferentially bind free *Sia*, they often fail to selectively recognize *Sia* at termini cell-surface glycans.[365] The 4-isoquinolineboronic acid has recently showed highest binding affinity to Neu5Ac (formation constant 5390 ± 190 M^{-1}) compared to common neutral saccharides (glucose, fructose, sorbitol, *etc.*), catechol, ribose-5-P, lactic acid and gluconic acid in aqueous phosphate buffer (pH 3) due to the formation of a ternary quaternary heterocyclic nitrogen containing 4-isoquinolineboronic acid-Neu5Ac-phosphate complex unlike vicinal diol complexes. Thus, at neutral pH, the affinity of 4-isoquinolineboronic acid to catechol, sorbitol, fructose became higher compared to Neu5Ac (formation constant 83 ± 23 M^{-1}) and glucose (formation constant 8.9 ± 1.4 M^{-1}).[366]

5.2 Colourimetry-spectrophotometry

Colourimetry and spectrophotometry were the dominant classical assays of *Sia* in early days. Blix, being one of the discoverers of *Sia*, used direct Ehrlich reagent (*i.e.*, 5% w/v *p*-dimethylaminobenzaldehyde in 1 : 1 v/v ethanol (95% v/v) and concentrated HCl) to identify and quantify total *Sia* from a purple coloured product having absorbance maxima (λ_{max}) at 565 nm.[6] To avoid possible interference from pyrrole derivatives and alkali-treated mucopolysaccharides in direct Ehrlich assay, Klenk *et al.*, the other pioneer of *Sia*, used modified Bial's method (*i.e.*, orcinol, $FeCl_3$, concentrated HCl, 100 °C) producing a red-violet product having λ_{max} at 572 nm; but this colourimetric assay of *Sia* could not avoid the interference of pentose, fructose, sorbose, 2-furaldehyde, uronic acids, keto-hexoses.[4] The modified Dische's assay with 0.5% diphenylamine solution in glacial acetic acid containing 5% H_2SO_4 was also used to quantify total *Sia* from a pink coloured supernatant having λ_{max} at 530 nm, but it also suffered the interference from tryptophan and indole-3-acetic acid.[367,368] Svennerholm proposed resorcinol in HCl with catalytic amount of $CuSO_4$ for colourimetric assay of total *Sia* at λ_{max} 580 nm, but encountered interferences from pentose, keto-hexoses and 2-deoxyhexose.[369] Furthermore, the low molar absorption coefficients (ε) in the range 5300–6900 M^{-1} cm^{-1} (for Neu5Ac) of those chromophores resulted into poor sensitivity of these colorimetric assays. The HIO_4-resorcinol assay followed by extraction of the chromophore (having λ_{max} at 630 nm) in tertiary-butanol significantly improved the sensitivity of colourimetric assay owing to higher value of ε (27 900 M^{-1} cm^{-1} for Nue5Ac).[370] Furthermore, 10–60 μg of total *Sia* was determined by spectrophotometry at λ_{max} 307 nm in 0.01% *o*-phenanthroline solution in 0.1 M NaCl (pH 6.0).[371] To separately quantify free, bound and total *Sia*, Spyridaki *et al.* used different HIO_4 treatments (*i.e.* at 0 °C for 10/30 min for free/total *Sia*; at 37 °C for 35 min for bound *Sia*) before the acidic resorcinol treatment followed by extraction of the chromophore (having λ_{max} at 625 nm) with tertiary-butanol. The linear dynamic range (LDR) and a limit of detection (LOD) for Neu5Ac were also improved to 20–200 μM and 1 μM, respectively, due to an increase of ε to 35 435 M^{-1} cm^{-1}.[372]

Warren and Aminoff independently made a breakthrough in the spectrophotometric assay of *Sia* in 1959. Warren incubated *Sia* for 30 min at 37 °C with 0.2 M HIO_4 in 9 M H_3PO_4 to produce aldehyde, which after removal of excess HIO_4 by 10% $NaAsO_2$ in 0.5 M Na_2SO_4 + 0.1 N H_2SO_4, reacted with 0.6% thiobarbituric acid in 0.5 M Na_2SO_4 while heating at 100 °C for 15 min. The chromophore extracted with cyclohexanone showed a red colour with λ_{max} at 549 nm (ε = 61 000 M^{-1} cm^{-1} for Nue5Ac; 50 000 M^{-1} cm^{-1} for Neu5Gc).[373] Aminoff slightly modified this method by incubating *Sia* for 30 min at 37 °C with 0.025 M HIO_4 in 0.125 N H_2SO_4 at pH 1.2 to produce aldehyde, which after removal of excess HIO_4 by 2% $NaAsO_2$ in 0.5 N HCl, reacted with 0.1 M thiobarbituric acid in water (at pH 9.0) while heating at 100 °C for 15 min. The red colour chromophore extracted with 1-butanol containing 5% (v/v) of 12 N HCl had λ_{max} at 549 nm and ε 70 000 and 51 000 M^{-1} cm^{-1} for Nue5Ac and Neu5Gc, respectively.[374] These two methods were well adopted for several years by different research groups to determine *Sia* in biological samples owing to high sensitivity of assay by virtue of high ε values. However, both methods were limited to only free *Sia* and suffered interference from 2-keto-3-deoxygluconic acid and hexoses. Furthermore, these methods failed to produce reliable values in the concentration range 0.l–1.0 μg of *Sia*. The LDR of colourimetric assay of *Sia* was brought down to 225 ng–3.09 μg by modifying the thiobarbituric acid treatment followed by extraction steps of Aminoff. There, the aldehyde was allowed to react with 0.1 M thiobarbituric acid (at pH 9.0) in a boiling water bath for 10 min followed by cooling in an ice bath for 2 min. Then the reaction mixture was incubated in water bath at 37 °C for 2 min and the chromophore was extracted with 1-butanol containing 5.7% (v/v) of 10.5 N HCl.[375]

Massamiri *et al.* developed a 3-methyl-2-benzothiazolone hydrazone based method avoiding acid hydrolysis pre-treatment step. In this method, biological samples were shaken in 0.05–2.00 mM $NaIO_4$ in phosphate buffer saline (PBS) at pH 7.4 in the dark for 15 min at 4 °C. Then formaldehyde in equivalent amount to bound *Sia* was released in the solution. The supernatant was successively treated with 10% (w/v) $ZnSO_4$ in 1 N NaOH for 5 min and 0.01 M 3-methyl-2-benzothiazolone hydrazone in phosphate buffer for 20 min at room temperature. Then 5% (w/v) $FeCl_3$ was added into the reaction mixture, vigorously shaken and left for 15 min before the absorbance was read at 625 nm. However, this assay was not specific for *Sia* as 2-deoxyribose and hexoses interfered with the measurement and there was a chance of over-estimation of *Sia* due to the presence of endogenous formaldehyde.[376] Later, in another spectrophotometric assay, *Sia* was reacted with 2% (w/v)

ninhydrin in a solution of DMSO-lithium acetate buffer (at pH 5.2) and glacial acetic acid on a boiling water bath for 10 min followed by cooling in ice-bath for 2 min. Its chromophore showed λ_{max} at 470 nm (ε = 66 400 M^{-1} cm^{-1} for Nue5Ac). In this method the interference from L-tryptophan (having λ_{max} at 385 nm), L-cystine (having λ_{max} at 485 nm), L-proline (having λ_{max} at 510 nm) and L-cysteine (having λ_{max} at 560 nm) could be eliminated by using a small column of cation-exchange resin before the spectrometric assay.[377] This method, with a little modification, has recently been used for the spectrophotometry-based flow batch analysis of *Sia* in the whole, semi-skimmed and skimmed milks. The mixture of *Sia* in sample/standard, 0.1 M HCl and 0.16 M ninhydrin of equal volume was pumped into the batch flow chamber and mixed for 5 min at 75 °C, pH 1.6 and the absorbance of the product was recorded at 470 nm. The LDR and LOD of the method were reported as 1.0–10.0 mg L^{-1} and 0.239 mg L^{-1}, respectively, for Nue5Ac with no significant interference from L-cystine, L-cystein, L-tryptophan and ammonia.[378]

No significant progress, except two recent works reported by Jayeoye *et al.*, was observed in the development of spectrophotometric assays for the determination of *Sia* in present times. Aqueous suspension of gold nanoparticles (AuNPs) of average diameter 13 nm was prepared by citric acid reduction method and 3-aminophenylboronic acid was electrostatically assembled on the surface of AuNPs in 1 mM phosphate buffer solution at pH 5.6. The dispersion of boronic acid modified AuNPs was of red wine colour having λ_{max} at 520 nm (ε = 2.7 × 10^8 M^{-1} cm^{-1}), which after incubation with *Sia* for 5 min at room temperature changed to blue with appearance of a new absorbance peak at 700 nm due to aggregation of AuNPs linked through *Sia* (Fig. 7[A]). Hence, the ratio of absorbances at 700 nm to 520 nm was used for spectrophotometric assay of *Sia* in the LDR 0.15–1.0 mM and LOD 0.06 mM without significant interference from glucose, fructose, galactose, mannose and disaccharide sucrose. This assay was successfully tested with known concentration of spiked *Sia* in the simulated human saliva.[379] Later, the LOD of this assay was further improved to 35 μM with two LDRs 80–250 and 300–700 μM by modifying the surface of AuNPs with dithiobis(succinimidylpropionate) through a ligand exchange mechanism at room temperature without changing the basic UV-vis absorbance profile of AuNPs having λ_{max} at 520 nm. Again no significant interference was observed from glucose, mannose, lactose, fructose, sucrose, maltose and galactose in this assay, which was successfully tested with *Sia* spiked in the commercial human serum extracted from human male AB plasma.[380]

Here, we summarize the perspective of colourimetric and spectrophotometric assay of *Sia*. For this purpose, we have compared the LDR and LOD mentioned in either M or g L^{-1} units in the above-mentioned publications considering 309.273 g mol^{-1} molar mass of Neu5Ac for interconversion of units, if required. The AuNPs-boronic acid based spectrophotometric method, although recently developed, could not produce lower LOD compared to classical dye-based colourimetric assay, but it minimized the interferences of other saccharides in the quantification of Neu5Ac. The lowest LOD reported for AuNPs-boronic acid based spectrophotometric assay was 35 μM having two separate LDRs of 80–250 and 300–700 μM.[380] On the other hand, acidic ninhydrin dye based flow-batched spectrophotometric assay could provide lowest LOD of 0.77 μM (converted from 0.239 mg L^{-1}) with narrow LDR of 3.23–32.3 μM (converted from 1.0–10.0 mg L^{-1}) without interference from L-cystine, L-cystein, L-tryptophan and ammonia.[378] Therefore, enough scope exists to develop new ultrasensitive spectrophotometric assay of *Sia* in real biological and food samples.

5.3 Photoluminescence

Photoluminescence assay showed higher sensitivity compared to spectrophotometric or colorimetric assay of *Sia*.[381,382] In the reaction of both bound and free *Sia* with 5 mM 3,5-diaminobenzoic acid in 0.125 N HCl at 100 °C for 16 h, a green fluorescent product having excitation and photoluminescence maxima at 405 and 510 nm, respectively, was produced. While this fluorometric assay produced a good LDR of 0.15–2.0 μmol of *Sia* per 50 μL of 3,5-diaminobenzoic acid, it could not overcome strong interference of hexoses. Furthermore, dihydrochloride salt of 3,5-diaminobenzoic acid was commercially unavailable and thus had to be prepared from the commercially available precursors.[381] Hammond followed the Aminoff's thiobarbituric acid process, but instead of measuring absorbance at 549 nm, the 1-butanol extract was excited at 550 nm. It emitted a fluorescence light having intensity peak at 565 nm suitable for fluorometric assay of Neu5Ac with LDR 10–250 ng (*i.e.*, 32–800 pmol), but suffered interference of 2-deoxyribose.[382] In contemporary times, another fluorometric assay was reported for the reaction of free *Sia* with pyridoxamine dihydrochloride, zinc acetate and pyridine in methanol at 70 °C for 45 min. The excitation of the fluorophore with 395 nm light resulted to a photoluminescence having intensity peak at 470 nm. This assay was suitable for the LDR 0.1–10.0 μg of free Nue5Ac, but α-ketoacids interfered in the measurement.[383] On the other hand, mild oxidation of free *Sia* by 1 mM $NaIO_4$ in PBS (pH 7.2) at 4 °C for 15 min in the dark could quantitatively produce formaldehyde, which after removal of excess periodate by 2% $NaAsO_2$ in 0.5 N HCl, was allowed to incubate at 60 °C for 10 min with a mixture of acetylacetone, ammonium acetate, glacial acetic acid and distilled water. Free Nue5Ac was assayed from the fluorescence intensity of a light-yellow fluorophore (having excitation and luminescence maxima at 410 and 510 nm, respectively) with the LDR of 2–10 μg and a LOD of 0.1 μg (0.3 nmol). *o*-Acetylated (at either C-8 or C-9 position) *Sia* could not be oxidized by $NaIO_4$, thus *o*-deacetylation by 0.1 M NaOH should be a pre-treatment step for this assay, which suffered interference from endogenous pyruvate.[384] In 2008, Matsuno *et al.* reported a comparatively less hazardous fluorometric assay for both free and bound *Sia* by oxidising with 10 mM $NaIO_4$ at 0 °C for 45 min to quantitatively produce formaldehyde followed by removal of

excess periodate by reaction with 50 mM $Na_2S_2O_3$ solution. The fluorophore, having excitation and luminescence maxima at 388 and 471 nm, respectively, was produced from the reaction of formaldehyde with 4 M ammonium acetate (at pH 7.5) and ethanolic solution of 0.1 M acetoacetanilide for 10 min at room temperature. The LDR and LOD of this fluorometric assay of Nue5Ac were reported as 0.3–27 nmol and 4 pmol, respectively. However, this photoluminescence assay suffered a strong interference from the glucose derived sorbitol, which could eventually produce two equivalents of formaldehydes.[385] Alves *et al.* reported a solid-phase fluorometric assay of Nue5Ac with LDR and LOD 0.4–2000.0 and 0.4 mg L^{-1}, respectively, by incubating Nue5Ac with Eu(III)-coordinated silica modified by sodium thenoyltrifluoroacetonate in ethanol (carbonate buffer pH 6) for 3 min and measuring the fluorescence intensity at 615 nm for a photoexcitation at 345 nm.[386]

Several photoluminescence assays based on phenylboronic acid linked established fluorophores *viz.* CdTe, fluorescein isothiocyanate, *etc.* exploited the preferential affinity of phenylboronic acid to Nue5Ac. Wang *et al.* covalently conjugated CdTe (excitation and fluorescence maxima at 330 and 502 nm, respectively) with *Sambucus nigra* bark lectin, which specifically recognised *Sia* and increased the fluorescence intensity. The LDR and LOD of this assay were reported as 12–680 and 0.67 ng mL^{-1}, respectively. This method was successfully implemented to quantify *Sia* in different egg products *viz.* whole egg, yolk and egg white powders, egg noodles, cake and steamed bun.[387] Wang *et al.*, on the one hand, prepared amine-functionalized magnetic Fe_3O_4 nanoparticles (NH_2–Fe_3O_4) by modifying polyethylene glycol 400 coated Fe_3O_4 nanoparticles with 3-aminopropyl triethoxysilane and tetraethylorthosilicate. On the other hand, they prepared fluorescent 3-mercaptopropionic acid capped CdTe quantum dots from a solution of Cd(II), NaHTe and 3-mercaptopropionic acid. Then they covalently linked 3-mercaptopropionic acid capped CdTe quantum dots on modified Fe_3O_4 nanoparticles to prepare the fluorescence probe for assay of *Sia* (Fig. 7[B]). The probe was incubated with Nue5Ac in 5 mM PBS (pH 7.4) at 37 °C for 3 h and magnetically separated from the reaction mixture, washed and dispersed again in 5 mM PBS (pH 7.4) for measuring the fluorescence intensity at ~550 nm. The fluorescence intensity of the probe was linearly quenched with the concentration of Nue5Ac resulting LDR and LOD 0.05–1.5 mg mL^{-1} and 16 μg mL^{-1} without any significant interference from Na^+, K^+, Mg^{2+}, Ca^{2+}, Zn^{2+}, Cu^{2+}, Hg^{2+}, Pb^{2+}, Mn^{2+}, Fe^{3+}, dopamine, glucose, galactose, mannose and fructose. Hence, this assay of Nue5Ac was validated with commercial infant formula.[388] A comparatively simpler strategy was proposed by Hao *et al.*, where aminophenylboronic acid was covalently linked to fluorescein isothiocyanate producing the fluorescence probe having excitation and luminescence intensity peak at 493 and 515 nm, respectively, in Tris-HCl (pH 7.40). The fluorescence intensity was completely quenched in the presence of 90 mg reduced graphene oxide dispersion due to the Förster resonance energy transfer from fluorescence probe stacks to reduced graphene oxide. The fluorescence intensity was regained, and simultaneously reduced graphene oxide was precipitated out upon incubation of this dispersion with Nue5Ac at room temperature for 2–3 h owing to the higher affinity of aminophenylboronic acid modified fluorescein isothiocyanate to Nue5Ac than reduced graphene oxide. The LDR and LOD of this assay for Neu5Ac were reported as 0.5–5.0 and 0.044 mM, respectively.[389]

Xu *et al.* hydrothermally synthesised boronic-acid-functionalized carbon dots of average diameter 3.5 nm having luminescence maxima at 390 nm by heating the aqueous solution of 3-pyridylboronic acid at 160 °C for 8 h and used it for fluorometric assay of Nue5Ac by incubating at room temperature for 4 min with Neu5Ac in 10 mM PBS (pH = 5.5) from the decrease of fluorescence intensity linearly to concentration of Nue5Ac in the LDR 0.08–4.0 mM. This method could detect Nue5Ac down to 54 μM without any interference from glucose, mannose and galactose. Hence, this fluorometric assay was validated to quantify Nue5Ac in real human serum samples.[390] Wang *et al.* have recently reported a similar methodology by using dispersion of fluorescent B-, N-doped carbon dots of diameter 2–7 nm having excitation and luminescent maxima at 560 and 645 nm (quantum yield 8.56% with respect to rhodamin 6G), respectively, in 10 mM glycine buffer (pH 5.5). B-, N-doped carbon dots were prepared from a mixture of 10 : 1 (w/w) *o*-phenylenediamine : 3-aminophenylboronic acid (w : w 10 : 1) by hydrothermal synthesis at 160 °C for 6 h. The fluorescence intensity of the dispersion at 645 nm increased upon incubation with Nue5Ac at 37 °C for 30 min because of the favourable complex formation between *Sia* and boronic acid groups present on the surface of B-, N-doped carbon dots. The LDR and LOD of Neu5Ac assay were reported as 0.02–1.0 mM and 9.24 μM, respectively, without any significant interference from urea, isoleucine, proline, galactose, maltose, Na^+, K^+, Ca^{2+}, NH_4^+, SCN^- and Cl^-. Thus, the assay was validated for quantifying spiked known amount of Nue5Ac in simulated human saliva samples.[391]

Wang *et al.* have recently developed an indicator-displacement photoluminescence assay for *Sia* by preparing fluorescein sodium dye anchored covalent organic framework, TpPa-1, as fluorescent indicator having excitation and luminescence maxima at 437 and 514 nm, respectively. A hydrogel mould of the fluorescent indicator was prepared with sodium alginate and was immersed in $Cr(NO_3)_3$ solution for 2 h and then washed thoroughly. The luminescence of the fluorescent indicator was significantly quenched by Cr^{3+} by virtue of strong indicator-receptor interaction. The fluorescence intensity of the indicator hydrogel was partially regained in the presence of *Sia* in neutral water due to partial displacement of Cr^{3+} from the hydrogel matrix to the solution by the electrostatic attraction to negatively charged *Sia* present in the solution. The LDR and LOD of this fluorometric assay were reported as 10 nM–10 mM (in logarithmic scale) and 7.08 nM, respectively, with no significant interference from $CaCl_2$, $MgCl_2$, KCl, NaCl, $NaHCO_3$, glucose, L-proline and urea. An on–off–on sequential action of this method was validated for quantifying *Sia* in real human serum samples.[392] Yu *et al.* have recently reported the use of photoluminescent UiO–66-NH_2@B(OH)$_2$ (having excitation and luminescence maxima at 320 and ~470 nm, respectively) to determine Neu5Ac in the LDR 0.05–2.5 mM with

a LOD of 0.025 mM owing to the preferential interaction of the diol of Neu5Ac with the boronic acid functional group at pH 7.4.[393] A molecular logic-gate has also been successfully designed by incorporating 4-carboxyphenylboronic acid in $Eu(atpt)_{1.5}(phen)(H_2O)_n$ metal–organic-framework to detect *Sia* from the fluorescence intensity ratio at $\lambda_{470}/\lambda_{614}$ nm.[394] Wang *et al.* prepared a fluorescent polydiacetylene based liposome type structure by UV-light assisted polymerization with three monomers *viz.* 10,12-pentacosadiynoic acid-phenylboronic acid (as *Sia* recognising unit), 10,12-pentacosadiynoic acid-1,8-naphthalimide (as fluorescent unit with excitation and luminescence maxima at 420 and 535 nm, respectively) and 10,12-pentacosadiynoic acid-ethyl acrylate with molar ratio 4.5 : 1.0 : 4.5 in methylene chloride containing 10% methyl alcohol (v/v). The prepared liposome suffered from self-quenching fluorescence due to transfer of energy from 1,8-naphthalimide unit to polydiacetylene backbone. The pendent side chain configuration was disturbed in the presence of *Sia*-boronic acid complex and the original fluorescence of 1,8-naphthalimide was restored. This assay reported LDR up to 0.4 mM with a LOD of 14 μM with little spectral deformation in the presence of glucose, galactose and mannose.[395] Yue *et al.* used 6-carboxyfluorescein (excitation and emission maxima at 494 and 520 nm, respectively) tagged aptamer (5′-6-carboxyfluorescein-TAGGGAATTCGTCGACGGAT-3) to quantify Neu5Ac in LDR 20–1000 nM with tolerable interference of Neu5Gc, KDN, glucose, sucrose and maltose. The aptamer tagged fluorophore lost photoluminescence after adsorbing on the dispersed graphene oxide in solution, but Neu5Ac brought the aptamers back into the solution due their preferential affinity resulting into the development of the photoluminescence of 6-carboxyfluorescein.[396]

Binding of different family members of *Sia* to lactose-specific lectin–peanut agglutinin slightly varies with respect to the core composition of binding domain Asp–Pro–Ala–Asp peptides. A panel consisting of 6 types of dipeptide combinations labelled with fluorescein (excitation and emission maxima at 470 and 514 nm, respectively) could discriminate Neu5Ac, Neu5Gc, KDN, *N*-acetylneuraminic acid methyl ester, *N*-acetyl-2,3-didehydro-2-deoxyneuraminic acid, 2,4,7,8,9-penta-*O*Ac-*N*-acetylneuraminic acid methyl ester.[397] Furthermore, the fluorescence intensity of pyrene-conjugated-histidine (excitation and emission maxima at 330 and 385/410 nm, respectively) decreased in the presence of Neu5Ac and 2,3′-sialyllactose due to hindrance in gelation, which usually occurred in the presence of other monosaccharides and sialic acid analogues. The fluorometric dynamics of gel-formation of pyrene-conjugated-histidine can be used to recognise Neu5Ac in complex matrix.[398] Neu5Ac significantly enhanced the fluorescence intensity (at 658.8 nm) of phenylboronic acid functionalised squarylium cyanine dyes having shorter alkyl chain due to formation of J-aggregate (Nue5Ac : dye as 2 : 1) complex through multipoint interaction of dye with Neu5Ac compared to other monosaccharides. On the other hand, no such enhancement was observed by Neu5Ac for similar dyes having longer alkyl chain due to formation of H-aggregate (Nue5Ac : dye as 1 : 1) complex similar to other monosaccharides. This method is useful to discriminate Neu5Ac in biological samples.[399]

Here, we summarize the perspective of photoluminescence assay of *Sia*. For this purpose, we have compared the LDR and LOD mentioned in either M or g L^{-1} units in the above-mentioned publications considering 309.273 g mol^{-1} molar mass of Neu5Ac for interconversion of units, if required. Most of the photoluminescence assays of *Sia* reported LDR within ~20–5000 μM with LOD ~10–60 μM.[388–391,393] The solid-phase fluorometric assay could provide a wide LDR 1.3–6500 μM with a LOD of 1.3 μM.[386] The ultra-sensitive Cr(III)-displacement fluorometric assay with fluorescein sodium dye anchored TpPa-1 could provide a wide LDR of 10 nM–10 mM (although in logarithmic scale) with sufficiently low LOD (7.08 nM) without interference from L-proline and urea.[392] However, the fluorescent CdTe quantum dots modified with *Sambucus nigra* bark lectin could provide lowest LOD (2.1 nM; converted from 0.67 ng mL^{-1}) for fluorometric assay of *Sia* with a moderately wide LDR 3.88 nM–2.2 μM (converted from 12–680 ng mL^{-1}) in linear scale without interference in commercial egg products.[387] Therefore, the research towards the development of ultrasensitive photoluminescence assay of *Sia* in real biological and food samples is open to further investigations.

5.4 Enzymatic analysis

The enzymatic reactions of *Sia* can produce secondary assayable chemicals *viz.* H_2O_2, reduced nicotinamide adenine dinucleotide (NADH), *etc.* Exo-α-sialidase can release *Sia* from the terminal residue of sialylated glycoproteins, glycolipids and oligosaccharides having α2,3-, α2,6- and α-2,8-glycosidic bonds (reaction 1). However, 4*O*-acetylated *Sia* is irresponsive to this enzyme.[400] Sialic acid aldolase can reversibly convert Neu5Ac to ManNAc and pyruvate during incubation at 37 °C and pH 7.1 for 15 min (reaction 2). At equilibrium, the molar ratio of Neu5Ac : ManNAc : pyruvate attained 1 : 9 : 9 with an equilibrium constant 0.064 ± 0.020 M at 37 °C.[401,402] The optimum pH and Michaelis constant of the reaction were reported as 7.1–7.3 and 3.3×10^{-3} M, respectively. Neu5Ac almost completely cleaved at concentrations <1 mM, but a significant amount of un-reacted Neu5Ac remained in the solution at equilibrium at higher concentrations. The enzymatic cleavage reaction could be stopped by increasing the temperature of the incubated solution to 100 °C for 2 min.[403] This enzymatic reaction is also equally effective for Neu5Gc producing *N*-glycolyl-D-mannosamine and pyruvate under similar condition but is ineffective for *O*-acetylated *Sia*. Therefore, Neu5Ac could be quantitatively assayed indirectly through either of four different options by measuring either ManNAc or pyruvate.

$$\text{Sialylated Glycoproteins/Glycolipids/Oligosaccharides} \xrightarrow{\textit{Exo}\text{-}\alpha\text{-sialidase(EC:3.2.1.18)}} \text{Free Neu5Ac/Nue5Gc} \quad \text{(Reaction 1)}$$

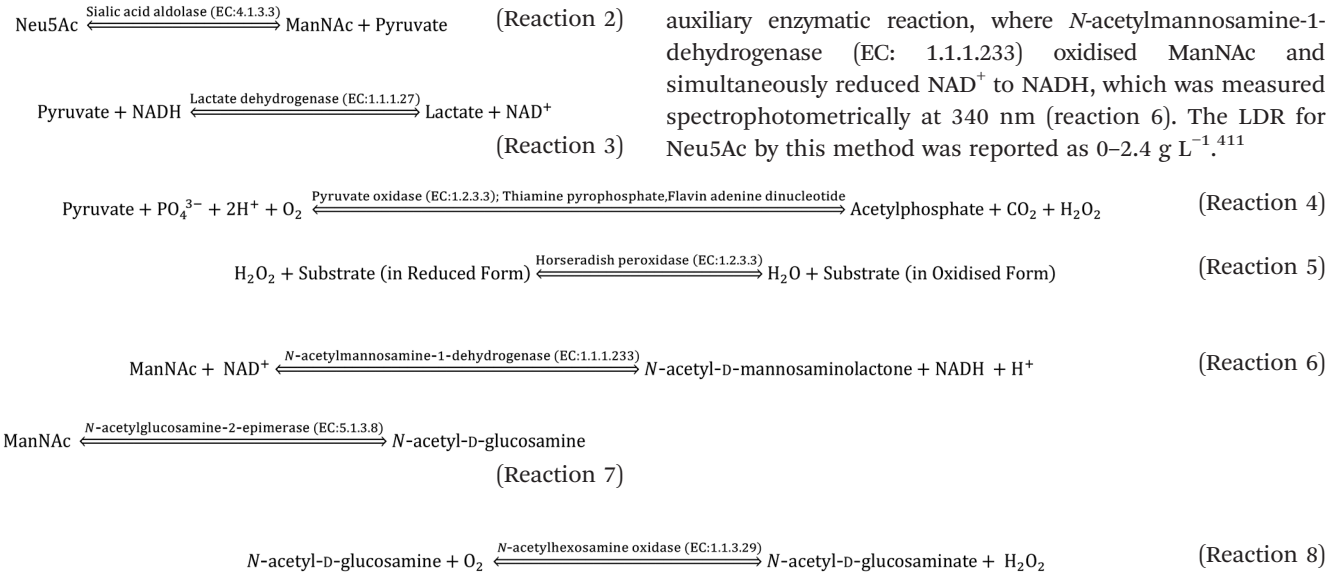

Option 1. The first option is to measure pyruvate by spectrophotometry or fluorometry through the auxiliary enzymatic reaction of lactate dehydrogenase (EC: 1.1.1.27) and NADH (previously known as reduced diphosphopyridine nucleotide) substrate. Lactate dehydrogenase enzymatically reduces pyruvate to lactate and at the same time, the co-reactant NADH is oxidised to NAD^+ (previously known as oxidised diphosphopyridine nucleotide) (reaction 3). Lactate dehydrogenase solution has UV-B absorbance with maxima at 285 nm, while NADH has both UV-C and UV-A absorbances with maxima at 250 and 340 nm ($\varepsilon_{340} = 6.22 \times 10^3\ M^{-1}\ cm^{-1}$). Furthermore, NADH exhibits blue colour fluorescence with broad luminescence peak ~440–460 nm upon exciting with a light source at 340 nm.[404] Although NAD^+ has intrinsic UV-C absorbance with λ_{max} at 250 nm, it does not absorb light above 300 nm.[405] Therefore, the concentration of pyruvate produced after the aldolase reaction can be assayed from the difference of peak intensities of absorbance (measured at 340 nm) or fluorescence (measured at 446 nm) of NADH just before and after the reaction with Lactate dehydrogenase. However, the endogenous pyruvate and enzymatic impurity *viz.* NADH oxidase interfere in this assay.[406,407]

Option 2. Pyruvate oxidase (EC: 1.2.3.3) quantitatively produces H_2O_2 from pyruvate in the presence of dissolved oxygen, inorganic phosphate, thiamine pyrophosphate and flavin adenine dinucleotide (reaction 4). The produced H_2O_2 can be measured spectrophotometrically from the concentration of oxidised form of an auxiliary substrate by the action of horseradish peroxidase (EC: 1.2.3.3). The frequently used auxiliary substrate include 4-aminoantipyrine along with 4-chlorophenol (probing at 505 nm),[408] *N*-ethyl-*N*-(3-sulfopropyl)-3,5-dimethoxyaniline (probing at 590 nm),[409] *N*-ethyl-*N*-2-hydroxyethyl-3-toluidine,[410] 10-acetyl-3,7-dihydroxyphenoxazine (probing at 570 nm), *etc.* (reaction 5).

Option 3. The first two options suffered from the interference of endogenous pyruvate and that could be eliminated by an auxiliary enzymatic reaction, where *N*-acetylmannosamine-1-dehydrogenase (EC: 1.1.1.233) oxidised ManNAc and simultaneously reduced NAD^+ to NADH, which was measured spectrophotometrically at 340 nm (reaction 6). The LDR for Neu5Ac by this method was reported as 0–2.4 g L^{-1}.[411]

Option 4. H_2O_2 could be quantitatively produced by the successive enzymatic reactions of ManNAc with *N*-acetylglucosamine-2-epimerase and *N*-acetylhexosamine oxidase (EC: 1.1.3.29) in the presence of dissolved oxygen (reaction 7 and 8).[409] Furthermore, ManNAc can also be measured down to 10 μg by modified Elson and Morgan method (spectrophotometrically by using Ehrlich's reagent).[412]

The enzymatic assays of *Sia* are very specific and selective, but the high cost of purified enzymes and their stability in diverse sample conditions sometimes limit applications. Readers should be aware of the fact that except one publication,[411] none of the above-mentioned enzymatic assay provided information about the LDR and LOD for *Sia*.

5.5 Chromatography

5.5.1 Chromatography with UV-vis detector (UV-vis). The research and development on the chromatographic assay of *Sia* started relatively later than colourimetric, spectrophotometric and enzymatic methods mentioned above. Svennerholm showed that *Sia* could be separated from complex biological matrix by an anion exchange resin, Dowex 2 × 8 in acetate form followed by assayed using spectrophotometric resorcinol method.[413] Extending this concept, Krantz *et al.* reported in 1975 about the use of an automated anion exchange (by using Rexyn-201(Cl^-) resin in acetate form) chromatography coupled with Aminoff's spectrophotometric detection methodology for the quantification of Neu5Ac. The chromatographic peak area was found to be linear for 1.5–12.0 nmole of Neu5Ac. However, the retention time of Neu5Ac and Neu5Gc was found to be similar (*i.e.*, 20 min).[414] On the other hand, Neu5Ac was silylated with *N*,*O*-bis(trimethylsilyl)-trifluoroacetamide and quantified down to 8 ng by gas–liquid chromatography using 2% (w/w) OV-17 column, flame

ionization detector and *trans*-stilbene as an internal standard.[415,416] In contemporary times, *Sia* was identified by high-resolution mass-spectrometry after converting carboxyl and hydroxyl groups of *Sia* to methyl ester and tri-methyl-silyl derivatives, respectively.[417] Silver *et al.* developed an isocratic HPLC method for quantification of Neu5Ac in the LDR 0.32–6.5 μmol mL^{-1} and LOD of 0.8 nmol mL^{-1} by using Aminex HPX-87 cation-exchange resin, UV detector (fixed at 206 nm) and Neu5Gc as an internal standard. The peak height ratio of Neu5Ac (at retention time 7.8 min) to Neu5Gc (at retention time 11.36 min) was used in this HPLC-UV-vis assay.[418] Shukla *et al.* compared the performance of cation-exchange resin (DC-6A) and anion-exchange resin (DA-X8-11) for the quantification of Neu5Ac, Neu5Gc and their *O*-acetylated derivatives. They found that the retention time (20.2 and 20.6 min for Neu5Ac and Neu5Gc, respectively), LOD (1 μg *i.e.*, 3 nmol) and sensitivity of cation-exchanger with 0.4 M sodium citrate buffer (pH 6.0) were better compared to those (22.0 and 28.6 min for Neu5Ac and Neu5Gc, respectively; LOD 3 μg *i.e.*, 10 nmol) of anion-exchanger with 0.8 M borate including 0.3 M sodium acetate buffer (pH 8.55). However, the resolution of *Sia* in the cation-exchanger was inferior compared to the anion-exchanger.[419] They further modified the HPLC method to effectively separate and quantify *N*,*O*-acetylated derivatives of *Sia* including cytidine-5′-monophospho-Neu5Ac, sialyloligosaccharides, neutral sugars and *N*-acylmannosamines within 16 min. Here the authors used Aminex A-28 anion-exchange resin, 0.75 mM Na_2SO_4 solution as mobile phase and UV detectors set at 195 and 215 nm. The LOD of *Sia* by this HPLC-UV-vis assay was reported as 6 ng (*i.e.*, 20 pmol).[420] Karamanos *et al.* used per-*O*-benzoylation (by using 10% (w/v) benzoic anhydride and 5% (w/v) *p*-dimethylaminopyridine in pyridine) of Neu5Ac and Neu5Gc and eluted the mixture through reversed-phase HPLC (C18 column) by 67% (v/v) aqueous acetonitrile and measured Neu5Ac down to 30 pmol (*i.e.*, 10 ng) by UV detector set at 231 nm.[421] Unland *et al.* performed Folch partition just before and after the benzoylation of hydrolysed Neu5Ac and Neu5Gc to separate and individually quantify both Neu5Ac and Neu5Gc down to 20 ng through HPLC equipped with UV detector set at 230 nm.[422] Although HPLC provided better separation efficiency among the family members of *Sia* as well as from the other saccharides compared to other classical assays, the use of UV detector restricted the selective assay of *Sia* in complex biological matrix. Therefore, an effort was made to elute the chromophore produced from the reaction of Neu5Ac with Aminoff's reagent through HPLC column by *n*-butanol 5% (v/v) in 12 N HCl and setting the visible detector at 549 nm to assay Neu5Ac in picomole ranges.[423] Recently, Ye *et al.* studied hydrophilic chromatography along with HPLC equipped with UV detector (at 205 nm) to determine *Sia* in the LDR and LOD 5–100 and 0.2 μg mL^{-1}, respectively. The hydrophilic chromatographic column improved the retention behaviour of *Sia* on the HPLC column.[29] Levonis *et al.* used a reversed-phase HPLC-UV-vis assay for separately quantifying Neu5Ac and Neu5Gc in the LDR 0.05–0.40 and 0.025–0.200 mM, respectively, in unprocessed bovine milk. They reported the LOD 5.5 μM for Neu5Ac and 0.4 μM for Neu5Gc.[424] The interference of other organic compounds in the UV-vis detection compromise the specificity and sensitivity of HPLC-UV-vis assay. Hence, most of the HPLC assays of *Sia* are based on the hyphenation of reversed-phase HPLC with either fluorescence detection (FLD), pulsed-amperometry detection (PAD) or mass-spectrometry detection (MS).

5.5.2 Chromatography with fluorescence detection (FLD). In HPLC-FLD assay, the *Sia* (post-hydrolysing samples) were tagged with the fluorophore molecules *viz.* 4′-hydrazino-2-stilbazole (excitation and luminescence maxima at 415 and 550 nm, respectively),[425] malononitrile (excitation and luminescence maxima at 360 and 430 nm, respectively),[426,427] *o*-phenyldiamine dihydrochloride (excitation and luminescence maxima at 232 and 420 nm, respectively),[428] 1,2-diamino-4,5-methyleneoxybenzene (DMB, excitation and luminescence maxima at 369 and 453 nm),[429–433] 4-(*N*,*N*-dimethylaminosulfonyl)-7-piperazino-2,1,3-benzoxadiazole (excitation and luminescence maxima at 450 and 560 nm, respectively),[434,435] *o*-phenylenediamine (excitation and luminescence maxima at 337 and 417 nm, respectively),[436] 4,5-dimethylbenzene-1,2-diamine (excitation and luminescence maxima at 379 and 432 nm, respectively),[437] *etc.* before passing through HPLC column followed by detection at the respective emission wavelength upon exposing the specific excitation light. The stilbazole method was free from the interference of α-keto acids other than *Sia* with respect to specific retention time but suffered interference from pyruvate and two suspicious peaks just adjacent to the peak of Neu5Ac. Furthermore, 4′-hydrazino-2-stilbazole derivative of *Sia* was found to be unstable in light and stable for maximum 2 h in the dark.[425] A malononitrile method showed LDR 3–60 nmol and a LOD of 400 pmol for both Neu5Ac and Neu5Gc and little interference from other carbohydrates, amino acids, amines, aldehydes, α-keto acids and carboxylic acids. However, a few amino sugars, deoxy sugars and catecholamines could also form similar derivatives and interfered in the measurements.[427] Later this method was also used for the determination of Neu5Ac with LDR 30–1000 ng mL^{-1} and a LOD of 2 ng mL^{-1} in human serum.[426] The LDR of *o*-phenyldiamine method was reported as 2–450 pmol of Neu5Ac, but accurate quantification of *Sia* by this method was required at least 5–6 blank runs due to the high self-fluorescence of the anthanilic acid.[428] Hara *et al.* tagged Neu5Ac and Neu5Gc with DMB prior to HPLC pass and found 40 fmol (*i.e.*, 12 pg) LOD (S/N 2) for both *Sia* for 10 μL sample volume.[429] Further, with minor modification they could reach LOD 25 fmol (*i.e.*, 7.7 pg) of Neu5Ac and 23 fmol (*i.e.*, 7.5 pg) of Neu5Gc (S/N 2) for the same volume of sample.[430] They also extended this method for determination of *O*-acetylated Neu5Ac with LDR 57–192 fmol for 10 μL sample volume.[431] Stanton *et al.* hydrolysed the human pituitary gonadotropins *viz.* follitropin and lutropin in 0.1 M trifluoroacetic acid at 80 °C for 1 h to

release Neu5Ac, which was tagged with DMB followed by HPLC analysis with Neu5Gc as an internal standard and reported LDR of 3.5–28 pmol.[432] Martín *et al.* used this DMB based HPLC-FLD assay for the quantification of Neu5Ac in commercial infant formula with the LDR 25–250 ng and a LOD of 3.71 ng of Neu5Ac.[433] However, DMB is highly light sensitive and an expensive reagent. It is only stable at room temperature for a couple of hours and must be stored below −20 °C in dark in inert gas chamber for making it stable for at least 24 h. Therefore, Orozco-Solano *et al.* developed a semi-automated methodology consisting of ultrasound-assisted hydrolysis, solid-phase extraction (for pre-concentration and clean-up) and DMB derivatisation followed by insertion of sample to μ-liquid-chromatography column equipped with fluorescence detector. The ultrasound shortened the time of DMB derivatisation to 20 min compared to 180 min required in conventional heating method and furthermore, separation and quantification of *Sia* were completed within 20 min. The authors reported LDR 0.1–100 ng mL^{-1} (for Neu5Ac) and 0.5–500 ng mL^{-1} (for Neu5Gc). The LOD of Neu5Ac was found in the range 0.1–0.8 pg (*i.e.*, 0.1–0.8 ng mL^{-1}) in different samples.[438] Ota *et al.* used 4-(*N*,*N*-dimethylaminosulfonyl)-7-piperazino-2,1,3-benzoxadiazole fluorophore for simultaneous assay of Neu5Ac and its oxidised product ADOA by hydrophilic-interaction-HPLC-FLD with LDR 576 fmol–2.0 nmol (for Neu5Ac) and 556 fmol–2.0 nmol (for ADOA). The LOD of this assay was reported as 173 fmol (for Neu5Ac) and 167 fmol (for ADOA) and they demonstrated first the presence of ADOA in human saliva.[435] Recently, Kawasaki *et al.* slightly improved the LDR to 221 fmol–1.5 nmol (for Neu5Ac) and 44 fmol–1.5 nmol (for ADOA) as well as LOD to 67 fmol (for Neu5Ac) and 13 fmol (for ADOA).[434] The derivatization of Neu5Ac with fluorescent molecule *viz.* *O*-phenylenediamine, followed by HPLC equipped with diode array detector was also used to determine Neu5Ac in the fat globule membrane of yak milk with LDR 50–500 μg mL^{-1} and LOD 10 μg mL^{-1}.[436] The HPLC-FLD assay with 4,5-dimethylbenzene-1,2-diamine as tagged fluorophore was used to determine both free and total Neu5Ac and Neu5Gc in foetal bovine serum and glycoprotein fetuin. The authors reported the LOD of the assay as 6.00 pg (for Neu5Ac) and 8.80 pg (for Neu5Gc).[437] UiO–66-NH_2, which is a zirconium metal organic framework conjugated with 2-aminoterephthalic acid was used to tag *Sia* for reversed phase HPLC-FLD assay of Neu5Ac and Neu5Gc in the LDR 10–1000 pmol L^{-1} with LODs of 0.11 and 0.16 pmol, respectively.[439]

5.5.3 Chromatography with pulsed-amperometric detection (PAD). Manzi *et al.* first reported a new separation process for *Sia* at neutral pH by using carbopac PA1 anion-exchange column of pellicular resin followed by post-column addition of 0.3 M NaOH for PAD with potentiostatic pulse sequence of 0.05 V for 2 s followed by 0.6 V for 2 s and −0.8 V for 5 s for a total duration of 1 min with measurable current in the range 100–300 nA.[440] Although the potential for PAD is not very critical, the potential of the first pulse, which could oxidise the analyte of interest should be kept within 0.0–0.05 V for better S/N. The frequently used durations for the first, second and third potentiostatic pulses were 0.2, 0.2 and 0.4 s, respectively. The objectives of the second and third pulses were oxidative cleaning and reductive reactivation of the electrode, respectively.[441] Rohrer *et al.* performed a high-performance anion-exchange chromatography for simultaneously measuring Neu5Ac and Neu5Gc by using KDN as an internal standard. They reported LDR 10–500 pmol and a LOD of 2 pmol for both Neu5Ac and Neu5Gc. However, they found that the accuracy of measurement was compromised with the age of the gold electrode, because over the time of experiment the upper layer of gold electrode was dissolved into the solution during the oxidative cleaning step. This recession of the detector electrode down to its original position increased the thickness of the thin-layer channel and decreased the velocity of fluid flow over the electrode leading to the compromised electrode response.[442] Rocklin *et al.* addressed this issue and designed a new quadruple-potential waveform consisting of the potentiostatic pulse sequence of 0.1 V for 0.2 s for oxidative measurement followed by −2.0 V for 0.01 s for reductive cleaning, 0.6 V for 0.01 s for activation through oxide growth and −0.1 V for 0.05 s for generation of catalytic sites by oxide reduction.[443]

5.5.4 Chromatography with mass-spectrometry detection (MS). *Shaw et al.* first used HPLC-MS assay to determine Neu5Ac and Neu5Gc by using reversed phase HPLC column coupled with positive-ion mode electron-spray-ionization (ESI) source and *N*-acetylneuraminic acid methyl ester as an internal standard. The areas of the chromatographic peaks at retention time 5.88 min (*m*/*z* 324) for the internal standard, 7.23 min (*m*/*z* 326) for Neu5Gc and 8.00 min (*m*/*z* 310) for Neu5Ac were used to plot the individual calibration curves in the LDR 5–100 μg mL^{-1} with LOD of 0.5 ng for Neu5Ac and 1.0 ng for Neu5Gc.[444] van der Ham *et al.* extended this technique to quantify free and total-Neu5Ac in human urine by using reversed phase HPLC coupled with negative mode ESI source, quadrupole MS/MS detector and 1,2,3-$^{13}C_3$ Neu5Ac as an internal standard in isotope dilution method. Here, the negatively charged Neu5Ac (at *m*/*z* 308.2) and internal standard (at *m*/*z* 311.2) having same retention time (*i.e.*, 2.6 min), were fragmented by collision induced dissociation to daughter products (*m*/*z* 87.0 for Neu5Ac and 90.0 for 1,2,3-$^{13}C_3$ Neu5Ac), whose relative intensities were used to measure the concentration of conjugated Neu5Ac in urine from the difference between concentrations of total and free Neu5Ac. The LDR of this assay was extended up to 7800 μmol L^{-1} for both forms of Neu5Ac, whereas the LOD of total and free Neu5Ac was 1.7 and 0.3 μM, respectively.[445] Allevi *et al.* modified the reversed phase column with 1-decylboronic acid, used both 1,2,3-$^{13}C_3$ Neu5Ac and 1,2,3-$^{13}C_3$ Neu5Gc for isotope dilution and replaced quadrupole MS/MS by quadrupole ion-trap MS/MS detector. This modification resolved the chromatographic peaks of Neu5Ac (at retention time 8.81 min) and Neu5Gc (at retention time 7.21 min) and showed LDR of 0.1–80 mg L^{-1} for both *Sia*.[446]

A similar HPLC-MS assay was developed by Hammad *et al.* by using an aminopropyl-bonded silica phase column and negative-ion multiple-reaction-monitoring mode mass spectrometer for the simultaneous determination of Neu5Ac (LDR 0.1–3.0 ng μL^{-1}; LOD 5 pg) and Neu5Gc (LDR 0.01–0.3 ng μL^{-1}; LOD 1 pg) along with other monosaccharides derived from glycoprotein and blood serum.[447] The reversed phase HPLC coupled with negative-ion mode ESI source and triple quad MS/MS detector successfully quantified Neu5Ac in edible bird nest.[26] Shi *et al.* used isotope dilution hydrophilic interaction chromatography coupled with positive-ion mode ESI source and selective reaction monitor tandem MS/MS detector for assay of Neu5Ac and *N*-acetylmannosamine in human plasma with LDR 25.0–10 000 ng mL^{-1} for Neu5Ac.[448] The ultra-HPLC coupled with positive-ion mode ESI source and selective reaction monitor tandem quadrupole MS/MS detector were also used to determine Neu5Ac in the milk-based commercial infant formulas with LDR 0.05–5.0 μg mg^{-1}.[449] However, the formation of $Na^+/K^+/NH_4^+$ adduct with the COO^- functional group of *Sia* sometimes limits the direct HPLC-MS assay.

Fernando *et al.* protected the carboxyl group of Neu5Ac with fluorophore 1,2-diamine-4,5-dimethoxyl benzene dihydrochloride (excitation and luminescence maxima at 369 and 453 nm, respectively) and carried out the HPLC-MS assay coupled with scanning fluorescence detector, positive ion mode ESI source and quadrupole mass spectrometer with an internal standard α-keto glutaric acid. The LOD of this assay was calculated as 7 pg from the MS peak of fluorophore derivative of Neu5Ac at *m*/*z* 442.[450] Xia *et al.* extracted glycoprotein from the root of a Tibetan plant *Potentilla anserina* L. and released Neu5Ac and Neu5Gc from that glycoprotein by acid hydrolysis. They used 3-methyl-1-(naphthalen-2-yl)-1*H*-pyrazol-5(4*H*)-one in ammonia solution to make pre-derivatives of the *Sia* and eluted the fluorophore derivatives of *Sia* through reversed phase HPLC coupled with UV detector (at 254 nm) for measurement and both positive- and negative-ion mode ESI sources, ion-trap mass spectrometer for identification. They could produce LDR 0.25–10.0 μM for both Neu5Ac and Neu5Gc with LOD 1.09 pmol (for Neu5Ac) and 1.06 pmol (for Neu5Gc).[31] Hayama *et al.* pre-derivatised Neu5Ac and Neu5Gc with heptadecafluoroundecylamine in the presence of 4-(4,6-dimethoxy-1,3,5-triazin-2-yl)-4-methylmorpholinium chloride and used fluorous-phase fluophase reversed-phase HPLC column coupled with positive mode ESI source and Qtrap tandem mass spectrometer to assay Neu5Ac and Neu5Gc in the LDR 1–100 μM (for Neu5Ac) and 0.05–10 μM (for Neu5Gc).[451] The pre-derivatization with HCl-*n*-butanol and reversed phase isotope dilution mass-spectrometry in positive-mode ESI source and tandem mass-spectrometer showed LDR and LOD 2–1000 and 0.42 μM, respectively, for Neu5Ac.[452] Wang *et al.* followed a similar strategy *i.e.*, isotope dilution of Neu5Ac with 1,2,3-$^{13}C_3$ Neu5Ac, inclusion of ketodeoxynonulosonic acid as an internal standard followed by pre-derivatisation with 3,4-diaminotoluene and eluting through ultra-HPLC coupled with positive ion mode ESI source and multiple reaction monitoring with Qtrap MS/MS detector. They used the *m*/*z* transition 396 → 253 at retention time 3.6 min for the assay of Neu5Ac with LDR 20.0–2.00 × 10^4 ng mL^{-1}.[453] Priego-Capote *et al.* used derivatives of Neu5Ac and Neu5Gc with DMB and pre-concentrated by a solid-phase extractor (hysphere polymeric polydi-vinylbenzene resin) online coupled with reversed phase chromatography having both positive- and negative-ion mode ESI source and multiple reaction monitoring with QqQ MS/MS detector. They reported LDR 0.2–500 ng mL^{-1} for both the target analytes in urine and serum samples with LOD 0.03 ng mL^{-1} for Neu5Ac and 0.04 ng mL^{-1} for Neu5Gc.[454] Yesilyurt *et al.* used DMB derivative of Neu5Ac for HPLC-MS assay in the egg jelly coat of the sea urchin *Paracentrotus lividus* by using capillary liquid chromatography coupled with positive ion mode ESI source and ultra-ion trap tandem MS/MS detector.[455]

In the present day, the HPLC-FLD and HPLC-MS/MS (with or without fluorescence tagging) methods are the most reliable techniques for ultra-sensitive assays of *Sia* in the clinical and commercial food samples. The DMB based HPLC-FLD assay could produce a moderately wide LDR of 0.32–320 nM with a LOD of 0.32 nM of Neu5Ac.[438] On the other hand, a DMB derivative of Neu5Ac preconcentrated by hysphere polymeric polydi-vinylbenzene resin online coupled with HPLC-ESI-MS/MS analyser resulted to wider LDR of 0.65 nm–1.6 μM of Neu5Ac with the lowest reported LOD of 97 pM.[454]

5.6 Capillary electrophoresis

Chen *et al.* used sialic acid aldolase for the enzymatic reaction of Neu5Ac to produce ManNAc, which was derivatised with the anionic fluorescent dye 8-aminopyrene-1,3,6-trisulfonic acid (having excitation and luminescence maxima at 425 and 503 nm, respectively) for the quantification of Neu5Ac by capillary electrophoretic separation followed by laser-induced fluorescence detection in the LDR 0.1–10 nmol.[456] On the other hand, Neu5Ac was directly derivatised with 2-aminoacridone (having excitation and photoluminescence maxima at 429 and 529 nm, respectively), but monitored at 260 nm after capillary electrophoresis. The LDR and LOD of this assay were reported as 10–120 and 1 μM of Neu5Ac, respectively.[457] Dong *et al.* used only high-performance capillary electrophoresis (HPCE) coupled with UV detection at 195 nm for assay of Neu5Ac without any pre- or post-derivatisation. The reported the LDR and LOD for Neu5Ac as 0.064–6.40 mM and 9.6 μM, respectively.[458] Strousopoulou *et al.* derivatised Neu5Ac to per-*O*-benzoylated Neu5Ac by benzoic anhydride and quantified it with capillary zone electrophoresis coupled with diode-array detector fixed at 231 nm. They reported the LDR and LOD of Neu5Ac as 5–5000 μg mL^{-1} and 2 μM, respectively.[459] Taga *et al.* developed a capillary electrophoresis assay featured with in-capillary sialidase digestion for the determination of Neu5Ac in sialoglycans and sialoglycoproteins. They introduced the samples into a running 50 mM acetate buffer (pH 5.0) containing exo-α-

sialidase (of concentration 250 mU mL^{-1}) from the cathodic end of the capillary and then applied 5 kV for 20 min followed by 20 kV for 5 min between two ends of the capillary. The authors achieved good linear response in the concentration range 0.025–10.0 mg mL^{-1} with a UV detector fixed at 200 nm.[460]

Ortner *et al.* developed an assay method for the simultaneous determination of Neu5Ac and Neu5Gc by capillary zone electrophoresis coupled with negative-ion mode ESI source and ion-trap MS detector. They reported LDR and LOD 10–100 and 2 μg mL^{-1}, respectively, for both *Sia* released from the glycoproteins after acid hydrolysis.[461] *Zheng et al.* oxidised Neu5Ac to β-formyl pyruvic acid by HIO_4–H_2SO_4 treatment and then derivatised with electroactive 2-thiobarbituric acid. This derivatised Neu5Ac was assayed by sample-stacking capillary electrophoresis coupled with amperometric detection on a carbon disc electrode kept at 0.950 V *vs.* saturated calomel electrode. They reported the LDR and LOD as 2–200 and 0.5 μg mL^{-1}, respectively, with distinguishable signal of excess 2-thiobarbituric acid, 2-deoxy-D-ribose, fucose, glucose, formaldehyde, acetaldehyde and propaldehyde.[462] Wang *et al.* developed a capillary electrophoresis method in conjugation with capacitively coupled contactless conductivity detection based on synergistic electrophoretic stacking technique of field-amplified sample injection and moving chemical reaction boundary. This method was found to be suitable for the assay of both Neu5Ac and Neu5Gc in the commercial milk and milk powder samples with LDR 0.02–2.0 μg mL^{-1} (in milk) and 0.01–2.0 μg g^{-1} (in milk powder). The LOD of Neu5Ac and Neu5Gc in real samples was reported as 2.2 ng mL^{-1} (in milk); 1.7 ng mL^{-1} (in milk powder) and 2.0 ng mL^{-1} (in both milk and milk powder), respectively.[463]

In summarising electrophoretic analytical approaches to *Sia* quantitation, it could be conferred that although this method is not as ultra-sensitive as chromatographic assays, it is simpler to operate to quantify *Sia* in commercial food samples at moderately trace-levels. The pre-derivatization of Neu5Ac with fluorophores *viz.* 2-aminoacridone and benzoic anhydride followed by capillary electrophoresis could result in LDR of 10–120 and 16–16 000 μM, respectively, with LOD of 1 and 2 μM, respectively.[457,459] The lowest possible LDR (65–6500 nM; converted from 0.02–2.0 μg mL^{-1}) and LOD (5.5 nM; converted from 1.7 ng mL^{-1}) for capillary electrophoretic assay of *Sia* was achieved by coupling with capacitively coupled contactless conductivity detection technique.[463] Hence, there is scope for scientific research and development for ultra-sensitive electrophoretic assays of *Sia* in clinical samples and food products.

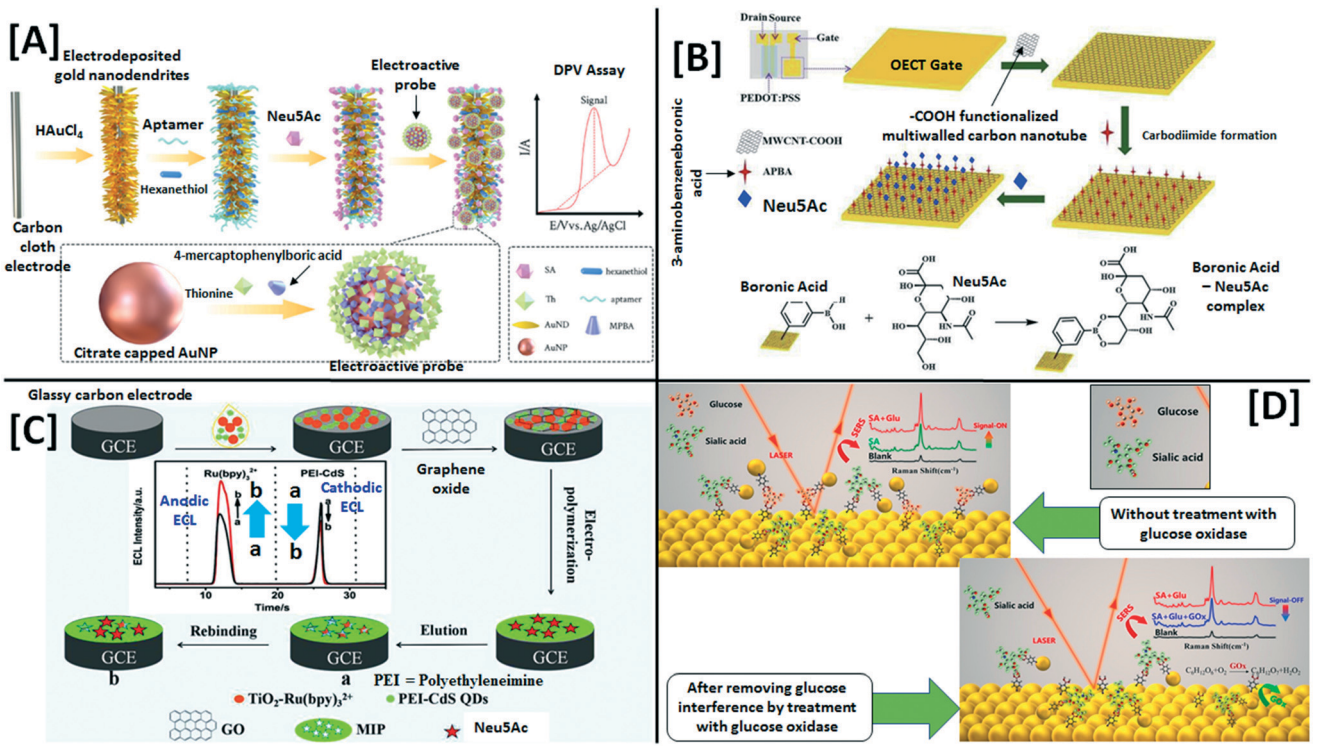

Fig. 8 [A] DPV assay of Neu5Ac by using aptamer coated gold nanodendrites electrochemical platform and thionine-4-marcaptophenylboronic acid electroactive probe (figures reproduced with permission from ref. 472) Copyright 2020 John Wiley and Sons. [B] Interaction of Neu5Ac with 3-aminobenzeneboronic acid covalently linked to carboxylic acid functionalized multiwalled carbon nanotubes placed on the gate of OECT (figures reproduced with permission from ref. 476) Copyright 2020 Elsevier. [C] Ratiometric MIP based ECL assay of Neu5Ac on glassy carbon electrode modified with TiO_2–$Ru(bpy)_3^{2+}$ nanoparticles, polyethyleneimine (PEI) capped CdS quantum dots and graphene oxide (figures reproduced with permission from ref. 479) Copyright 2020 Elsevier. [D] SERS assay of Neu5Ac in the presence of glucose by using glucose oxidase pre-treatment (figures reproduced with permission from ref. 488) Copyright 2020 American Chemical Society.

5.7 Electrochemistry and electroluminescence

5.7.1 Amperometry. Amperometry was first used as only a detection technique of HPLC-PAD in 1998, but its first-step towards direct electrochemical assay of *Sia* happened 10 years later, when Marzouk *et al.*, developed a prototype amperometric biosensor for *Sia* by utilising the concept of enzymatic reactions of *Sia* as discussed in the Section 5.4. They co-immobilized 4% (w/v) sialic acid aldolase and 6% (w/v) pyruvate oxidase by 0.9% (w/v) glutaraldehyde in the presence of 9% (w/v) bovine serum albumin in phosphate buffer (pH 6.3). They optimised aldolase/oxidase as 1.5; glutaraldehyde/(aldolase + oxidase + albumin) as 0.05 and (aldolase + oxidase)/albumin as 1.1 for best sensitivity of *Sia* and 15 μL of this mixture in phosphate buffer (pH 6.3) was drop-dried over 25 mm diameter microporous polyester membrane. On the other hand, 1,3-diaminobenzene was electropolymerized as a thin layer on a platinum working electrode using a potentiodynamic method for protecting the platinum surface and the dry-enzyme contained polyester membrane was fixed at the top of the modified platinum electrode by using a Teflon cap. This polyester membrane helped to reduce the interference, contain and protect the enzymes and increase the reproducibility of the sensor. The amperometry was recorded at 0.6 V *vs.* Ag/AgCl reference electrode in PBS (pH 6.3 and 37 °C) containing 0.5 mM thiamine pyrophosphate cofactor and Neu5Ac. The response was linear up to 200 μM with a LOD of 10 μM for Neu5Ac.[464] Later, they extended this methodology by constructing an amperometric flow-through cell detector as an attachment of immobilized enzyme reactors to achieve better LDR and LOD as 10 μM–5 mM and 2 μM, respectively, for Neu5Ac.[465] Fatoni *et al.* developed a porous conducting network of chitosan-grafted polyaniline cryogel for amperometric assay of *Sia*. They initially prepared polyaniline (a conducting polymer) from aniline in 0.1 M HCl by ammonium peroxodisulphate oxidation and dispersed it along with ferrocene (a redox mediator), bovine serum albumin and 5.0% glutaraldehyde (a cross-linker) in chitosan. Then that mixture was drop-casted on a multi-walled carbon nanotube modified gold electrode (to enhance the current) and immediately stored at −20 °C overnight for cryogelation followed by thawing at 4 °C for 1 h. Using this procedure, the authors prepared a porous cryogenic conducting polymer network on the working electrode that could host 2 : 1 sialic acid aldolase : pyruvate oxidase along with 5.0% glutaraldehyde in 0.1 M phosphate buffer (pH 7.0). Instead of probing H_2O_2, they probed the amperometric current of ferrocene redox reaction at 0.2 V *vs.* Ag/AgCl in 0.05 M phosphate buffer (pH 8). The pyruvate oxidase converted pyruvate to acetylphosphate, H_2O_2 and CO_2 (see section 5.4) and itself was regenerated by ferrocinium/ferrocene redox reaction. The amperometric assay was suitable to determine Neu5Ac in the LDR 0.025–15.0 mM with a LOD of 18 μM without any significant interference of ascorbic acid, uric acid and pyruvic acid. This assay was successfully validated to quantify *Sia* in blood plasma samples.[466]

5.7.2 Potentiometry. A potentiometric assay of *Sia* was first reported by Zhou *et al.* They electrochemically reduced graphene oxide on glassy carbon electrode onto which 3-aminophenylboronic acid was electropolymerised to prepare a modified electrode capable of forming a stable complex with Neu5Ac interacting through the boronic acid functional group of 3-aminophenylboronic acid in 0.1 M PBS (pH 4.75). The open-circuit potential of the cell as a function of time changed in the presence of Neu5Ac compared to that in the absence of Neu5Ac. The change in the open-circuit potential of the modified electrode as a function of the concentration of Neu5Ac was found to be linear in the LDR 2 μM–1.38 mM with a LOD of 0.8 μM. They successfully quantified the concentration of *Sia* in the human blood serum by this potentiometric assay.[467] The same research group prepared a molecularly imprinted polymer (MIP) based electrode with 3-aminophenylboronic acid electropolymerised on the hydrophilic carbon cloth in the presence of NaF (a polymerization catalyst) and Neu5Ac complex of 3-aminophenylboronic acid as the template. The potentiometric assay was carried out in 0.1 M PBS (pH 4.8) with an equilibration time of 100 s. The change in the electrode potential of the MIP modified electrode was found to be linear over 40–440 μM of Neu5Ac with a LOD of 0.5 μM. The authors successfully employed this potentiometric assay for measuring Neu5Ac levels in infant formulas.[468] Huang *et al.* prepared a similar MIP, but on carboxylated multi-walled carbon nanotube casted glassy carbon electrode. They developed this potentiometric assay for the quantification of Neu5Ac in human serum samples with LDR 80 μM–8.2 mM and a LOD of 60 μM in the physiological pH.[469] Shishkanova *et al.* showed that chemically bound 3-aminophenylboronic acid (through carbodiimide protocol) on electropolymerised 3-aminobenzoic acid could also be employed for the potentiometric assay of Neu5Ac with a sensitivity of −38 ± 6 mV and a LOD of 21 μM.[470]

5.7.3 Voltammetry and electrochemical impedance spectroscopy (EIS). Sun *et al.* reported the differential pulse voltammetry (DPV) study for the determination of Neu5Ac on a paper-based electrode in the different parts of pea seedlings. They placed a piece of carbon tape on a conductive indium-tin-oxide coated glass plated and modified with multiwalled carbon nanotubes. The effective detection area (*i.e.*, 4 mm diameter) of the modified electrode was treated under oxygen plasma for 1 min. Then small samples (taken from different zones of pea seedling) were acquired with a sample punch and were directly placed on the effective electrode area one at a time. The sample was covered by a piece of filter-paper soaked with phosphate buffer (pH 7.5) and a clasp with platinum and Ag/AgCl wires was placed on it to act as counter and reference electrodes, respectively. This voltammetric assay resulted to a LDR of 1–100 μM of Neu5Ac.[30] Liu *et al.* reported a non-enzymatic indicator displacement voltammetry assay of Neu5Ac in human blood and urine samples pre-treated using ion-exchange column. Aqueous dispersion of *meso*-tetra(4-carboxyphenyl)-porphine

and graphene oxide (1 : 2 w/w) was drop-casted on the glassy carbon electrode and dopamine was covalently linked on it by the carbodiimide route. Then 2-fluorophenylboronic acid was allowed to be adsorbed on the electrode surface owing to the interaction of the boronic acid functional group with the catecholamine dopamine. A DPV scan of the dopamine modified electrode in 0.1 M PBS (pH 7.0) showed an anodic peak at 0.25 V corresponding to oxidation of dopamine. After modification with 2-fluorophenylboronic acid, the anodic current at 0.25 V decreased and a new peak appeared at 0.6 V corresponding to the oxidation of an ester boronic acid–dopamine complex. In the presence of Neu5Ac in the electrolyte solution, the anodic peak at 0.6 V disappeared and the anodic current at 0.25 V increased due to the preferential bonding of 2-fluorophenylboronic acid with Neu5Ac in the solution compared to the diol unit of dopamine present on the electrode surface. The DPV peak current at 0.25 V proportionally increased with the concentration of Neu5Ac in the range 0.1–7.5 mM with a LOD of 28.5 μM. This voltammetric assay suffered significant interference from ascorbic acid, glucose and uric acid and thus samples were required to be pre-treated with an ion-exchange column.[471] Lv *et al.* reported an aptamer based voltammetric sensor for the determination of *Sia* in hospital acquired human blood samples (Fig. 8[A]). Carbon cloth electrode was electrochemically modified with gold nanodendrites and incubated in the solution of aptamer sequence (*i.e.*, TCCCT ACGGC GCTAA CCGAT AGGTG TAGCG TGGGG CACAT GTTCG CGCCA CCGTG CTACA AC) of *Sia* for 12 h at room temperature. The non-specific binding sites of this aptasensor base were blocked by 1-hexanethiol. On the other hand, an electroactive probe was prepared by 4-mercaptophenylboric acid and thionine modified and citrate-capped AuNPs. Then the aptasensor base was incubated in the aqueous solution of Neu5Ac in 0.1 M phosphate buffer (pH 4.5) for 3 h at room temperature followed by incubation with the electroactive probe in the same buffer for 5 h. Finally, Neu5Ac was assayed indirectly from the equivalent cathodic peak of thionine by DPV through potential scan from 0.4 V to −0.4 V in 0.1 M phosphate buffer (pH 4.5) in the LDR 0.1–440 μM with a LOD of 0.08 μM.[472] Hai *et al.* synthesised pyridylboronic acid to specifically bind *Sia* in lower pH (5–6) and used it along with the poly-3,4-ethylenedioxythiophene to determine Neu5Ac in the LDR 0.1–3.0 mM with a LOD 0.1 mM by using ferri-/ferrocyanide as a redox probe for the DPV assay.[473] Ding *et al.* reported an electrochemical impedance spectroscopy (EIS) based stimuli-responsive polymer electrode hyphenated with *in vivo* microdialysis for electrochemical assay of Neu5Ac for Alzheimer disease in live rat brain microdialysates. They electrochemically deposited gold nanoflowers on a screen-printed carbon electrode and prepared a copolymer consisting of *N*-isopropylacrylamide, acryloyl-3-amidophenylboronic acid, acryloyl-3,5-bis(trifluoromethyl)-phenylthiourea and *S*-benzyl dithiobenzoate with the mole ratio of 170 : 15 : 15 : 2 through a reversible addition–fragmentation chain transfer polymerization mechanism. Here, *S*-benzyl dithiobenzoate anchored the copolymer on the gold nanoflowers, the amide group of poly-(*N*-isopropylacrylamide) made hydrogen bonds with the N–H functionality of acryloyl-3,5-bis(trifluoromethyl)-phenylthiourea and O–H functionality of acryloyl-3-amidophenylboronic acid provided a gated-channel polymeric network to the approach of the redox-probe (*i.e.*, $[Fe(CN)_6]^{3-/4-}$) towards the working electrode surface. In the presence of Neu5Ac in the assay electrolyte, the hydrogen bond between poly-(*N*-isopropylacrylamide) and acryloyl-3-amidophenylboronic acid became weaker due to the higher affinity of Neu5Ac towards the boronic acid functional group and the polymeric network became more open towards the passage of the redox-probe to/from electrode surface. The authors used 0.1 M artificial cerebrospinal fluid buffer solution containing $[Fe(CN)_6]^{3-/4-}$ redox probe and EIS assay was carried out at 0.14 V with a sine potential perturbation of 5 mV amplitude and frequency range 0.01–10^5 Hz. The charge-transfer-resistance linearly decreased with the concentration of Neu5Ac in the range 1 pM–10 μM with a LOD of 0.4 pM without any significant interference from glucose, mannose, galactose, fucose, xylose, fructose, K^+, Na^+, Ag^+, Ca^{2+}, Mg^{2+}, Zn^{2+}, Cu^{2+}, Co^{2+}, Fe^{2+}, Mn^{2+}, Ni^{2+}, Cd^{2+}, Fe^{3+}, Al^{3+}, amino acids (Glu, Gly, Phe, Met, Val, Cys, His, Iso, Lys, Leu, Tyr), ascorbic acid, uric acid, dopamine, lactate, 3,4-dihydroxyphenylacetic acid and 5-hydroxytryptamine.[474] Broncová *et al.* electropolymerized 3,4-diaminobenzoic acid on a platinum electrode and covalently anchored 3-aminophenylboronic acid by a two-step carbodiimide modification. Authors performed EIS assay in the frequency range 0.1 Hz–100 kHz at 0 V with an amplitude of 10 mV in 0.04 M Britton–Robinson buffer (pH 7.0) and found that the difference between polarization and solution resistances linearly varied with the concentration (in logarithmic scale) of Neu5Ac in range 25 μM–0.998 mM.[475]

5.7.4 Organic electrochemical transistor (OECT). Chen *et al.* have recently reported the assay of *Sia* in human serum by an OECT. It was fabricated by coating Cr (of 10 nm thick) and Au (of 100 nm thick) layers on a glass plate followed by photolithographic patterning (Fig. 8[B]). Then poly-(3,4-ethylenedioxythiophene) doped with poly-(styrene sulfonate) along with 5% glycerin and 5% dimethyl sulfoxide (V/V) were spin-coated on that platform to form a conducting channel between drain and source. On the other hand, carboxylic acid functionalized multiwalled carbon nanotubes were drop-casted on the gate followed by covalent immobilization of 3-aminobenzeneboronic acid *via* carbodiimide formation. Then Neu5Ac in 0.01 M PBS (pH 7.4) was incubated on the OCET for 10 min at room-temperature and the drain-source current was recorded for 300 s at 0.9 V gate voltage and 50 mV drain voltage compared to source, which was effectively grounded. The current response was found to be linear in the 0.1–7.0 mM concentration range of Neu5Ac without any significant interference from glucose, mannose, lactose, fructose,

sucrose, maltose, galactose, ribose, dopamine, ascorbic acid and uric acid. The authors successfully used this assay to quantify Neu5Ac in the serum samples collected from the lung cancer patients and healthy people.[476]

5.7.5 Photoelectrochemical and electrochemiluminescence (ECL). Wang *et al.* have recently developed a photoelectrochemical assay of *Sia*. They prepared a composite polymer from poly-[(9,9-di-*n*-octyfluorenyl-2,7-diyl)-alt-(benzo[2,1,3]thiadia-zol-4,8-diyl)], poly-(styrene-co-maleic anhydride) and photosensitizer tetraphenylporphyrin mixed in the weight ratio 20 : 4 : 1. Then the composite polymer was mixed with equal amount of rutile TiO_2 and a monoclonal antibody was anchored to TiO_2-composite polymer mixture. On the other hand, a glassy carbon electrode was modified with fullerene to increase the electrochemical current response and successively that was modified with AuNPs to chemically anchor 4-mercaptophenylboronic acid for the recognition of *Sia*. Then, Neu5Ac was incubated on the modified electrode surface for 40 min at room temperature in 0.1 M PBS (pH 7.4) and the Neu5Ac modified electrode was allowed to react with the monoclonal antibody anchored TiO_2-composite polymer mixture by incubation for another 40 min at room temperature. The photocurrent (recorded in the potential range 0.5–0.6 V *vs.* Ag/AgCl reference electrode) and the temperature (recorded upon laser irradiation at 808 nm, 1.0 w cm^{-2}) of the system linearly increased with concentration (in logarithmic scale) of Neu5Ac in the range 3.5×10^{-5}–35.0 ng mL^{-1} with a LOD of 1.2×10^{-5} ng mL^{-1}. The authors successfully employed this photoelectrochemical assay to measure Neu5Ac in blood samples collected from human volunteers.[477]

Fang *et al.* have recently developed a self-enhanced and renewable biosensor for ultra-sensitive detection of *Sia* in human serum though ECL assay. For this purpose, the ECL bio-probe was prepared by mixing $Ru(bpy)_3^{2+}$ with TiO_2 mesocrystals for 6 h followed by addition of 4-mercaptobenzoic acid and bismuth nano-belts. The monoclonal antibody was anchored to this surface *via* a carbodiimide route. On the other hand, fullerene followed by TiO_2 mesocrystals were drop-casted on a glassy carbon electrode and 4-mercaptophenylboronic acid was also added on this surface. Furthermore, the nonspecific sites available on the modified electrode were blocked by adding 1% bovine serum albumin. For the ECL assay, the modified electrode was incubated with the solution of Neu5Ac in 0.1 M PBS (pH 8.0) for 40 min at room temperature and further incubated for another 40 min after adding the ECL bio-probe. The ECL response of Neu5Ac recorded in the potential range 0.8–1.5 V in 0.1 M PBS (pH 8.0) was found to be linear with concentration (in logarithmic scale) of Neu5Ac in the range 3.5×10^{-5}–350 ng mL^{-1} with a LOD of 1.17×10^{-5} ng mL^{-1}. Interestingly, the modified electrode could be regenerated by simply immersing into 0.1 M PBS (pH 6.0) when Neu5Ac conjugated with the ECL bio-probe detached from the modified electrode surface, which can be re-used for the next assay with fresh bio-probe.[478]

A ratiometric MIP based ECL sensor was developed by Cao *et al.* in 2020 for sensitive and selective detection of Neu5Ac in the commercially available synthetic human serum and EBN (Fig. 8[C]). Initially, TiO_2–$Ru(bpy)_3^{2+}$ nanoparticles and polyethyleneimine capped CdS quantum dots (w : w 1 : 4) were drop-casted on a glassy carbon electrode and covered with a few layers of graphene oxide to enhance the overall conductivity of the modified electrode suitable for electrochemical applications. The MIP was potentiodynamically electropolymerized on the modified electrode in a solution of 0.3 mM 3-aminophenylboronic acid and 0.2 mM Neu5Ac (acted as template) in 0.1 M PBS (pH 4.5). After removal of the template, the modified electrode was incubated in a solution of Neu5Ac (to be assayed) in 0.1 M PBS (pH 4.5) for 180 s followed by washing and drying. The ECL assay was carried out in 0.1 M PBS (pH 7.5) solution containing 50 mM H_2O_2 by cyclic voltammetry in the range −1.6 V to 1.2 V at a scan rate of 200 mV s^{-1}. In this assay, Neu5Ac and H_2O_2 both acted as co-reactants for the anodic ECL of TiO_2–$Ru(bpy)_3^{2+}$; whereas only H_2O_2 acted as reactant for cathodic ECL of PEI-CdS quantum dots. Thus, in the presence of Neu5Ac, the intensity of the anodic ECL increased due to the availability of both co-reactants, but the intensity of the cathodic ECL of PEI-CdS quantum dots decreased due to the blockage of the available passage of H_2O_2 through imprinted cavities by Neu5Ac occupancy in the MIP.[479]

In the perspective of electrochemical assays as discussed in the above sub-sections, it should be mentioned that current electrochemical assays of *Sia* are competing well with expensive and time-consuming chromatographic and electrophoretic assays. The amperometric and potentiometric assays could provide a good LDR within about 20 μM–15 mM range for Neu5Ac.[464,466–469] The aptamer based DPV assay could detect *Sia* at ultra-trace levels down to 80 nM in clinical samples[472] and the EIS assay was able to bring the LOD further down to 0.4 pM with a LDR of 1 pM–10 μM.[474] There are few reports published on the OECT, photoelectrochemical and ECL based electrochemical assays, although the ECL assay showed interesting results for quantifying Neu5Ac in the wide LDR 0.11 pM–1.13 μM (converted from 3.5×10^{-5}–350 ng mL^{-1}) with a very competitive LOD of ~38 fM (converted from 1.17×10^{-5} ng mL^{-1}) to HPLC-MS/SM assays.[478] Therefore, this branch of electrochemical assay of *Sia* can inspire further research.

5.8 Quartz crystal microbalance (QCM)

In the year 2000, Kugimiya *et al.* coated two different types of MIPs on 9 MHz AT-cut platinum QCMs for assay of *Sia* in methanol (or water) in pyridine (99 : 1 v/v). The first type of MIP was prepared with *p*-vinylbenzeneboronic acid as a chemical receptor of *Sia*, whereas the second type of MIP was prepared with *p*-vinylbenzeneboronic acid and *N*,*N*,*N*-trimethylaminoethyl methacrylate, which could provide additional attractive electrostatic force to the carboxylate

Table 3 Summary of LDR, LOD and nature of tested samples of the analytical methods (as discussed in Section 5.2–5.10) validated to quality *Sia* in either biological or commercial samples

Assay method	LDR	LOD	Method validated by determination of *Sia* in	Ref.
Colourimetry and spectrophotometry	1.0–10.0 mg L^{-1}	0.239 mg L^{-1}	Whole, semi-skimmed and skimmed milks	378
	0.15–1.0 mM	0.06 mM	Simulated human saliva	379
	80–250, 300–700 μM	35 μM	Commercial human serum extracted from human male AB plasma	380
Photoluminescence	12–680 ng mL^{-1}	0.67 ng mL^{-1}	Whole egg, yolk and egg white powders, egg noodles, cake and steamed bun	387
	0.05–1.5 mg mL^{-1}	16 μg mL^{-1}	Commercial infant formula	388
	0.08–4.0 mM	54 μM	Real human serum	390
	0.02–1.0 mM	9.24 μM	Simulated human saliva	391
	10 nM–10 mM (in logarithmic scale)	7.08 nM	Real human serum	392
HPLC-UV–vis	0.05–0.40 mM (Neu5Ac); 0.025–0.200 mM (Neu5Gc)	5.5 μM (Neu5Ac); 0.4 μM (Neu5Gc)	Unprocessed bovine milk	424
HPLC-FLD	30–1000 ng mL^{-1}	2 ng mL^{-1}	Human serum	426
	3.5–28 pmol	—	Human pituitary gonadotropins *viz.* follitropin and lutropin	432
	25–250 ng	3.71 ng	Commercial infant formula	433
	576 fmol–2.0 nmol (Neu5Ac); 556 fmol–2.0 nmol (ADOA)	173 fmol (Neu5Ac); 167 fmol (ADOA)	Human saliva	435
	50–500 μg mL^{-1}	10 μg mL^{-1}	Fat globule membrane of yak milk	436
	—	6.00 pg (Neu5Ac); 8.80 pg (Neu5Gc)	Foetal bovine serum and glycoprotein fetuin	437
HPLC-MS	<7800 μmol L^{-1}	1.7 (total); 0.3 μM (free)	Human urine	445
	0.1–3.0 ng μL^{-1} (Neu5Ac); 0.01–0.3 ng μL^{-1} (Neu5Gc)	5 pg (Neu5Ac); 1 pg (Neu5Gc)	Glycoprotein and blood serum	447
	25.0–10 000 ng mL^{-1}	—	Human plasma	448
	0.05–5.0 μg mg^{-1}	—	Milk-based commercial infant formulas	449
	0.25–10.0 μM (Neu5Ac; NeuGc)	1.09 pmol (Neu5Ac); 1.06 pmol (Neu5Gc)	Extracted glycoprotein from the root of a Tibetan plant *Potentilla anserina* L.	31
	20.0–20 000 ng mL^{-1}	20 ng mL^{-1} (LOQ)	Human plasma	453
	0.2–500 ng mL^{-1}	0.03 ng mL^{-1} (Neu5Ac); 0.04 ng mL^{-1} (Neu5Gc)	Urine and serum	454
Capillary electrophoresis	2–200 μg mL^{-1}	0.5 μg mL^{-1}	Human saliva	462
	0.02–2.0 μg mL^{-1} (Neu5Ac, Neu5Gc in milk); 0.01–2.0 μg g^{-1} (Neu5Ac, Neu5Gc in milk powder)	2.2 ng mL^{-1} (Neu5Ac in milk); 1.7 ng mL^{-1} (Neu5Ac in milk powder); 2.0 ng mL^{-1} (Neu5Gc in milk and milk powder)	Commercial milk and milk powder	463
Amperometry	>200 μM	10 μM	Epotin, blood, and serum samples of human	464
	0.025–15.0 mM	18 μM	Blood plasma	466
Potentiometry	2 μM–1.38 mM	0.8 μM	Human blood serum	467
	40–440 μM	0.5 μM	Infant formulas	468
	80 μM–8.2 mM	60 μM	Human serum	469
Voltammetry and EIS	1–100 μM	—	Pea seedlings	30
	0.1–7.5 mM	28.5 μM	Human blood and urine samples	471
	0.1–440 μM	0.08 μM	Human blood	472
	1 pM–10 μM	0.4 pM	Live rat brain microdialysates	474
	25 μM–0.998 mM		Artificial human urine	475
OECT	0.1–7.0 mM	—	Human serum	476
Photoelectrochemical and ECL	3.5×10^{-5}–35.0 ng mL^{-1} (logarithmic scale)	1.2×10^{-5} ng mL^{-1}	Human blood	477
	3.5×10^{-5}–350 ng mL^{-1} (logarithmic scale)	1.17×10^{-5} ng mL^{-1}	Human serum	478
	1.0 nM–0.1 mM (logarithmic scale)	0.017 nM	Synthetic commercially available human serum and bird's nest	479
QCM	0.025–0.50 μM	1.0 nM	Artificial human urine	482
SERS	1–200 mg dL^{-1}	—	Human saliva	487

Table 3 *(continued)*

Assay method	LDR	LOD	Method validated by determination of *Sia* in	Ref.
	0.25–1.5 μM	0.25 μM	Human blood plasma	488

functional group of *Sia*. The *p*-vinylbenzeneboronic acid ester of *Sia* was used as a template molecule during formation of both MIPs. The resonance oscillation frequency of both the modified QCMs linearly varied with the concentration of *Sia* in the range 20–250 nmol.[480] Twelve years later, Duan *et al.* used a gold QCM and modified it with a monolayer of 4-mercaptophenylboronic acid for a direct assay of *Sia* solely relying on the special affinity of boronic acid to *Sia*. The LDR and LOD of this QCM assay reported as 0.50–5.0 and 0.15 mM, respectively.[481] In 2018, Qiu *et al.* modified gold QCM with allylmercaptane to introduce an allyl group on the QCM surface and then prepared a MIP on it by using *Sia* (as template molecule), 4-aminophenylboronic acid (as functional monomer), *N*,*N*-methylene-bis(acrylamide) (as cross-linker) and ammonium persulfate (as polymerisation initiator). This assay provided the best LDR and LOD of 0.025–0.50 μM and 1.0 nM, respectively, for *Sia* in 50 mM phosphate buffer (pH 7.7) among all QCM assays of *Sia*.[482] Hence, the research on the QCM assay of *Sia* can be considered as rare, being less reported compared to other assays.

5.9 Surface plasmon resonance (SPR)

In 2001, Kugimiya *et al.* prepared *p*-vinylbenzeneboronic acid ester of Neu5Ac by azeotropic distillation in dry pyridine and used the ester as a template molecule for a thin MIP layer prepared on a gold-coated SPR chip. The MIP was prepared by co-polymerizing *N*,*N*,*N*-trimethylaminoethyl methacrylate, 2-hydroxyethyl methacrylate, ethyleneglycol dimethacrylate and 2,2′-azobis(dimethylvaleronitrile) in DMF. In the assay, the sample was passed along with 20 mM Tris-HCl buffer (pH 8.0) carrier solution over the SPR chip and the SPR resonance angle was monitored at 660 nm. The authors observed no change in the SPR resonance angle for free Neu5Ac compared to the control, but the SPR resonance angle linearly changed for sialylated gangliosides in the concentration range 0.1–1.0 mg mL^{-1}.[483] After a long gap until 2018, Li *et al.* developed a new SPR assay of *Sia* owing to the synchronous amplification of the opto-electric response of localised SPR during linear sweep of electrochemical potential. They sputter coated SiO_2 layer of 100 nm thickness on the nanocone array of (poly)ethylene-terephthalate substrate fabricated by laser interference lithography followed by reaction ion etching. Then, AuNPs of diameter ~40 nm were deposited on it by electron-beam evaporation technique. They also electrodeposited silver nanoparticles (AgNPs) of diameter ~30–50 nm on it by using a potentiodynamic method to enhance the conductivity of the platform and hence sensitivity of the nanochip, while modifying the surface of AuNPs with mercaptophenyl boronic acid for selective adsorption of Neu5Ac. The localised SPR was recorded in the wavelength range 400–650 nm in 0.01 M PBS (pH 7.4) during the sweep of electrode potential in the range 0.0–0.3 V *vs.* Ag/AgCl at a scan rate of 0.05 V s^{-1}. The applied electrochemical potential increased the sensitivity of localised SPR. The refractive index of the SPR-chip and water interface increased in the presence of Neu5Ac because of the preferential binding of *Sia* by the boronic acids and the SPR peak intensity decreased while shifting to higher wavelengths. At the same time, the adsorbed *Sia* on the SPR-chip hindered the movement of the redox-probe (the name was not specified in the manuscript) towards the electrode decreasing voltammetric peak current in the presence of *Sia* in the test solution. Hence, using localised SPR signal recorded during the potential sweep authors could quantify Neu5Ac in the LDR 0.05–5.00 mM with a LOD of 17 μM.[484] However, it can be easily understood now that SPR based analysis of *Sia* is another neglected branch of science along with QCM assay.

5.10 Surface-enhanced Raman spectroscopy (SERS)

In 2014, Vinogradova *et al.* first reported the possibility of SERS assay of *Sia* by using citrate capped AgNPs. Density functional calculation suggested that the negatively charged Neu5Ac could be chemisorbed on the surface of AgNPs *via* competitive adsorption of the carboxylate functional groups. The Raman peak of Neu5Ac at 1391 cm^{-1} enhanced significantly after the adsorption on citrate capped AgNPs upon excitation with 785 nm light.[485] In order to understand the mechanism of adsorption of Neu5Ac on citrate capped AgNPs, Hernández-Arteaga *et al.* extended the experimental and DFT studies on Neu5Ac adsorbed on citrated capped AgNPs in comparison to propanethiol capped AgNPs. It was revealed that citrates could form aggregate structures on AgNPs leaving enough vacant sites available for the adsorption of Neu5Ac on silver by competitive surface adsorption of carboxylate functional groups, whereas propanethiol could uniformly coat AgNPs and hence did not allow adsorption of Nue5Ac on the silver surface.[486] They further extended this study for the diagnosis of breast cancer through the SERS assay of Neu5Ac in human plasma. They used a special logarithmic equation with the average intensities of the SERS peaks at 1391 cm^{-1} (corresponding to stretching of –COOH), 1237 cm^{-1} (corresponding to C–N

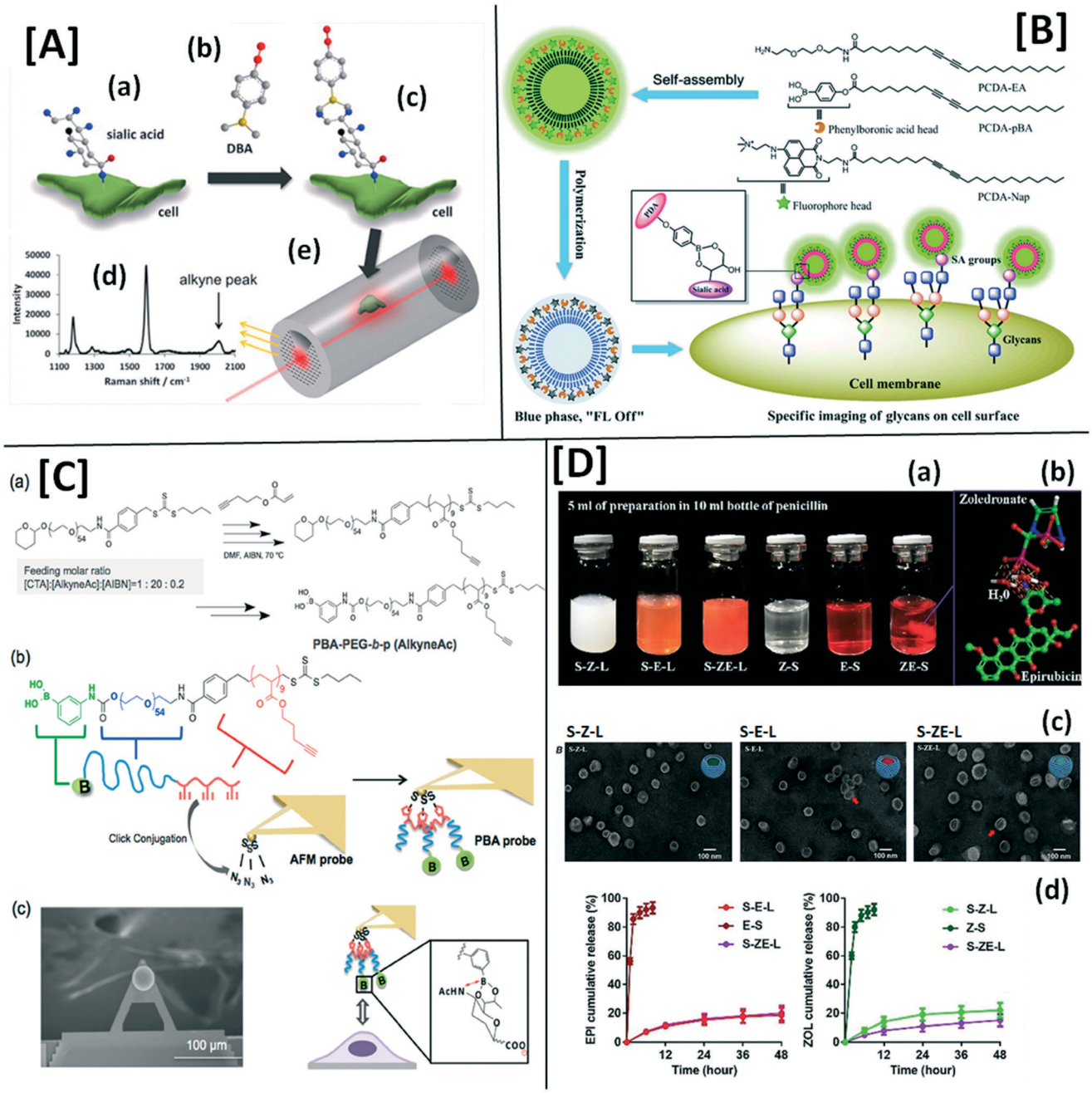

Fig. 9 [A] Illustration of highly sensitive SERS method for detection and quantification method of *Sia* on single cell using photonic-crystal fiber with gold nanoparticles: (a) chemical structure of *Sia* on cell surface; (b) chemical structure of 4-(dihydroxyborophenyl) acetylene (DBA); (c) DBA-bonded *Sia* on the membrane of a cell at the C-8,9 diol of *Sia*; (d) Raman spectrum detected from DBA tagged cell in a solid core photonic crystal fiber, the 2000 cm^{-1} peak corresponded to alkyne group from DBA; (e) schematic of solid core photonic crystal fiber as a SERS platform for detection of *Sia* on a single cell (figures reproduced with permission from ref. 517) Copyright 2015 Elsevier. [B] UV-light assisted self-assembly of 10,12-pentacosadiynoic acid–phenylboronic acid (PCDA–pBA as *Sia* recognising unit), 10,12-pentacosadiynoic acid–1,8-naphthalimide (PCDA–Nap as fluorescent unit with excitation and luminescence maxima at 420 and 535 nm, respectively) and 10,12-pentacosadiynoic acid–ethyl acrylate (PCDA–EA) to form a composite polydiacetylene (PDA) based liposome and the schematic illustration of the as-prepared PDA liposomes for specific cell-glycan imaging (figures reproduced with permission from ref. 395) Copyright 2018 Royal Society of Chemistry. [C] Preparation of a phenylboronic acid (PBA) end functionalised poly-(ethylene glycol) (PEG) onto a cantilever of atomic force microscope (AFM) for dynamic *Sia* specific imaging on human breast cancer cell surfaces with sub-micrometer scale resolution: (a) synthetic scheme for PBA end-functionalized polymer; (b) installation of the polymer to an AFM cantilever by click chemistry. (c) Scanning electron microscopy image of the prepared PBA-modified AFM cantilever and schematic representation of its interaction with *Sia* on cell surface (figures reproduced with permission from ref. 530) Copyright 2020 American Chemical Society. [D] (a) The appearance of liposome (L) composed of hydrogenated soy phosphatidylcholine, cholesterol and *Sia*-octadecylamine in solution of epirubicin (S-E-L), zoledronate (S-Z-L), mixture of epirubicin and zoledronate (S-ZE-L) in comparison to solution of epirubicin (E-S), zoledronate (Z-S), mixture of epirubicin and zoledronate (ZE-S); (b) stable complex of epirubicin and zoledronate with water molecules, (c) transmission electron micrographs of the liposomes S-Z-L, S-E-L and S-ZE-L (scale bar: 100 nm, the red arrows mark the low-solubility aggregates); (d) *in vitro* drug release from S-E-L, S-Z-L and S-ZE-L liposomes in comparison to E-S and Z-S (n = 3) (figures reproduced with permission from ref. 531) Copyright 2021 Elsevier.

mode of amide III) and 1002 cm^{-1} (corresponding to breathing of pyranose ring) in the concentration range 1–200 mg dL^{-1} of Neu5Ac.[487]

Recently, Teng *et al.* reported an enzyme assisted SERS assay of Neu5Ac in the human blood serum (Fig. 8[D]). They drop-casted citrate capped AuNPs on an indium-tin-oxide coated glass plate and submerged that into 0.1 mM 4-mercaptophenylboronic acid solution in dilute ethanol (pH 9.18) for 24 h at room temperature to make a sensing platform. Then, Neu5Ac and glucose were incubated on the sensing platform for 2 h followed by incubation with 0.1 mM 4-mercaptophenylboronic acid solution in dilute ethanol (pH 9.18) for another 24 h at room temperature. Then, that sensing platform was thoroughly washed and again immersed into the colloidal dispersion of citrate capped AuNPs for 18 h at room temperature to form a sandwich structure with AuNPs. To eliminate the interference of glucose, the same procedure was followed but after incubation of the test solution of *Sia* containing glucose with glucose oxidase at 37 °C for 2 h. The SERS signal intensities of Neu5Ac both with and without glucose interference were independently recorded using a confocal Raman instrument set with 785 nm laser line and subtracted to calculate the concentration of Neu5Ac. The LDR and LOD of this SERS assay were reported as 0.25–1.5 and 0.25 μM, respectively.[488] The SERS detection of *Sia*, although promising for clinical applications, is understudied to date compared to other assays for detection and quantification of *Sia*.

Table 3 represents a summary of LDR, LOD and nature of tested samples of the analytical methods (as discussed in Section 5.2–5.10) validated to quality *Sia* in either biological or commercial samples.

5.11 Commercially available *Sia* assay kits

The commercially available assay kits of *Sia* are mostly limited to either colourimetric-spectrophotometric, fluorometric or HPLC-FLD methods. The colorimetric assay kit E-BC-K068[489] and MBS2540448[490] & MBS2563693[491] are microplate-reader and spectrophotometer based reagents containing *Sia* standard (*i.e.*, reagent 1) and a mixture of methyl resorcinol and an oxidant (*i.e.*, reagent 2). The incubation of serum, plasma, saliva, urine, hydrothorax, tissue and cell samples containing *Sia* with reagent 2 produces a purplish red complex having λ_{max} at 560 nm. The concentration of *Sia* in the sample can be determined within 60 min (total assay time) from the absorbance value of the sample with respect to standard in LDR 0.022–7.0 mM. The majority of colourimetric/fluorometric assay kits of *Sia* follow either of enzymatic or improved Warren method. The assay kits K566,[492] EnzyChrom ESLA,[493] LS-K187,[494] PK-CA577-K566,[495] ab83375,[496] ABIN411705,[497] CAK1183,[498] MBS8309610,[499] MBS841610,[500] S1013-31Q,[501] & A0535-01A,[502] Kit-1099[503] and Kit-2477[504] produce equivalent amount of H_2O_2 from free *Sia* by the successive enzymatic reactions of sialic acid aldolase and pyruvate oxidase (reactions 2 and 4 of Section 5.4). Either absorbance (at 570 nm) or fluorescence (excitation and emission maxima at 535 and 587 nm, respectively) of the oxidised product of the reaction between H_2O_2 and amplex red (also known as amplisyn red, 10-acetyl-3,7-dihydroxyphenoxazine and Oxi-Red probe) in the presence of horseradish peroxidase enzyme (reaction 5 of Section 5.4) is used for quantification of free *Sia* in LDR 0.1–10 nmol (0.02–1.0 mM (colourimetric) and 0.002–0.100 mM (fluorometric)) in 40–60 min (assay time). On the other hand, the assay kits KA1655,[505] DSLA,[506] S1013-31P,[507] MAK314,[508] Kit-0783[509] and BA0058[510] oxidise *Sia* by periodate to formylpyruvic acid, which produces a pink-coloured product (having absorbance at 549 nm and excitation/emission maxima at 555/585 nm) from reaction with thiobarbituric acid. These kits can quantify free *Sia* in LDR 0.005–1.0 mM (colourimetric) and 0.0005–0.100 mM (fluorometric) in 40–60 min (assay time).

The commercially available *Sia* assay kit SIALICQ can determine both bound and free *Sia* through successive enzymatic reactions of exo-α-sialidase, sialic acid aldolase and lactate dehydrogenase in the presence of NADH, whose absorbance is monitored at 340 nm (reactions 1–3 of Section 5.4).[511]

The *Sia* assay kits 4400[512] and GKK-407[513] use (ultra) HPLC-FLD methods with a pre-DMB derivatization step for the determination of free and bound (by additional hydrolysis step) *Sia* down to fmols. The assay kits LT-KDMB-A1[514] and GS24-SAP[515] follow similar procedure and it provided *Sia* reference panels containing Neu5Ac, Neu5Gc, $Neu5,7Ac_2$, $Neu5,9Ac_2$, Neu5,Gc9Ac, $Neu5,7,(8),9Ac_3Gc$ along with quantitative standards of Neu5Ac and Neu5Gc.

6. Indirect utilization of *Sia* in cytosensing, therapy and imaging of living cells

As discussed in the previous section, the SERS based assay is underutilised to date with respect to quantification of *Sia*, however Song *et al.* have recently used this technique to capture images of *Sia* on living cells. They prepared a SERS probe of gold nanoflower modified with 5,50-dithio-bis(2-nitrobenzoic acid) (as Raman reporter) and 3-mercaptophenylboronic acid (as *Sia* receptor). This modified nanoflower can bind to the cell surface *Sia* at physiological pH (*i.e.*, 7.4) with the boronic acid group, which will also be available to make a sandwich detection system by anchoring another SERS probe made of poly*Sia* and 5,50-dithio-bis(2-nitrobenzoic acid) modified poly(amidoamine) encapsulated AuNPs. This sandwich-based SERS technique was used to image the cell surface over-expression of *Sia* on the human breast adenocarcinoma (MCF-7) cells in comparison to normal immortalized human keratinocytes (HaCaT) cells.[516] Gong *et al.* synthesised 4-(dihydroxyborophenyl) acetylene for dual role. It results in an interference-free Raman signal as well as binding to *Sia*

on cell surface. Upon loading the mixture of AuNPs and test cells incubated with 4-(dihydroxyborophenyl) acetylene at the side panel of the photonic crystal fibre and propagating laser light through central core, they could measure the average *Sia* concentration even on a single-cell by utilising the Raman peak at 2000 cm^{-1} corresponding to acetylene unit (-Fig. 9[A]).[517] Similarly, He *et al.* modified AgNPs of average diameter 60 nm, by both 4-mercaptophenylboronic acid (as *Sia* binding unit) and 4-mercaptobenzenitrile (as Raman reporter) to quantify the average cell surface *Sia* concentration from the interference-free SERS peak at 2232 cm^{-1} corresponding to cyanide unit.[518] Liang *et al.* modified AgNPs of average diameter of 40 nm by 4-mercaptophenylboronic acid and used confocal SERS technique at 1074 and 1570 cm^{-1} for measuring and imaging the overexpression of *Sia* on HepG2, HeLa, BNL.CL2 cells to diagnose breast cancer.[519] Shinde *et al.* prepared a SiO_2 (as core of diameter ~200 nm) and fluorescent-MIP (as shell of thickness ~10 nm) based composite material for selective imaging of sialylated glycans on cell surfaces. They used nitrobenzoxadiazole (as fluorescence reporter having excitation and luminescence peaks at 411 and 509 nm, respectively), ester of polyvinylphenylboronic acid and Neu5Ac (as template) and 2-aminoethyl-methacrylate hydrochloride (as additional hydrogen bonding agent) and 2-(-3-(4-nitrobenzo[*c*][1,2,5]oxadiazo-7-yl)ureido)-ethylmethacrylate (as additional carboxylate recognition site for *Sia*) in the MIP shell. This core–shell fluorescence probe was successfully used to image the sialylated glycans on surfaces of the prostate cancer cell lines DU145, PC3 and leukemic cell line Jurkat T cells.[520] As discussed in section 5.3, the fluorescent polydiacetylene based liposome was prepared for the fluorescence-based assay of free *Sia*. 100 μM of this fluorescence probe was also used for imaging sialylated glycans expressed on MCF-7 cells through confocal microscopy (Fig. 9[B]).[522] Peng *et al.* prepared tetraphenylethene tagged peptidylboronic acids having aggregation-induced emission at 460 nm (maxima). The change in luminescent intensity was selective for *Sia* compared to other monosaccharides and this phenomenon was used to label and image cancer cells owing to higher *Sia* expressions on their cell surfaces.[521] Recently, Geng *et al.* modified AgNPs of average diameter ~50 nm with 4-mercaptophenylboronic acid to recognise *Sia* and used it in a non-linear optical imaging technique known as four-wave-mixing to visualize *Sia* on A549, HeLa, HepG2 and MCF-7 cells.[522] Almeida-Marrero *et al.* recently synthesised a photosensitizer by covalently linking dendritic zinc(II) phthalocyanine with 3 units of Neu5Ac for the photodynamic therapy through *in situ* generation of photoinduced singlet oxygen and other reactive species in the lysosome. The amphiphilic Neu5Ac modified photosensitizer formed non-photoresponsive self-assembled nano-aggregates and enters into the cellular lysosome, where it could regain its photoresponse.[523] Yang *et al.* modified a gold coated QCM with mercaptobutanedioic acid followed by concanavalin A lectin to specifically attach mannose of the cell surface of RBC. Then AuNPs modified with 4-aminobenzeneboronic acid were added on the modified QCM with RBC to measure the average number of *Sia* $2.1 \pm 0.2 \times 10^8$ on RBC of healthy person compared to $8.2 \pm 0.7 \times 10^7$ on RBC of a diabetic patient.[524]

Qian *et al.* demonstrated a multivalent recognition and signal amplification strategy for cancer cell cytosensing and dynamic evaluation of cell surface *Sia* using graphene oxide functionalised with 3-aminophenylboronic acid for cell capture and *Sambucus nigra* agglutinin and thionine conjugated to gold nanoparticles. The DPV based electrochemical method was used to monitor the changes in expression of *Sia* in response to addition of sialidase enzyme.[525] A similar approach combined 3-aminophenylboronic acid modified carbon nanospheres for *Sia* recognition with horseradish peroxidase decorated gold nanoparticles for signal amplification. The electrochemical cytosensor realised an identification system using *Sambucus nigra* agglutinin and 3-aminophenylboronic acid modified carbon nanospheres for cancer cell capture with measurement of the expression level of *Sia* on MCF-7 cells *vs.* control cell lines (LOD of 25 cells per mL).[526] Zhang *et al.* electrochemically prepared poly-pyrrole on a gold electrode allowing physical inclusion of bovine serum albumin incorporated silver submicron particles into the polymer matrix. Then the electrode was modified with 3-aminophenylboronic acid through the cross-linking agent *p*-phenylene-diisothiocyanate. This modified electrode was used to diagnose renal cell carcinoma from the change of charge-transfer resistance of $[Fe(CN)_6]^{3-/4-}$ electrochemical reaction with LDR and LOD 17–1.7×10^6 and 6 Cell786-O per mL (S/N = 3), respectively.[527] Matsumoto *et al.* used 3-aminophenylboronic acid end-functionalised poly(ethylene glycol) modified gold electrode for potentiometric determination of a blood-circulating glycoprotein fetuin at pH 7.4.[528]

Landa *et al.* modified AuNPs of average diameter 20 nm with Neu5Ac to generate a negatively charged nanoprobe of zeta potential −13.21 ± 1.87 mV and absorption maxima at 520 nm in neutral pH. This nanoprobe was agglomerated in the presence of gram-positive bacteria *viz. Staphylococcus aureus* and methicillin resistant *Staphylococcus aureus* extending the absorption to longer wavelengths, but did not show any changes in the presence of Gram-negative bacteria *viz. Pseudomonas aeruginosa*. This method was effective to discriminate Gram-positive and Gram-negative bacteria at high concentration ~10^5 CFU mL^{-1} in tryptic soy broth medium and serum sample.[529]

Finally, a phenylboronic acid end functionalised poly-(ethylene glycol) was decorated onto a cantilever of atomic force microscope for dynamic *Sia* specific imaging on human breast cancer cell surfaces with sub-micrometer scale resolution (Fig. 9[C]). A greater extent of probe-surface interaction was observed for the high *Sia* expressed MCF-7 as compared to health control cell lines, taking advantage

of the reversible and pH dependant boronic acid-*Sia* binding chemistry.[530] *Sia* receptors are usually over-expressed on the surface of tumour-associated macrophages. Sui *et al.* reported that sequential administration of *Sia* (0.2 mg mL^{-1}) modified epirubicin (0.056 mg mg^{-1} of lipid) liposome followed by (after 24 h) *Sia* modified zoledronate (0.08 mg mg^{-1} of lipid) liposome (Fig. 9[D]) could kill the tumour-associated macrophages and restrict tumour growth in mice.[531]

The commercially available EZClick™ sialic acid (ManAz) modified glycoprotein assay kit K441 uses direct feeding of modified ManAc precursor into the cell for biosynthesis of *Sia* followed by its participation in *N*-glycosylation of cell surface protein, which can be mapped and quantified by using fluorescence-activated cell sorting method following the click reaction with an alkyne-containing dye. This assay is very useful to identify the altered sialylation of tumour-cell surfaces.[532] Similarly, the GlyS Kit is used to screen the terminal *Sia* content of glycans in protein of interest even in the presence of host cell glycoproteins in crude samples by high throughput Octet system.[533]

7. Future direction

Sia is widely distributed in free, polymeric and conjugated forms in living creatures. However, the discovery and identification of new members of the *Sia* family is yet an open science. Furthermore, with the advancement of analytical methodologies to achieve ultra-trace LODs, exploration of *Sia* in different parts of plants has a great opportunity to either discover green resources of *Sia* or confirm the absence of *Sia* in plants, fruits and vegetables.

The involvement of *Sia* in important physiology including brain development and formation of central nervous system during foetal and neonatal stages has been studied mostly on animals *viz.* laboratory rats and pigs and correlated to human physiology. The participation of *Sia* in the human immune system has been studied, and has keen ongoing interest, especially given the inconclusive evidence of *Sia*'s involvement in several bacterial and viral infections including SARS-CoV-2 causing COVID-19 disease. The over-/under-expression of *Sia* in human cells/tissues/fluids during physiological disorders and onset of cancers are now in high surveillance to promote *Sia* as one of the potential biomarkers for a number of human diseases.

The correlated case studies of *Sia* in human lactation and infant cognition produced sufficient evidence to receive regulatory approval for use of Neu5Ac.2H_2O, 3′-sialyllactose sodium salt and 6′-sialyllactose sodium salt in infant formula and commercial food products as nutrition additives. This has definitely boosted the demand of *Sia* in commercial domain, although the number of economic and large-scale production of *Sia* suitable for safe consumption by humans is very limited at present.

The emerging biological relevance of *Sia* in human health and clinical sciences along with its commercial role in human health and nutrition has increased the importance of development of robust sensors and diagnostic methods for *Sia* in complex clinical and food matrices. There is a vast scope of research and development in this direction as presented in this review. In summary, it should be mentioned that knowledge of the biological role and participation of *Sia* in human physiology is expanding day-by-day. Hence, the extension of the analytical horizons of *Sia* beyond the current state of the art will underpin further explorations in the expansive *Sia* galaxy.

Symbols and abbreviations

Symbols

ε	Molar absorption coefficient
λ_{Max}	Absorbance maxima
C	Carbon
n	Number of samples/persons/patients

Abbreviations

ACE2	Angiotensin-converting enzyme 2
ADOA	4-(Acetylamino)-2,4-dideoxy-D-*glycero*-D-galacto-octonic acid
AgNPs	Silver nanoparticles
AuNPs	Gold nanoparticles
cGMP	Caseinoglycomacropeptide
CMP	Cytidine-5′-monophosphate
CoV	Corona virus
CTD	C-Terminal domain
DMB	1,2-Diamino-4,5-methyleneoxybenzene
DPV	Differential pulse voltammetry
EBN	Edible bird's nest
ECL	Electrochemiluminescence
EIS	Electrochemical impedance spectroscopy
ESI	Electron spray ionization
HMOs	Human milk oligosaccharides
HPLC-FLD	High performance liquid chromatography coupled with fluorescence detection
HPLC-MS	High performance liquid chromatography coupled with mass-spectrometry detection
HPLC-PAD	High performance liquid chromatography coupled with pulsed-amperometry detection
HPLC-UV–vis	High performance liquid chromatography coupled with UV–Vis detection
KDN	2-Keto-3-deoxy-D-*glycero*-D-galacto-nononic acid
LDR	Linear dynamic range
LOD	Limit of detection
ManNAc	*N*-Acetyl-D-mannosamine
MERS-CoV	Middle east respiratory syndrome coronavirus
MIP	Molecularly imprinted polymer
NADH	Reduced nicotinamide adenine dinucleotide
NCAM	Neural cell adhesion molecule
ND	Not detected
Neu5Ac	*N*-Acetyl-D-neuraminic acid

Neu5Gc	*N*-Glycolyl-D-neuraminic acid
NMR	Nuclear magnetic resonance
NR	Not reported
NTD	N-terminal domain
OECT	Organic electrochemical transistors
PBS	Phosphate buffer saline
PEC	Photoelectrochemistry
poly*Sia*	Poly-sialic acid
QCM	Quartz crystal microbalance
RBC	Red blood cells
SAMPs	Self-associated molecular patterns
SARS-CoV	Severe acute respiratory syndrome coronavirus
SARS-CoV-2	Severe acute respiratory syndrome coronavirus 2 (novel corona virus)
SERS	Surface-enhanced Raman spectroscopy
Sia	Sialic acid
Siglec	Sialic acid binding immunoglobulin like lectin
SPR	Surface plasmon resonance
ST8SiaII	ST8-α-*N*-Acetyl-neuraminide-α-2,8-sialyltransferase-2
ST8SiaIV	ST8-α-*N*-Acetyl-neuraminide-α-2,8-sialyltransferase-4
T2DM	Type 2 diabetic mellitus
UDP-GlcNAc	Uridine diphosphate-*N*-acetylglucosamine

8. Funding source

This project has received funding from the Enterprise Ireland and the European Union's Horizon 2020 Research and Innovation Programme under the Marie Skłodowska-Curie Career FIT PLUS grant agreement no. 847402 (Project No. MF20200140).

Author contributions

Dr. Saurav K. Guin has completed the literature survey and written the original draft. Dr. Eithne Dempsey and Dr. Trinidad Velasco-Torrijos reviewed and edited the manuscript. Dr. Dempsey and Dr. Guin are jointly involved in conceptualisation, funding acquisition and administration of this project.

Conflicts of interest

There are no conflicts to declare.

Acknowledgements

Dr. Guin wishes to acknowledge the Open-Access Publication Policy of Enterprise Ireland and the European Union's Horizon 2020 Research and Innovation Programme under the Marie Skłodowska-Curie Career FIT PLUS fellowship for dissemination of work to wider community. The authors acknowledge Dr. Fergal Lawless and Glanbia Ingredients Ireland. Dr. Guin wishes to thank Dr. P.K. Pujari, Director of Radiochemistry and Isotope Group and Dr. S. Kannan, Head of Fuel Chemistry Division in Bhabha Atomic Research Centre for approving his visit (on leave) in Ireland.

References

1 R. Schauer and J. P. Kamerling, in *Glycoproteins II*, ed. J. Montreuil, J. F. G. Vliegenthart and H. Schachter, Elsevier Science Publishers B.V, Amsterdam, 1997, pp. 243–372.
2 T. Janas and T. Janas, *Biochim. Biophys. Acta, Biomembr.*, 2011, **1808**, 2923–2932.
3 E. Klenk, *Biol. Chem.*, 1935, **235**, 24–36.
4 E. Klenk, H. Langerbeins and E. Schumann, *Biol. Chem.*, 1941, **270**, 185–193.
5 E. Klenk, *Biol. Chem.*, 1941, **268**, 50–58.
6 F. G. Blix, *Biol. Chem.*, 1936, **240**, 43–54.
7 G. Blix, L. Svennerholm and I. Werner, *Acta Chem. Scand.*, 1952, **6**, 358–362.
8 T. Yamakawa and S. Suzuki, *J. Biochem.*, 1951, **38**, 199–212.
9 A. Gottschalk, *Nature*, 1951, **176**, 845–847.
10 J. R. E. Hoover, G. A. Braun and P. György, *Arch. Biochem. Biophys.*, 1953, **47**, 216–217.
11 F. Zilliken, G. A. Braun and P. György, *Arch. Biochem. Biophys.*, 1955, **54**, 564–566.
12 K. Richard, R. Brossmer and M. von W. Schulz, *Chem. Ber.*, 1954, **87**, 123–127.
13 A. Gottschalk, *Nature*, 1955, **176**, 881–882.
14 F. G. Blix, A. Gottschalk and E. Klenk, *Nature*, 1957, **179**, 1088.
15 L. Warren and H. Felsenfeld, *J. Biol. Chem.*, 1962, **237**, 1421–1431.
16 M. E. Tanner, *Bioorg. Chem.*, 2005, **33**, 216–228.
17 L. Shaw and R. Schauer, *Biol. Chem. Hoppe-Seyler*, 1988, **369**, 477–486.
18 T. Hayakawa, Y. Satta, P. Gagneux, A. Varki and N. Takahata, *Proc. Natl. Acad. Sci. U. S. A.*, 2001, **98**, 11399–11404.
19 P. S. K. Ng, R. Böhm, L. E. Hartley-Tassell, J. A. Steen, H. Wang, S. W. Lukowski, P. L. Hawthorne, A. E. O. Trezise, P. J. Coloe, S. M. Grimmond, T. Haselhorst, M. Von Itzstein, A. W. Paton, J. C. Paton and M. P. Jennings, *Nat. Commun.*, 2014, **5**, 5750.
20 S. A. Springer, S. L. Diaz and P. Gagneux, *Immunogenetics*, 2014, **66**, 671–674.
21 M. Jahan, P. C. Thomson, P. C. Wynn and B. Wang, *Food Chem.*, 2021, **343**, 128439.
22 S. Inoue and K. Kitajima, *Glycoconjugate J.*, 2006, **23**, 277–290.
23 S. Ghosh, *Sialic acid and biology of life: An introduction*, Elsevier B.V., 2020/01/17, 2020.
24 M. Yang, S. H. Cheung, S. C. Li and H. Y. Cheung, *Food Chem.*, 2014, **151**, 271–278.
25 O. Mahaq, M. A. Mohd, M. Jaoi Edward, N. Mohd Hanafi, S. Abdul Aziz, H. Abu Hassim, M. H. Mohd Noor and H. Ahmad, *Brain Behav.*, 2020, **10**, e01817.

26 G. K. Chan, K. Y. Zheng, K. Y. Zhu, T. T. Dong and K. W. Tsim, *The Journal of Ethnobiology and Traditional Medicine*, 2013, **120**, 620–628.
27 R. Zeleny, D. Kolarich, R. Strasser and F. Altmann, *Planta*, 2006, **224**, 222–227.
28 A. N. Samraj, O. M. T. Pearce, H. Läubli, A. N. Crittenden, A. K. Bergfeld, K. Band, C. J. Gregg, A. E. Bingman, P. Secrest, S. L. Diaz, N. M. Varki, A. Varki and S. A. Kornfeld, *Proc. Natl. Acad. Sci. U. S. A.*, 2015, **112**, 542–547.
29 L. Ye, L. Mu, G. Li and Y. Bao, *J. Food Compos. Anal.*, 2020, **87**, 103393.
30 L. J. Sun, Y. Xie, Y. F. Yan, H. Yang, H. Y. Gu and N. Bao, *Sens. Actuators, B*, 2017, **247**, 336–342.
31 L. Xia, L. Liu, F. Qu, R. Kong, G. Li and J. You, *Chromatographia*, 2017, **80**, 861–872.
32 R. Schauer and J. P. Kamerling, *Exploration of the Sialic Acid World*, Elsevier Inc., 1st edn, 2018, vol. 75.
33 H. Yang, L. Lu and X. Chen, *Biotechnol. Adv.*, 2021, **46**, 107678.
34 M. Huizing, M. E. Hackbarth, D. R. Adams, M. Wasserstein, M. C. Patterson, S. U. Walkley, W. A. Gahl, K. Dobrenis, J. Foglio, B. Gasnier, M. Hackbarth, M. Lek, M. C. V. Malicdan, L. E. Paavola, R. Reimer, R. Y. Wang and R. Zoncu, *Neurosci. Lett.*, 2021, **755**, 135896.
35 R. Heida, Y. C. Bhide, M. Gasbarri, Ö. Kocabiyik, F. Stellacci, A. L. W. Huckriede, W. L. J. Hinrichs and H. W. Frijlink, *Drug Discovery Today*, 2021, **26**, 122–137.
36 P. Burzy, K. Mikołajczyk, M. Jodłowska and E. Ja, *Biomolecules*, 2021, **11**, 831.
37 E. Gianchecchi, A. Arena and A. Fierabracci, *Int. J. Mol. Sci.*, 2021, **22**, 5774.
38 X. Zhou, G. Yang and F. Guan, *Cell*, 2020, **9**, 273.
39 R. Lacomba, J. Salcedo, A. Alegría, M. Jesús Lagarda, R. Barberá and E. Matencio, *J. Pharm. Biomed. Anal.*, 2010, **51**, 346–357.
40 J. Cheeseman, G. Kuhnle, D. I. R. Spencer and H. M. I. Osborn, *Bioorg. Med. Chem.*, 2021, **30**, 115882.
41 V. Andriukaitis, *Official Journal of the European Union*, 2017, **L 337**, 63–67.
42 A. B. Engin, E. D. Engin and A. Engin, *Environ. Toxicol. Pharmacol.*, 2020, **79**, 103436.
43 P. Wielgat, K. Rogowski, K. Godlewska and H. Car, *Cell*, 2020, **9**, 1963.
44 X.-L. Sun, *Glycobiology*, 2021, cwab032.
45 W. Zhao, T. L. L. Chen, B. M. Vertel and K. J. Colley, *J. Biol. Chem.*, 2006, **281**, 31106–31118.
46 F. Tokumasu, G. R. Ostera, C. Amaratunga and R. M. Fairhurst, *Exp. Parasitol.*, 2012, **131**, 245–251.
47 S. E. Quaggin, *J. Clin. Invest.*, 2007, **117**, 1480–1483.
48 A. Varki, *Glycobiology*, 2011, **21**, 1121–1124.
49 X. Wang, N. Mitra, I. Secundino, K. Banda, P. Cruz, V. Padler-Karavani, A. Verhagen, C. Reid, M. Lari, E. Rizzi, C. Balsamo, G. Corti, G. De Bellis, L. Longo, W. Beggs, D. Caramelli, S. A. Tishkoff, T. Hayakawa, E. D. Green, J. C. Mullikin, V. Nizet, J. Bui and A. Varki, *Proc. Natl. Acad. Sci. U. S. A.*, 2012, **109**, 9935–9940.
50 P. R. Crocker, J. C. Paulson and A. Varki, *Nat. Rev. Immunol.*, 2007, **7**, 255–266.
51 H. Läubli and A. Varki, *Cell. Mol. Life Sci.*, 2020, **77**, 593–605.
52 S. Pillai, I. A. Netravali, A. Cariappa and H. Mattoo, *Annu. Rev. Immunol.*, 2012, **30**, 357–392.
53 B. S. Blaum, J. P. Hannan, A. P. Herbert, D. Kavanagh, D. Uhrín and T. Stehle, *Nat. Chem. Biol.*, 2015, **11**, 77–82.
54 C. Q. Schmidt, A. L. Hipgrave Ederveen, M. J. Harder, M. Wuhrer, T. Stehle and B. S. Blaum, *Glycobiology*, 2018, **28**, 765–773.
55 B. A. H. Smith and C. R. Bertozzi, *Nat. Rev. Drug Discovery*, 2021, **20**, 217–243.
56 K. Sołkiewicz, H. Krotkiewski, M. Jędryka and E. M. Kratz, *Sci. Rep.*, 2021, **11**, 5586.
57 J. Finne, *J. Biol. Chem.*, 1982, **257**, 11966–11970.
58 C. Weisgerber, M. Husmann, M. Frosch, C. Rheinheimer, T. W. Peuckert and I. Gorgen, *J. Neurochem.*, 1990, **55**, 2063–2071.
59 J. Ahrens, N. Foadi, A. Eberhardt, G. Haeseler, R. Dengler, A. Leffler, M. Mühlenhoff, R. Gerardy-Schahn and M. Leuwer, *Pharmacology*, 2011, **87**, 311–317.
60 J. Nakayama, M. N. Fukuda, B. Fredette, B. Ranscht and M. Fukuda, *Proc. Natl. Acad. Sci. U. S. A.*, 1995, **92**, 7031–7035.
61 M. S. Skog, J. Nystedt, M. Korhonen, H. Anderson, T. A. Lehti and M. I. Pajunen, *Stem Cell Res. Ther.*, 2016, **7**, 113.
62 P. M. Drake, J. K. Nathan, C. M. Stock, P. V. Chang, M. O. Muench, D. Nakata, J. R. Reader, P. Gip, K. P. K. Golden, B. Weinhold, R. Gerardy-Schahn, F. A. Troy and C. R. Bertozzi, *J. Immunol.*, 2008, **181**, 6850–6858.
63 T. M. Villanueva-Cabello, L. D. Gutiérrez-Valenzuela, D. V. López-Guerrero, M. E. Cruz-Muñoz, H. M. Mora-Montes and I. Martínez-Duncker, *Glycobiology*, 2019, **29**, 557–564.
64 S. Werneburg, F. F. R. Buettner, M. Mühlenhoff and H. Hildebrandt, *Stem Cell Res.*, 2015, **14**, 339–346.
65 U. Yabe, C. Sato, T. Matsuda and K. Kitajima, *J. Biol. Chem.*, 2003, **278**, 13875–13880.
66 S. Curreli, Z. Arany, R. Gerardy-schahn, D. Mann and N. M. Stamatos, *J. Biol. Chem.*, 2007, **282**, 30346–30356.
67 R. W. Nelson, P. A. Bates and U. Rutishauser, *J. Biol. Chem.*, 1995, **270**, 17171–17179.
68 S. S. Mendiratta, N. Sekulic, A. Lavie and K. J. Colley, *J. Biol. Chem.*, 2005, **280**, 32340–32348.
69 S. S. Mendiratta, N. Sekulic, F. G. Hernandez-Guzman, B. E. Close, A. Lavie and K. J. Colley, *J. Biol. Chem.*, 2006, **281**, 36052–36059.
70 J. L. Brusés and U. Rutishauser, *J. Cell Biol.*, 1998, **140**, 1177–1186.
71 P. C. Hallenbeck, E. R. Vimr, F. Yu, B. Basslero and A. Troyn, *J. Biol. Chem.*, 1987, **262**, 3553–3561.
72 C. D. Hunter and C. Cairo, *ChemRxiv*, 2021, DOI: 10.26434/chemrxiv.14065025.v1.
73 A. Mori, M. Hane, Y. Niimi, K. Kitajima and C. Sato, *Glycobiology*, 2017, **27**, 834–846.
74 F. Miragall, G. Kadmon, M. Husmann and M. Schachner, *Dev. Biol.*, 1988, **129**, 516–531.
75 L. Bonfanti, *Prog. Neurobiol.*, 2006, **80**, 129–164.

76 U. Rutishauser, *Nat. Rev. Neurosci.*, 2008, **9**, 26–35.
77 C. Sato and K. Kitajima, *Sialic Acids in Neurology*, Elsevier Inc., 1st edn, 2019, vol. 76.
78 P. Simon, S. Bäumner, O. Busch, R. Röhrich, M. Kaese, P. Richterich, A. Wehrend, K. Müller, R. Gerardy-schahn, M. Mühlenhoff, H. Geyer, R. Geyer, R. Middendorff and S. P. Galuska, *J. Biol. Chem.*, 2013, **288**, 18825–18833.
79 R. D. Astronomo and D. R. Burton, *Nat. Rev. Drug Discovery*, 2010, **9**, 308–324.
80 Y. Wang and H. Neumann, *J. Neurosci.*, 2010, **30**, 3482–3488.
81 J. Roth, C. Zuber, P. Komminoth, T. Sata, W. P. Li and P. U. Heitz, *Histochem. Cell Biol.*, 1996, **106**, 131–148.
82 C. Sato and K. Kitajima, *Mol. Aspects Med.*, 2020, 100892, In press.
83 K. F. Boligan, J. Oechtering, C. W. Keller, B. Peschke, R. Rieben, N. Bovin, L. Kappos, R. D. Cummings, J. Kuhle, S. von Gunten and J. D. Lünemann, *Neurol. Neuroimmunol. Neuroinflamm.*, 2020, **7**, e676.
84 R. Sandhoff and K. Sandhoff, *FEBS Lett.*, 2018, **592**, 3835–3864.
85 L. Svennerholm, in *Cholera and Related Diarrheas 43rd Nobel Symposium*, Stockholm, 1978, pp. 80–87.
86 L. Svennerhom, *Gangliosides and Synaptic Transmission*, Springer, Boston, MA, 1980.
87 L. Svennerholm, *Prog. Brain Res.*, 1994, **101**, xi–xiv.
88 R. K. Yu, T. Ariga, M. Yanagisawa and G. Zeng, in *Glycoscience*, ed. B. O. Fraser-Reid, K. Tatsuta and J. Thiem, 2008, pp. 1671–1695.
89 R. K. Yu, Y. Nakatani and M. Yanagisawa, *J. Lipid Res.*, 2009, **50**, S440–S445.
90 S. Ando, N. C. Chang and R. K. Yu, *Anal. Biochem.*, 1978, **89**, 437–450.
91 M. Sarbu, A. C. Robu, R. M. Ghiulai, Ž. Vukelić, D. E. Clemmer and A. D. Zamfir, *Anal. Chem.*, 2016, **88**, 5166–5178.
92 M. Sarbu, Ž. Vukelić, D. E. Clemmer and A. D. Zamfir, *Analyst*, 2018, **143**, 5234–5246.
93 M. Sarbu, L. Dehelean, C. V. A. Munteanu, Ž. Vukelić and A. D. Zamfir, *Anal. Biochem.*, 2017, **521**, 40–54.
94 M. Sarbu, S. Raab, L. Henderson, D. Fabris, Z. Vukelic, D. E. Clemmer and A. D. Zam, *Biochimie*, 2020, **170**, 36–48.
95 N. Sasaki, M. Toyoda and T. Ishiwata, *Int. J. Mol. Sci.*, 2021, **22**, 5076.
96 M. Sarbu, L. Petrica, D. E. Clemmer, Ž. Vukelić and A. D. Zamfir, *J. Am. Soc. Mass Spectrom.*, 2021, **32**, 1249–1257.
97 M. Sarbu, D. E. Clemmer and A. D. Zamfir, *Biochimie*, 2020, **177**, 226–237.
98 E. Chiricozzi, E. Di Biase, M. Maggioni, G. Lunghi, M. Fazzari, D. Y. Pomè, R. Casellato, N. Loberto, L. Mauri and S. Sonnino, *J. Neurochem.*, 2019, **149**, 231–241.
99 N. Sasaki, Y. Itakura and M. Toyoda, *Int. J. Mol. Sci.*, 2019, **20**, 1–12.
100 S. Sipione, J. Monyror, D. Galleguillos, N. Steinberg and V. Kadam, *Front. Neurosci.*, 2020, **14**, 572965.
101 T. Mitsuda, K. Furukawa, S. Fukumoto, H. Miyazaki, T. Urano and K. Furukawa, *J. Biol. Chem.*, 2002, **277**, 11239–11246.
102 Y. Ohkawa, H. Momota, A. Kato, N. Hashimoto, Y. Tsuda, N. Kotani, K. Honke, A. Suzumura, K. Furukawa, Y. Ohmi, A. Natsume, T. Wakabayashi and K. Furukawa, *J. Biol. Chem.*, 2015, **290**, 16043–16058.
103 R. París, A. Morales, O. Coll, A. Sánchez-Reyes, C. García-Ruiz and J. C. Fernández-Checa, *J. Biol. Chem.*, 2002, **277**, 49870–49876.
104 R. De Maria, L. Lenti, F. Malisan, B. Tomassini, A. Zeuner, M. R. Rippo and R. Testi, *Science*, 1997, **277**, 1652–1655.
105 Y. Makino, K. Hamamura, Y. Takei, R. Hasan, Y. Ohkawa and G. Lauc, *Biochim. Biophys. Acta, Gen. Subj.*, 2016, **1860**, 1753–1763.
106 K. Furukawa, M. Kambe, M. Miyata, Y. Ohkawa, O. Tajima and K. Furukawa, *Cancer Sci.*, 2014, **105**, 52–63.
107 K. Hamamura, M. Tsuji, H. Hotta, Y. Ohkawa, M. Takahashi, H. Shibuya, H. Nakashima, Y. Yamauchi, N. Hashimoto, H. Hattori, M. Ueda, K. Furukawa and K. Furukawa, *J. Biol. Chem.*, 2011, **286**, 18526–18537.
108 Y. Liang, C. Wang, I. Wang, Y. Chen, L. Li, M. Ho, T. Chou, Y. Wang, S. Chiou, Y. Lin and J. Yu, *Oncotarget*, 2017, **8**, 47454–47473.
109 B. L. Mirkin, S. H. Clark and C. Zhang, *Cell Proliferation*, 2002, **35**, 105–115.
110 N. Kawashima, Y. Nishimiya, S. Takahata and K. I. Nakayama, *J. Biol. Chem.*, 2016, **291**, 21424–21433.
111 S. Kawamura, I. Sato, T. Wada, K. Yamaguchi, Y. Li, D. Li, X. Zhao, S. Ueno, H. Aoki, T. Tochigi, M. Kuwahara, T. Kitamura, K. Takahashi, S. Moriya and T. Miyagi, *Cell Death Differ.*, 2012, **19**, 170–179.
112 H. Wang, T. Isaji, M. Satoh, D. Li, Y. Arai and J. Gu, *Urology*, 2013, **81**, 210.E11–210.E15.
113 K. Shiga, K. Takahashi, I. Sato, K. Kato, S. Saijo, S. Moriya, M. Hosono and T. Miyagi, *Cancer Sci.*, 2015, **106**, 1544–1553.
114 H. J. Choi, T. W. Chung, S. K. Kang, Y. C. Lee, J. H. Ko, J. G. Kim and C. H. Kim, *Glycobiology*, 2006, **16**, 573–583.
115 K. Takahashi, M. Hosono, I. Sato, K. Hata, T. Wada, K. Yamaguchi, K. Nitta, H. Shima and T. Miyagi, *Int. J. Cancer*, 2015, **137**, 1560–1573.
116 T. W. Chung, H. J. Choi, S. J. Kim, C. H. Kwak, K. H. Song, U. H. Jin, Y. C. Chang, H. W. Chang, Y. C. Lee, K. T. Ha and C. H. Kim, *PLoS One*, 2014, **9**, e92786.
117 N. Sasaki, K. Hirabayashi, M. Michishita, K. Takahashi, F. Hasegawa, F. Gomi, Y. Itakura, N. Nakamura, M. Toyoda and T. Ishiwata, *Sci. Rep.*, 2019, **9**, 19369.
118 K. Nguyen, Y. Yan, B. Yuan, A. Dasgupta, J. Sun, H. Mu, K. A. Do, N. T. Ueno, M. Andreeff and V. Lokesh Battula, *Mol. Cancer Ther.*, 2018, **17**, 2689–2701.
119 A. Cazet, M. Bobowski, Y. Rombouts, J. Lefebvre, A. Steenackers, I. Popa, Y. Guérardel, X. Le Bourhis, D. Tulasne and P. Delannoy, *Glycobiology*, 2012, **22**, 806–816.
120 T. Iwasawa, P. Zhang, Y. Ohkawa, H. Momota, T. Wakabayashi, Y. Ohmi, R. H. Bhuiyan, K. Furukawa and K. Furukawa, *Int. J. Oncol.*, 2018, **52**, 1255–1266.

121 S. Yoshida, S. Fukumoto, H. Kawaguchi, S. Sato, R. Ueda and K. Furukawa, *Cancer Res.*, 2001, **61**, 4244–4252.
122 W. Aixinjueluo, K. Furukawa, Q. Zhang, K. Hamamura, N. Tokuda, S. Yoshida, R. Ueda and K. Furukawa, *J. Biol. Chem.*, 2005, **280**, 29828–29836.
123 S. Hyuga, N. Kawasaki, M. Hyuga, M. Ohta, R. Shibayama, T. Kawanishi, S. Yamagata, T. Yamagata and T. Hayakawa, *Int. J. Cancer*, 2001, **94**, 328–334.
124 S. H. Ha, J. M. Lee, K. M. Kwon, C. H. Kwak, F. Abekura, J. Y. Park, S. H. Cho, K. Lee, Y. C. Chang, Y. C. Lee, H. J. Choi, T. W. Chung, K. T. Ha, H. W. Chang and C. H. Kim, *Int. J. Mol. Sci.*, 2016, **17**, 652.
125 J. H. Hwang, J. S. Sung, J. M. Kim, Y. H. Chung, J. S. Park, S. H. Lee and I. S. Jang, *Am. J. Cancer Res.*, 2014, **4**, 801–810.
126 R. Rajan, A. R. Sheth and S. S. Rao, *Eur. J. Obstet. Gynecol. Reprod. Biol.*, 1983, **16**, 37–46.
127 M. H. Alvi, N. A. Amer and I. Sumerin, *Obstet. Gynecol.*, 1988, **72**, 171–174.
128 E. Salvolini, R. Di Giorgio, A. Curatola, L. Mazzanti and G. Fratto, *Br. J. Obstet. Gynaecol.*, 1998, **105**, 656–660.
129 N. Moretti, R. A. Rabini, L. Nanetti, G. Grechi, M. C. Curzi, N. Cester, L. A. Tranquilli and L. Mazzanti, *Metabolism*, 2002, **51**, 605–608.
130 M. Orczyk-Pawiłowicz, J. Floriański, J. Zalewski and I. Kątnik-Prastowska, *Glycoconjugate J.*, 2005, **22**, 433–442.
131 Y. Zhu and M. Li, *Int. J. Clin. Exp. Med.*, 2017, **10**, 12322–12328.
132 S. Martín-Sosa, M. J. Martín, L. A. García-Pardo and P. Hueso, *J. Pediatr. Gastroenterol. Nutr.*, 2004, **39**, 499–503.
133 B. Wang, J. Brand-Miller, P. McVeagh and P. Petocz, *Am. J. Clin. Nutr.*, 2001, **74**, 510–515.
134 E. B. Isaacs, B. R. Fischl, B. T. Quinn, W. K. Chong, D. G. Gadian and A. Lucas, *Pediatr. Res.*, 2010, **67**, 357–362.
135 M. K. Kim and J.-W. Choi, *Int. Breastfeed J.*, 2020, **15**, 83.
136 S. Mills, R. P. Ross, C. Hill, G. F. Fitzgerald and C. Stanton, *Int. Dairy J.*, 2011, **21**, 377–401.
137 J. Lis-Kuberka and M. Orczyk-Pawiłowicz, *Nutrients*, 2019, **11**, 306.
138 T. Urashima, J. Hirabayashi, S. Sato and A. Kobata, *Trends Glycosci. Glycotechnol.*, 2018, **30**, SE51–SE65.
139 M. K. McGuire, C. L. Meehan, M. A. McGuire, J. E. Williams, J. Foster, D. W. Sellen, E. W. Kamau-Mbuthia, E. W. Kamundia, S. Mbugua, S. E. Moore, A. M. Prentice, L. J. Kvist, G. E. Otoo, S. L. Brooker, W. J. Price, B. Shafii, C. Placek, K. A. Lackey, B. Robertson, S. Manzano, L. Ruíz, J. M. Rodríguez, R. G. Pareja and L. Bode, *Am. J. Clin. Nutr.*, 2017, **105**, 1086–1100.
140 D. S. Newburg, *Am. J. Clin. Nutr.*, 2017, **105**, 1027–1028.
141 EFSA NDA Panel (EFSA Panel on Dietetic Products Nutrition and Allergies), *EFSA J.*, 2014, **12**, 3760.
142 T. A. Lehti, M. I. Pajunen, M. S. Skog and J. Finne, *Nat. Commun.*, 2017, **8**, 1915.
143 S. Sakarya, G. T. Ertem, S. Oncu, I. Kocak, N. Erol and S. Oncu, *FEMS Immunol. Med. Microbiol.*, 2003, **39**, 45–50.
144 F. Schwarz, C. S. Landig, S. Siddiqui, I. Secundino, J. Olson, N. Varki, V. Nizet and A. Varki, *EMBO J.*, 2017, **36**, 751–760.
145 Z. Han, P. S. Thuy-Boun, W. Pfeiffer, V. F. Vartabedian, A. Torkamani, J. R. Teijaro and D. W. Wolan, *Sci. Rep.*, 2021, **11**, 4763.
146 T. D. Mubaiwa, E. A. Semchenko, L. E. Hartley-tassell, C. J. Day, M. P. Jennings and K. L. Seib, *Pathog. Dis.*, 2017, **75**, ftx063.
147 G. A. Jarvis and N. A. Vedros, *Infect. Immun.*, 1987, **55**, 174–180.
148 C. Jones, M. Virji and P. R. Crocker, *Mol. Microbiol.*, 2003, **49**, 1213–1225.
149 S. L. Xiang, M. Zhong, F. C. Cai, B. Deng and X. P. Zhang, *J. Neuroimmunol.*, 2006, **174**, 126–132.
150 R. Huizinga, W. Van Rijs, J. J. Bajramovic, M. L. Kuijf, J. D. Laman, J. N. Samsom and C. Jacobs, *J. Immunol.*, 2013, **191**, 5636–5645.
151 M. Bax, M. L. Kuijf, A. P. Heikema, W. van Rijs, S. C. M. Bruijns, J. J. García-Vallejo, P. R. Crocker, B. C. Jacobs, S. J. van Vliet and Y. van Kooyk, *Infect. Immun.*, 2011, **79**, 2681–2689.
152 S. Uchiyama, J. Sun, K. Fukahori, N. Ando, M. Wu, F. Schwarz and S. S. Siddiqui, *Proc. Natl. Acad. Sci. U. S. A.*, 2019, **116**, 7465–7470.
153 S. Weiman, S. Uchiyama, F.-Y. C. Lin, D. Chaffin, A. Varki, V. Nizet and A. L. Lewis, *Biochem. J.*, 2013, **428**, 163–168.
154 P. S. K. Ng, C. J. Day, J. M. Atack, L. E. Hartley-Tassell, L. E. Winter, T. Marshanski, V. Padler-Karavani, A. Varki, S. J. Barenkamp, M. A. Apicella and M. P. Jennings, *MBio*, 2019, **10**, e00422-19.
155 K. Hentrich, J. Löfling, A. Pathak, V. Nizet, A. Varki and B. Henriques-Normark, *Cell Host Microbe*, 2016, **20**, 307–317.
156 B. Khatua, A. Ghoshal, K. Bhattacharya, C. Mandal, B. Saha, P. R. Crocker and C. Mandal, *FEBS Lett.*, 2010, **584**, 555–561.
157 B. Khatua, K. Bhattacharya and C. Mandal, *J. Leukocyte Biol.*, 2012, **91**, 641–655.
158 S. Ram, J. Shaughnessy, R. B. De Oliveira, L. A. Lewis, S. Gulati and P. A. Rice, *Pathog. Dis.*, 2017, **75**, ftx049.
159 S. M. Spinola, W. Li, K. R. Fortney, D. M. Janowicz, B. Zwickl, B. P. Katz and R. S. Munson, *Infect. Immun.*, 2012, **80**, 679–687.
160 F. M. Tatum, L. B. Tabatabai and R. E. Briggs, *Microb. Pathog.*, 2009, **46**, 337–344.
161 A. Varki and P. Gagneux, *Proc. Natl. Acad. Sci. U. S. A.*, 2009, **106**, 14739–14740.
162 I. Moustafa, H. Connaris, M. Taylor, V. Zaitsev, J. C. Wilson, M. J. Kiefel, M. Von Itzstein and G. Taylor, *J. Biol. Chem.*, 2004, **279**, 40819–40826.
163 S. Almagro-Moreno and E. F. Boyd, *Infect. Immun.*, 2009, **77**, 3807–3816.
164 M. Unemo, M. Aspholm-Hurtig, D. Ilver, J. Bergström, T. Borén, D. Danielsson and S. Teneberg, *J. Biol. Chem.*, 2005, **280**, 15390–15397.
165 P. Zhou, J. Liu, X. Li, Y. Takahashi and F. Qi, *PLoS One*, 2015, **10**, e0143898.
166 H. Geyer, C. Holschbach, G. Hunsmann and J. Schneider, *J. Biol. Chem.*, 1988, **263**, 11760–11767.

167 Z. Zou, A. Chastain, S. Moir, J. Ford, K. Trandem, E. Martinelli, C. Cicala, P. Crocker, J. Arthos and P. D. Sun, *PLoS One*, 2011, **6**, e24559.
168 S. Varchetta, P. Lusso, K. Hudspeth, J. Mikulak, D. Mele, S. Paolucci, R. Cimbro, M. Malnati, A. Riva, R. Maserati, M. U. Mondelli and D. Mavilio, *Retrovirology*, 2013, **10**, 154.
169 J. Wang, Q. Fan, T. Satoh, J. Arii, L. L. Lanier, P. G. Spear, Y. Kawaguchi and H. Arase, *J. Virol.*, 2009, **83**, 13042–13045.
170 Q. Lu, G. Lu, J. Qi, H. Wang, Y. Xuan, Q. Wang, Y. Lia, Y. Zhang, C. Zheng, Z. Fana, J. Yan and G. F. Gao, *Proc. Natl. Acad. Sci. U. S. A.*, 2014, **111**, 8221–8226.
171 A. S. Kondratowicz, N. J. Lennemann, P. L. Sinn, R. A. Davey, C. L. Hunt, S. Moller-Tank, D. K. Meyerholz, P. Rennert, R. F. Mullins, M. Brindley, L. M. Sandersfeld, K. Quinn, M. Weller, P. B. McCray, J. Chiorini and W. Maury, *Proc. Natl. Acad. Sci. U. S. A.*, 2011, **108**, 8426–8431.
172 S. Yuan, L. Cao, H. Ling, M. Dang, Y. Sun, X. Zhang, Y. Chen, L. Zhang, D. Su, X. Wang and Z. Rao, *Protein Cell*, 2015, **6**, 814–824.
173 D. Perez-Zsolt, I. Erkizia, M. Pino, M. García-Gallo, M. T. Martin, S. Benet, J. Chojnacki, M. T. Fernández-Figueras, D. Guerrero, V. Urrea, X. Muñiz-Trabudua, L. Kremer, J. Martinez-Picado and N. Izquierdo-Useros, *Nat. Microbiol.*, 2019, **4**, 1558–1570.
174 C. W. Tan, C. H. Huan Hor, S. Sen Kwek, H. K. Tee, I. C. Sam, E. L. K. Goh, E. E. Ooi, Y. F. Chan and L. F. Wang, *Emerging Microbes Infect.*, 2019, **8**, 426–437.
175 J. Cime-Castillo, P. Delannoy, G. Mendoza-Hernández, V. Monroy-Martínez, A. Harduin-Lepers, H. Lanz-Mendoza, F. D. L. C. Hernández-Hernández, E. Zenteno, C. Cabello-Gutiérrez and B. H. Ruiz-Ordaz, *BioMed Res. Int.*, 2015, 504187.
176 G. Zocher, N. Mistry, M. Frank, I. Hähnlein-Schick, J. O. Ekström, N. Arnberg and T. Stehle, *PLoS Pathog.*, 2014, **10**, e1004401.
177 T. Imamura, M. Okamoto, S.-I. Nakakita, A. Suzuki, M. Saito, R. Tamaki, S. Lupisan, C. N. Roy, H. Hiramatsu, K.-E. Sugawara, K. Mizuta, Y. Matsuzaki, Y. Suzuki, H. Oshitani and S. Perlman, *J. Virol.*, 2014, **88**, 2374–2384.
178 L. T. Jae, M. Raaben, A. S. Herbert, A. I. Kuehne, A. S. Wirchnianski, T. K. Soh, S. H. Stubbs, H. Janssen, M. Damme, P. Saftig, S. P. Whelan, J. M. Dye and T. R. Brummelkamp, *Science*, 2014, **344**, 1506–1510.
179 F. Superti, B. Hauttecoeur, M. J. Morelec, P. Goldoni, B. Bizzini and H. Tsiang, *J. Gen. Virol.*, 1986, **67**, 47–56.
180 G. Ayora-Talavera, *J. Recept., Ligand Channel Res.*, 2018, **10**, 1–11.
181 K. Shinya, M. Ebina, S. Yamada, M. Ono, N. Kasai and Y. Kawaoka, *Nature*, 2006, **440**, 435–436.
182 N. Limsuwat, O. Suptawiwat, C. Boonarkart, P. Puthavathana, W. Wiriyarat and P. Auewarakul, *Arch. Virol.*, 2016, **161**, 649–656.
183 Z. Chen, W. Chen, Q. Wang, Y. Qin, X. Wang, T. Ma, P. Zhang, X. Li, X. Wang, L. Ding and Z. Li, *J. Mol. Struct.*, 2021, **1230**, 129859.
184 L. Ding, X. Fu, W. Guo, Y. Cheng, X. Chen, K. Zhang, G. Zhu, F. Yang, H. Yu, Z. Chen, X. Wang, X. Wang, X. Wang and Z. Li, *Int. J. Biol. Macromol.*, 2021, **184**, 339–348.
185 T. Ginex and F. J. Luque, *Expert Opin. Ther. Pat.*, 2021, **31**, 53–66.
186 R. E. Forgione, C. Di Carluccio, M. Kubota, Y. Manabe, K. Fukase, A. Molinaro, T. Hashiguchi, R. Marchetti and A. Silipo, *Sci. Rep.*, 2020, **10**, 1589.
187 M. Amonsen, D. F. Smith, R. D. Cummings and G. M. Air, *J. Virol.*, 2007, **81**, 8341–8345.
188 I. V. Alymova, A. Portner, V. P. Mishin, J. A. McCullers, P. Freiden and G. L. Taylor, *Glycobiology*, 2012, **22**, 174–180.
189 L.-Y. Huang, A. Patel, R. Ng, E. B. Miller, S. Halder, R. McKenna, A. Asokan and M. Agbandje-McKenna, *J. Virol.*, 2016, **90**, 5219–5230.
190 R. Burger-Calderon and J. Webster-Cyriaque, *Cancers*, 2015, **7**, 1244–1270.
191 N. J. Bayer, D. Januliene, G. Zocher, T. Stehle, A. Moeller and B. S. Blaum, *J. Virol.*, 2020, **94**, e01664-19.
192 C. K. Liu, G. Wei and W. J. Atwood, *J. Virol.*, 1998, **72**, 4643–4649.
193 D. M. Reiter, J. M. Frierson, E. E. Halvorson, T. Kobayashi, T. S. Dermody and T. Stehle, *PLoS Pathog.*, 2011, **7**, e1002166.
194 K. Reiss, J. E. Stencel, Y. Liu, B. S. Blaum, D. M. Reiter, T. Feizi, T. S. Dermody and T. Stehle, *PLoS Pathog.*, 2012, **8**, e1003078.
195 T. Haselhorst, F. E. Fleming, J. C. Dyason, R. D. Hartnell, X. Yu, G. Holloway, K. Santegoets, M. J. Kiefel, H. Blanchard, B. S. Coulson and M. Von Itzstein, *Nat. Chem. Biol.*, 2009, **5**, 91–93.
196 S. M. Cashman, D. J. Morris and R. Kumar-Singh, *Virology*, 2004, **324**, 129–139.
197 E. C. Nilsson, R. J. Storm, J. Bauer, S. M. C. Johansson, A. Lookene, J. Ångström, M. Hedenström, T. L. Eriksson, L. FräCurrency Signngsmyr, S. Rinaldi, H. J. Willison, F. P. Domellöf, T. Stehle and N. Arnberg, *Nat. Med.*, 2011, **17**, 105–109.
198 A. Lenman, A. Manuel Liaci, Y. Liu, L. Frängsmyr, M. Frank, B. S. Blaum, W. Chai, I. I. Podgorski, B. Harrach, M. Benko, T. Feizi, T. Stehle and N. Arnberg, *Proc. Natl. Acad. Sci. U. S. A.*, 2018, **115**, E4264–E42736.
199 D. X. Liu, J. Q. Liang and T. S. Fung, *Encyclopedia of Virology*, 2021, vol. 2, pp. 428–440.
200 L. Guruprasad, *Prog. Biophys. Mol. Biol.*, 2021, **161**, 39–53.
201 A. H. M. Wong, A. C. A. Tomlinson, D. Zhou, M. Satkunarajah, K. Chen, C. Sharon, M. Desforges, P. J. Talbot and J. M. Rini, *Nat. Commun.*, 2017, **8**, 1735.
202 X. Zhao, F. Guo, M. A. Comunale, A. Mehta, M. Sehgal, P. Jain, A. Cuconati, H. Lin, T. M. Block, J. Chang and J. T. Guo, *Antimicrob. Agents Chemother.*, 2015, **59**, 206–216.
203 R. J. G. Hulswit, Y. Lang, M. J. G. Bakkers, W. Li, Z. Li, A. Schouten, B. Ophorst, F. J. M. Van Kuppeveld, G. J. Boons, B. J. Bosch, E. G. Huizinga and R. J. De Groot, *Proc. Natl. Acad. Sci. U. S. A.*, 2019, **116**, 2681–2690.

204 W. Li, R. J. G. Hulswit, I. Widjaja, V. S. Raj, R. McBride, W. Peng, W. Widagdo, M. A. Tortorici, B. Van Dieren, Y. Lang, J. W. M. Van Lent, J. C. Paulson, C. A. M. De Haan, R. J. De Groot, F. J. M. Van Kuppeveld, B. L. Haagmans and B. J. Bosch, *Proc. Natl. Acad. Sci. U. S. A.*, 2017, **114**, E8508–E8517.
205 M. Örd, I. Faustova and M. Loog, *Sci. Rep.*, 2020, **10**, 16944.
206 M. Seyran, K. Takayama, V. N. Uversky, K. Lundstrom, G. Palù, S. P. Sherchan, D. Attrish, N. Rezaei, A. A. A. Aljabali, S. Ghosh, D. Pizzol, G. Chauhan, P. Adadi, T. Mohamed Abd El-Aziz, A. G. Soares, R. Kandimalla, M. Tambuwala, S. S. Hassan, G. K. Azad, P. Pal Choudhury, W. Baetas-da-Cruz, Á. Serrano-Aroca, A. M. Brufsky and B. D. Uhal, *FEBS J.*, 2021, **288**, 5010–5020.
207 M. Awasthi, S. Gulati, D. P. Sarkar, S. Tiwari, S. Kateriya, P. Ranjan and S. K. Verma, *Viruses*, 2020, **12**, 909.
208 L. Pruimboom, *Med. Hypotheses*, 2021, **146**, 110368.
209 E. Milanetti, M. Miotto, L. Di Rienzo, M. Nagaraj, M. Monti, T. W. Golbek, G. Gosti, S. J. Roeters, T. Weidner, D. E. Otzen and G. Ruocco, *Front. Mol. Biosci.*, 2021, **8**, 690655.
210 B. Li, L. Wang, H. Ge, X. Zhang, P. Ren, Y. Guo, W. Chen, J. Li, W. Zhu, W. Chen, L. Zhu and F. Bai, *Front. Chem.*, 2021, **9**, 659764.
211 V. C. Divya and B. Saravanakarthikeyan, *J. Oral Biosci.*, 2021, DOI: 10.1016/j.job.2021.08.004, In Press.
212 N. Z. Cuervo and N. Grandvaux, *eLife*, 2020, **9**, e61390.
213 W. Hao, B. Ma, Z. Li, X. Wang, X. Gao, Y. Li, B. Qin, S. Shang, S. Cui and Z. Tan, *Sci. Bull.*, 2021, **66**, 1205–1214.
214 A. Shajahan, S. Archer-Hartmann, N. T. Supekar, A. S. Gleinich, C. Heiss and P. Azadi, *Glycobiology*, 2021, **31**, 410–424.
215 Q. Yang, T. A. Hughes, A. Kelkar, X. Yu, K. Cheng, S. J. Park, W. C. Huang, J. F. Lovell and S. Neelamegham, *eLife*, 2020, **9**, e61552.
216 H. Chu, B. Hu, X. Huang, Y. Chai, D. Zhou, Y. Wang, H. Shuai, D. Yang, Y. Hou, X. Zhang, T. T. T. Yuen, J. P. Cai, A. J. Zhang, J. Zhou, S. Yuan, K. K. W. To, I. H. Y. Chan, K. Y. Sit, D. C. C. Foo, I. Y. H. Wong, A. T. L. Ng, T. T. Cheung, S. Y. K. Law, W. K. Au, M. A. Brindley, Z. Chen, K. H. Kok, J. F. W. Chan and K. Y. Yuen, *Nat. Commun.*, 2021, **12**, 134.
217 C. Dhar, A. Sasmal, S. Diaz, A. Verhagen, H. Yu, W. Li, X. Chen and A. Varki, *Glycobiology*, 2021, **31**, 1068–1071.
218 L. Nguyen, K. A. McCord, D. T. Bui, K. M. Bouwman, E. N. Kitova, M. Elaish, D. Kumawat, G. C. Daskhan, I. Tomris, L. Han, P. Chopra, T.-J. Yang, S. D. Willows, A. L. Mason, L. K. Mahal, T. L. Lowary, L. J. West, S.-T. D. Hsu, T. Hobman, S. M. Tompkins, G.-J. Boons, R. P. de Vries, M. S. Macauley and J. S. Klassen, *Nat. Chem. Biol.*, 2021, DOI: 10.1038/s41589-021-00924-1.
219 E. Song, C. Zhang, B. Israelow, A. Lu-Culligan, A. Vieites Prado, S. Skriabine, P. Lu, O.-E. Weizman, F. Liu, Y. Dai, K. Szigeti-Buck, Y. Yasumoto, G. Wang, C. Castaldi, J. Heltke, E. Ng, J. Wheeler, M. M. Alfajaro, E. Levavasseur, B. Fontes, N. G. Ravindra, D. V. Dijk, S. Mane, M. Gunel, A. Ring, S. A. J. Kazmi, K. Zhang, C. B. Wilen, T. L. Horvath, I. Plu, S. Haik, J.-L. Thomas, A. Louvi, S. F. Farhadian, A. Huttner, D. Seilhean, N. Renier, K. Bilguvar and A. Iwasaki, *J. Exp. Med.*, 2021, **218**, e20202135.
220 C. M. Salvatore, J.-Y. Han, K. P. Acker, P. Tiwari, J. Jin, M. Brandler, C. Cangemi, L. Gordon, A. Parow, J. DiPace and P. DeLaMora, *Lancet Child Adolesc. Health*, 2020, **4**, 721–727.
221 J. C. Silva-Filho, C. G. F. de Melo and J. L. de Oliveira, *Med. Hypotheses*, 2020, **144**, 110155.
222 R. Uraki and Y. Kawaoka, *Nat. Chem. Biol.*, 2021, DOI: 10.1038/s41589-021-00923-2.
223 T. A. Altalhi, K. Alswat, W. F. Alsanie, M. M. Ibrahim, A. Aldalbahi and H. S. El-Sheshtawy, *J. Mol. Struct.*, 2021, **1228**, 129459.
224 P. Colson, J. M. Rolain, J. C. Lagier, P. Brouqui and D. Raoult, *Int. J. Antimicrob. Agents*, 2020, **55**, 105932.
225 C. Prodromos and T. Rumschlag, *New Microbes New Infect.*, 2020, **38**, 100776.
226 N. Sinha and G. Balayla, *Postgrad. Med. J.*, 2020, **96**, 550–555.
227 J. K. Sun, Y. T. Chen, X. De Fan, X. Y. Wang, Q. Y. Han and Z. W. Liu, *Postgrad. Med.*, 2020, **132**, 604–613.
228 M. Wang, R. Cao, L. Zhang, X. Yang, J. Liu, M. Xu, Z. Shi, Z. Hu, W. Zhong and G. Xiao, *Cell Res.*, 2020, **30**, 269–271.
229 J. A. Al-Tawfiq, A. H. Al-Homoud and Z. A. Memish, *Travel Med. Infect. Dis.*, 2020, **34**, 101615.
230 A. N. Baker, S. J. Richards, C. S. Guy, T. R. Congdon, M. Hasan, A. J. Zwetsloot, A. Gallo, J. R. Lewandowski, P. J. Stansfeld, A. Straube, M. Walker, S. Chessa, G. Pergolizzi, S. Dedola, R. A. Field and M. I. Gibson, *ACS Cent. Sci.*, 2020, **6**, 2046–2052.
231 M. Renlund, M. A. Chester, A. Lundblad, P. Aula, K. O. Raivio, S. Autio and S.-L. Koskela, *Eur. J. Biochem.*, 1979, **101**, 245–250.
232 L. W. Hancock, M. M. Thaler, A. L. Horwitz and G. Dawson, *J. Neurochem.*, 1982, **38**, 803–808.
233 L. W. Hancock, A. L. Horwitz and G. Dawson, *Biochim. Biophys. Acta*, 1983, **760**, 42–52.
234 G. H. Thomas, J. Scocca, C. S. Miller and L. Reynolds, *Clin. Genet.*, 1989, **36**, 242–249.
235 G. Strecker, M.-C. Peers, J.-C. Michalski, T. Hondi-Assah, B. Fournet, G. Spik, J. Montreuil, J.-P. Farriaux, P. Maroteaux and P. Durand, *Eur. J. Biochem.*, 1977, **75**, 391–403.
236 M. F. Goldberg, E. Cotlier, L. G. Fichenscher, K. Kenyon, R. Enat and S. A. Borowsky, *Arch. Intern. Med.*, 1971, **128**, 387–398.
237 T. Yardeni, T. Choekyi, K. Jacobs, C. Ciccone, K. Patzel, Y. Anikster, W. A. Gahl, N. Kurochkina and M. Huizing, *Biochemistry*, 2011, **50**, 8914–8925.
238 C. Tran, L. Turolla, D. Ballhausen, S. C. Buros, T. Teav, H. Gallart-Ayala, J. Ivanisevic, M. Faouzi, D. J. Lefeber, I. Ivanovski, S. Giangiobbe, S. G. Caraffi, L. Garavelli and A. Superti-Furga, *Mol. Genet. Metab. Rep.*, 2021, **28**, 100777.
239 L. F. Mollashahi, M. Honarmand, A. Nakhaee and G. Mollashahi, *Int. J. High Risk Behav. Addict.*, 2016, **5**, e27969.
240 N. Kurtul and E. Gkpnar, *Mediators Inflammation*, 2012, **2012**, 619293.

241 N. Waszkiewicz, S. D. Szajda, A. Kępka, A. Szulc and K. Zwierz, *Biochem. Soc. Trans.*, 2011, **39**, 365–369.
242 J. Romppanen, K. Punnonen, P. Anttila, T. Jakobsson, J. Blake and O. Niemelä, *Alcohol.: Clin. Exp. Res.*, 2002, **26**, 1234–1238.
243 P. Ghosh, E. A. Hale and M. R. Lakshman, *Alcohol*, 2001, **25**, 173–179.
244 F. M. Wurst, N. Thon, W. Weinmann, S. Tippetts, P. Marques, J. A. Hahn, C. Alling, S. Aradottir, S. Hartmann and R. Lakshman, *Alcohol.: Clin. Exp. Res.*, 2012, **36**, 251–257.
245 B. Cylwik, L. Chrostek, A. Krawiec, Z. Supronowicz, A. Koput and M. Szmitkowski, *Alcohol*, 2010, **44**, 457–462.
246 P. Sillanaukee, M. Pönniö and K. Seppä, *Alcohol.: Clin. Exp. Res.*, 1999, **23**, 1039–1043.
247 T. Alam, R. Cherian, P. T. Raman and A. S. Balasubramanian, *J. Neurol., Neurosurg. Psychiatry*, 1976, **39**, 1201–1203.
248 Y. Nagata, A. Hirayama, S. Ikeda, A. Shirahata, F. Shoji, M. Maruyama, M. Kayano, M. Bundo, K. Hattori, S. Yoshida, Y.-I. Goto, K. Urakami, T. Soga, K. Ozaki and S. Niida, *Biomark. Res.*, 2018, **6**, 5.
249 J. Yadav, A. K. Verma, R. K. Garg, K. Ahmad, Shiuli, A. A. Mahdi and S. Srivastava, *Exp. Gerontol.*, 2020, **141**, 111092.
250 F. Mochel, F. Sedel, A. Vanderver, U. F. H. Engelke, J. Barritault, B. Z. Yang, B. Kulkarni, D. R. Adams, F. Clot, J. H. Ding, C. R. Kaneski, F. W. Verheijen, B. W. Smits, F. Seguin, A. Brice, M. T. Vanier, M. Huizing, R. Schiffmann, A. Durr and R. A. Wevers, *Brain*, 2009, **132**, 801–809.
251 E. Demirci, Y. Guler, S. Ozmen, M. Canpolat and S. Kumandas, *Clin. Psychopharmacol. Neurosci.*, 2019, **17**, 415–422.
252 X. Yang, S. Liang, L. Wang, P. Han, X. Jiang, J. Wang, Y. Hao and L. Wu, *Brain Res.*, 2018, **1678**, 273–277.
253 M. A. Crook, P. Tutt, H. Simpson and J. C. Pickup, *Clin. Chim. Acta*, 1993, **219**, 131–138.
254 T. Ozben, S. Nacitarhan and N. Tuncer, *Ann. Clin. Biochem.*, 1995, **32**, 303–306.
255 J. Roozbeh, A. Merat, F. Bodagkhan, R. Afshariani and H. Yarmohammadi, *Int. Urol. Nephrol.*, 2011, **43**, 1143–1148.
256 S. Shahvali, A. Shahesmaeili, M. Sanjari and S. Karami-Mohajeri, *Diabetol. Int.*, 2020, **11**, 19–26.
257 P. Khalili, J. Sundström, J. Jendle, F. Lundin, I. Jungner and P. M. Nilsson, *Prim. Care Diabetes*, 2014, **8**, 352–357.
258 R. B. Findik, F. M. Yilmaz, G. Yilmaz, H. Yilmaz and J. Karakaya, *Arch. Gynecol. Obstet.*, 2012, **286**, 913–916.
259 H. Dogan and H. Pagaoglu, *Acta Ophthalmol.*, 1992, **70**, 790–794.
260 I. Zipkin, S. E. Mergenhagen and R. Kass, *Biochem. Biophys. Res. Commun.*, 1961, **4**, 76–78.
261 S. R. Rathod, F. Khan, A. P. Kolte and M. Gupta, *J. Clin. Diagn. Res.*, 2014, **8**, 19–21.
262 A. Hernández-Cedillo, M. G. García-Valdivieso, A. C. Hernández-Arteaga, N. Patiño-Marín, Á. A. Vértiz-Hernández, M. José-Yacamán and H. R. Navarro-Contreras, *Oral Dis.*, 2019, **25**, 1627–1633.
263 S. Oktay, Ö. Ö. Bal, L. Kuru, A. Yarat and Ü. Noyan, *Niger. J. Clin. Pract.*, 2020, **23**, 603–609.
264 M. Crook, M. Haq, S. Haq and P. Tutt, *Angiology*, 1994, **45**, 709–715.
265 M. N. Li, S. H. Qian, Z. Y. Yao, S. P. Ming, X. J. Shi, P. F. Kang, N. R. Zhang, X. J. Wang, D. S. Gao, Q. Gao, H. Zhang and H. J. Wang, *BMC Cardiovasc. Disord.*, 2020, **20**, 404.
266 P. Khalili, J. Sundström, S. S. Franklin, J. Jendle, F. Lundin, I. Jungner and P. M. Nilsson, *J. Hypertens.*, 2012, **30**, 1718–1724.
267 L. Zhang, T. T. Wei, Y. Li, J. Li, Y. Fan, F. Q. Huang, Y. Y. Cai, G. Ma, J. F. Liu, Q. Q. Chen, S. L. Wang, H. Li, R. N. Alolga, B. Liu, D. S. Zhao, J. H. Shen, X. M. Wang, W. Zhu, P. Li and L. W. Qi, *Circulation*, 2018, **137**, 1374–1390.
268 M. T. Goodarzi, M. Rezaei, E. Moadel, S. Homayounfar and M. R. Safari, *Eur. J. Lipid Sci. Technol.*, 2008, **110**, 302–306.
269 S. Oktay, I. Basar, E. Emekli-Alturfan, E. Malali, E. Elemek, F. Ayan, L. Koldas, U. Noyan and N. Emekli, *Pathophysiol. Haemostasis Thromb.*, 2009, **37**, 67–71.
270 L. Råstam, G. Lindberg, A. R. Folsom, G. L. Burke, P. Nilsson-Ehle and A. Lundblad, *Int. J. Epidemiol.*, 1996, **25**, 953–958.
271 M. Crook and W. U-test, *Clin. Sci.*, 1992, **83**, 593–595.
272 P. A. Larnba, P. K. Pandey, G. S. Sarin and M. D. Mathur, *Acta Ophthalmol.*, 1993, **71**, 833–835.
273 M. Altay, M. A. Karakoç, N. Çakır, C. Yılmaz Demirtaş, E. T. Cerit, M. Aktürk, İ. Ateş, N. Bukan and M. Arslan, *J. Clin. Lab. Anal.*, 2017, **31**, e22034.
274 R. Baba, K. Yashiro, K. Nagasako and H. Obata, *Gastroenterol. Jpn.*, 1992, **27**, 604–610.
275 E. Gruszewska, B. Cylwik, M. Gudowska, A. Panasiuk, R. Flisiak and L. Chrostek, *Ann. Clin. Biochem.*, 2019, **56**, 118–122.
276 B. Cylwik, L. Chrostek, B. Zalewski, A. Dabrowski and M. Szmitkowski, *Dig. Dis. Sci.*, 2007, **52**, 2317–2322.
277 B. Cylwik, L. Chrostek, A. Panasiuk and M. Szmitkowski, *Clin. Chem. Lab. Med.*, 2010, **48**, 137–139.
278 T. Özben, *Ann. Clin. Biochem.*, 1991, **28**, 44–48.
279 F. Fuentes, N. Carrillo, K. J. Wilkins, J. Blake, P. Leoyklang, W. A. Gahl, J. B. Kopp and M. Huizing, *Kidney360*, 2020, **1**, 957–961.
280 S. S. Demir, H. Ç. Özcan, Ö. Balat, E. Öztürk, M. G. Uğur, R. Gündüz and S. Taysi, *J. Obstet. Gynaecol.*, 2018, **38**, 532–535.
281 F. M. Von Versen-Hoeynck, C. A. Hubel, M. J. Gallaher, H. S. Gammill and R. W. Powers, *Am. J. Hypertens.*, 2009, **22**, 687–692.
282 R. O'Kennedy, G. Berns, E. Moran, H. Smyth, K. Carroll, R. D. Thornes, A. O'Brien, J. Fennelly and M. Butler, *Cancer Lett.*, 1991, **58**, 91–100.
283 R. Iijima, H. Takahashi, S. Ikegami and M. Yamazaki, *Biol. Pharm. Bull.*, 2007, **30**, 580–582.
284 N. Kurtul and B. C. Arikan, *Acta Med.*, 2006, **49**, 97–100.
285 A. Cardenas, A. M. Bernard and R. R. Lauwerys, *Toxicol. Appl. Pharmacol.*, 1991, **108**, 547–558.

286 Y. Wang, A. Khan, A. Antonopoulos, L. Bouché, C. D. Buckley, A. Filer, K. Raza, K. P. Li, B. Tolusso, E. Gremese, M. Kurowska-Stolarska, S. Alivernini, A. Dell, S. M. Haslam and M. A. Pineda, *Nat. Commun.*, 2021, **12**, 2343.
287 R. E. Taylor, C. J. Gregg, V. Padler-Karavani, D. Ghaderi, H. Yu, S. Huang, R. U. Sorensen, X. Chen, J. Inostroza, V. Nizet and A. Varki, *J. Exp. Med.*, 2010, **207**, 1637–1646.
288 L. Le Berre, J. Rousse, P. A. Gourraud, B. M. Imbert-Marcille, A. Salama, G. Evanno, G. Semana, A. Nicot, E. Dugast, P. Guérif, C. Adjaoud, T. Freour, S. Brouard, F. Agbalika, R. Marignier, D. Brassat, D. A. Laplaud, E. Drouet, V. Van Pesch and J. P. Soulillou, *Clin. Immunol.*, 2017, **180**, 128–135.
289 Y. Chen, L. Pan, N. Liu, F. A. Troy and B. Wang, *J. Geophys. Res. Oceans*, 2014, **111**, 332–341.
290 L. Tolenaars, D. Romanazzi, E. Carpenter, S. Gallier and C. G. Prosser, *Int. Dairy J.*, 2021, **117**, 105012.
291 H. Li and X. Fan, *Open J. Prev. Med.*, 2014, **04**, 57–63.
292 H. L. Yao, L. P. Conway, M. M. Wang, K. Huang, L. Liu and J. Voglmeir, *Glycoconjugate J.*, 2016, **33**, 219–226.
293 M. Hedlund, V. Padler-Karavani, N. M. Varki and A. Varki, *Proc. Natl. Acad. Sci. U. S. A.*, 2008, **105**, 18936–18941.
294 A. N. Samraj, H. Läubli, N. Varki and A. Varki, *Front. Oncol.*, 2014, **4**, 33.
295 P. R. Sanjay, K. Hallikeri and A. R. Shivashankara, *Indian J. Dent. Res.*, 2008, **19**, 288–291.
296 K. S. C. Bose, P. V. Gokhale, S. Dwivedi and M. Singh, *J. Nat. Sci., Biol. Med.*, 2013, **4**, 122–125.
297 R. D. Xing, Z. S. Wang, C. Q. Li, Q. Y. Tang, C. B. Jiang and Y. Z. Zhang, *Int. J. Biol. Markers*, 1994, **9**, 239–242.
298 S. Wongkham, C. Boonla, S. Kongkham, C. Wongkham, V. Bhudhisawasdi and B. Sripa, *Clin. Biochem.*, 2001, **34**, 537–541.
299 C. Feijoo-Carnero, F. J. Rodríguez-Berrocal, M. Páez de la Cadena, D. Ayude, A. de Carlos and V. S. Martínez-Zorzano, *Int. J. Biol. Markers*, 2004, **19**, 38–45.
300 A. Semczuk, M. Cybulski, A. Paszkowska and H. Berbec, *Eur. J. Obstet. Gynecol. Reprod. Biol.*, 1998, **76**, 211–215.
301 S. Inoue, S. L. Lin, T. Chang, S. H. Wu, C. W. Yao, T. Y. Chu, F. A. Troy and Y. Inoue, *J. Biol. Chem.*, 1998, **273**, 27199–27204.
302 F. Wang, B. Xie, B. Wang and F. A. Troy, *Glycobiology*, 2015, **25**, 1362–1374.
303 D. Konukoglu, T. Akqay and A. Ergzenci, *Cancer Lett.*, 1995, **94**, 97–100.
304 T. Akqay, D. Konukoglua, S. Atausb, A. Dirican and C. Uygur, *Cancer Lett.*, 1994, **78**, 7–9.
305 M. Payazdan, S. Khatami, H. Galehdari, N. Delfan, M. Shafiei and S. Heydaran, *Gene Rep.*, 2021, **24**, 101218.
306 J. E. Martin, S. W. Tanenbaum and M. Flashner, *Carbohydr. Res.*, 1977, **56**, 423–425.
307 Z. C. F. Wong, G. K. L. Chan, K. Q. Y. Wu, K. K. M. Poon, Y. Chen, T. T. X. Dong and K. W. K. Tsim, *Food Funct.*, 2018, **9**, 5139–5149.
308 N. H. Jamalluddin, N. A. Tukiran, N. Ahmad Fadzillah and S. Fathi, *Food Control*, 2019, **104**, 247–255.
309 X. Ma, J. Zhang, J. Liang, X. Ma, R. Xing, J. Han, L. Guo and Y. Chen, *Food Res. Int.*, 2019, **125**, 108639.
310 N. Daud, S. Mohamad Yusop, A. S. Babji, S. J. Lim, S. R. Sarbini and T. Hui Yan, *Food Rev. Int.*, 2021, **37**, 177–196.
311 Y. Dai, J. Cao, Y. Wang, Y. Chen and L. Jiang, *Food Res. Int.*, 2021, **140**, 109875.
312 T. Nakano and M. Betti, *J. Dairy Res.*, 2020, **87**, 364–367.
313 R. J. McMahon, M. F. Locniskar, S. C. Rumsey, J. C. Anthony and R. Wantanagorn, US7951410B2, 2011.
314 https://www.thegreenpharmacy.com/sialex-90-caps-p6399.html (Accessed November 2021).
315 https://www.ecologicalformulas.net/ (Accessed November 2021).
316 https://www.ulprospector.com/en/na/Food/Detail/5331/190810/Lacprodan-CGMP—10 (Accessed November 2021).
317 S. J. Danishefsky, M. P. DeNinno and S. Hui Chen, *J. Am. Chem. Soc.*, 1988, **110**, 3929–3940.
318 C. De Meo and B. T. Jones, in *Advances in Carbohydrate Chemistry and Biochemistry*, ed. D. C. Baker, Elsevier, 75th edn, 2018, pp. 215–316.
319 N. Komura, K. Kato, T. Udagawa, S. Asano, H. N. Tanaka, A. Imamura, H. Ishida, M. Kiso and H. Ando, *Science*, 2019, **364**, 677–680.
320 A. M. Vibhute, N. Komura, H. N. Tanaka, A. Imamura and H. Ando, *Chem. Rec.*, 2021, **21**, 1–31.
321 X. Chen and A. Varki, *ACS Chem. Biol.*, 2010, **5**, 163–176.
322 C. C. Yu and S. G. Withers, *Adv. Synth. Catal.*, 2015, **357**, 1633–1654.
323 W. Li, J. B. McArthur and X. Chen, *Carbohydr. Res.*, 2019, **472**, 86–97.
324 A. S. Kooner, H. Yu and X. Chen, *Front. Immunol.*, 2019, **10**, 2004.
325 I. Maru, J. Ohnishi, Y. Ohta and Y. Tsukada, *J. Biosci. Bioeng.*, 2002, **93**, 258–265.
326 M. J. Dawson, D. Noble and M. Mahmoudian, USOO6156544A, 2000.
327 U. Kragl, D. Gygax, O. Ghisalba and C. Wandrey, *Angew. Chem., Int. Ed. Engl.*, 1991, **30**, 827–828.
328 J. Lee, J. Yi, S. Lee, S. Takahashi and B. Kim, *Enzyme Microb. Technol.*, 2004, **35**, 121–125.
329 X. Gao, F. Zhang, M. Wu, Z. Wu and G. Shang, *J. Agric. Food Chem.*, 2019, **67**, 6285–6291.
330 V. R. L. J. Bloemendal, S. J. Moons, J. J. A. Heming, M. Chayoua, O. Niesink, J. C. M. Van Hest, T. J. Boltje and F. P. J. T. Rutjes, *Adv. Synth. Catal.*, 2019, **361**, 2443–2447.
331 https://www.glycom.com/ (Accessed November 2021).
332 https://www.dsm.com/corporate/home.html (Accessed November 2021).
333 A. Schroven, G. Dekany and I. Vrasidas, WO2013088267Al, 2013.
334 M. Shiba and S. Koizumi, EP1484406B1, 2004.
335 D. Zhu, W. Xiao, L. Zhu and Y. Jiang, *J. Ind. Microbiol. Biotechnol.*, 2019, **46**, 125–132.
336 B. Wang, *Annu. Rev. Nutr.*, 2009, **29**, 177–222.

337 B. Wang, *Adv. Nutr.*, 2012, **3**, 465–472.
338 J. M. Gil-Robles and G. Zalm, *Official Journal of the European Communities*, 1997, **L43**, 1–6.
339 Report of the Scientific Committee on Food on the Revision of Essential Requirements of Infant Formulae and Follow-on Formulae, 2003.
340 B. Koletzko, S. Baker, G. Cleghorn, U. F. Neto, S. Gopalan, O. Hernell, Q. S. Hock, P. Jirapinyo, B. Lonnerdal, P. Pencharz, H. Pzyrembel, J. Ramirez-Mayans, R. Shamir, D. Turck, Y. Yamashiro and D. Zong-Yi, *J. Pediatr. Gastroenterol. Nutr.*, 2005, **41**, 584–599.
341 J. B. Fontelles and J. Korkeaoja, *Official Journal of the European Union*, 2007, **L12**, 3–18.
342 J.-L. Bresson, A. Flynn, M. Heinonen, K. Hulshof, H. Korhonen, P. Lagiou, M. Løvik, R. Marchelli, A. Martin, B. Moseley, H. Przyrembel, S. Salminen, S. (J. J.) Strain, S. Strobel, I. Tetens, H. van den Berg, H. van Loveren and H. Verhagen, *EFSA J.*, 2009, **7**, 1277.
343 S. S. H. Choi, N. Baldwin, V. O. Wagner, S. Roy, J. Rose, B. A. Thorsrud, P. Phothirath and C. H. Röhrig, *Regul. Toxicol. Pharmacol.*, 2014, **70**, 482–491.
344 J. P. Zimmer and C. M. Butt, US8703716B2, 2014.
345 Glycom A/S, GRAS Exemption Claim for N-Acetyl-D-neuraminic acid (NANA), http://www.fda.gov/Food/IngredientsPackagingLabeling/GRAS/NoticeInventory/default.htm.
346 Food Safety Authority of Ireland, *Safety Assessment of N-acetyl-D-neuraminic acid dihydrate (NANA)*, 2016.
347 ADVISORY COMMITTEE FOR NOVEL FOODS AND PROCESSES, N-Acetyl-D-Neuraminic Acid (NANA, Sialic Acid) DOSSIER 187, https://acnfp.food.gov.uk/sites/default/files/nana.pdf.
348 EFSA Panel on Dietetic Products, *EFSA J.*, 2017, **15**, 4918.
349 S. Peled and Y. D. Livney, *Food Hydrocolloids*, 2021, **120**, 106911.
350 X. Sun, S. Zhang, J. Ren and C. C. Udenigwe, *Crit. Rev. Food Sci. Nutr.*, 2020, 1846157.
351 X. Sun and J. Wu, *Trends Food Sci. Technol.*, 2017, **69**, 148–156.
352 K. R. Phipps, Š. Alica, N. J. Baldwin, B. Gilby, B. Lynch, D. R. Stannard, M. H. Mik and C. H. Röhrig, *J. Appl. Toxicol.*, 2019, **39**, 1378–1393.
353 K. R. Phipps, Š. Alica, N. J. Baldwin, B. Gilby, B. Lynch, D. R. Stannard, M. H. Mik and C. H. Röhrig, *J. Appl. Toxicol.*, 2019, **39**, 1444–1461.
354 Glycom A/S, GRAS Notice for 3 ' -Sialyllactose, https://www.fda.gov/food/generally-recognized-safe-gras/gras-notice-inventory.
355 Glycom A/S, GRAS Notice for 6 '-Sialyllactose, https://www.fda.gov/food/generally-recognized-safe-gras/gras-notice-inventory.
356 EFSA Panel on Nutrition, *EFSA J.*, 2020, **18**, 6098.
357 EFSA Panel on Nutrition, *EFSA J.*, 2020, **18**, 6097.
358 https://www.dsm.com/human-nutrition/en/early-life-nutrition/human-milk-oligosaccharides/GlyCare-3SL.html (Accessed November 2021).
359 https://www.dsm.com/human-nutrition/en_AP/early-life-nutrition/human-milk-oligosaccharides/GlyCare-6SL.html (Accessed November 2021).
360 F. Herrmann, A. Nieto-Ruiz, N. Sepúlveda-Valbuena, M. T. Miranda, E. Diéguez, J. Jiménez, R. De-Castellar, M. García-Ricobaraza, J. A. García-Santos, M. G. Bermúdez and C. Campoy, *J. Funct. Foods*, 2021, **83**, 104529.
361 J. Ma, S. Gong, Y. He, W. Gao, W. Hao and X. Lan, *Lett. Appl. Microbiol.*, 2021, **73**, 20–25.
362 X. Wu, Z. Li, X. X. Chen, J. S. Fossey, T. D. James and Y. B. Jiang, *Chem. Soc. Rev.*, 2013, **42**, 8032–8048.
363 H. Otsuka, E. Uchimura, H. Koshino, T. Okano and K. Kataoka, *J. Am. Chem. Soc.*, 2003, **125**, 3493–3502.
364 K. Djanashvili, L. Frullano and J. A. Peters, *Chem. – Eur. J.*, 2005, **11**, 4010–4018.
365 S. Nishitani, Y. Maekawa and T. Sakata, *ChemistryOpen*, 2018, **7**, 513–519.
366 N. Wellington, S. Macklai and P. Britz-McKibbin, *Chem. – Eur. J.*, 2019, **25**, 15277–15280.
367 E. L. Hess, J. W. Hahn and W. Ayala, *Exp. Biol. Med.*, 1956, **91**, 528–531.
368 E. L. Hess, A. F. Coburn, R. C. Bates and P. Murphy, *J. Clin. Invest.*, 1957, **36**, 449–455.
369 L. Svennerholm, *Biochim. Biophys. Acta*, 1957, **24**, 604–611.
370 G. W. Jourdian, L. Dean and S. Roseman, *J. Biol. Chem.*, 1971, **246**, 430–435.
371 G. D. Dimitrov, *Hoppe-Seyler's Z. Physiol. Chem.*, 1973, **354**, 121–124.
372 M. H. E. Spyridaki and P. A. Siskos, *Anal. Chim. Acta*, 1996, **327**, 277–285.
373 L. Warren, *J. Biol. Chem.*, 1959, **234**, 1971–1975.
374 D. Aminoff, *Virology*, 1959, **7**, 355–357.
375 I. E. Horgan, *Clin. Chim. Acta*, 1981, **116**, 409–415.
376 Y. Massamiri, G. Durand, A. Richard, J. Féger and J. Agneray, *Anal. Biochem.*, 1979, **97**, 346–351.
377 K. Yao and T. Ubuka, *Acta Med. Okayama*, 1987, **41**, 237–241.
378 J. B. Joicy, N. T. G. de Paula, P. A. B. da Silva, G. C. S. de Souza, A. P. S. Paim and A. F. Lavorante, *Microchem. J.*, 2019, **147**, 782–788.
379 T. J. Jayeoye, W. Cheewasedtham, C. Putson and T. Rujiralai, *Microchim. Acta*, 2018, **185**, 409.
380 T. J. Jayeoye, W. Cheewasedtham, C. Putson and T. Rujiralai, *J. Mol. Liq.*, 2019, **281**, 407–414.
381 H. Hess and E. Rolde, *J. Biol. Chem.*, 1964, **239**, 3215–3220.
382 K. S. Hammond and D. S. Papermaster, *Anal. Biochem.*, 1976, **74**, 292–297.
383 J. I. Murayama, M. Tomita, A. Tsuji and A. Hamada, *Anal. Biochem.*, 1976, **73**, 535–538.
384 A. K. Shukla and R. Schauer, *Hoppe-Seyler's Z. Physiol. Chem.*, 1982, **363**, 255–262.
385 K. Matsuno and S. Suzuki, *Anal. Biochem.*, 2008, **375**, 53–59.
386 A. D. A. Alves, M. F. Belian and A. F. Lavorante, *Luminescence*, 2014, **29**, 779–783.
387 Q. Wang, B. Wang, M. Ma and Z. Cai, *J. Food Sci.*, 2014, **79**, C2434–C2440.

388 J. Wang, G. Xu, F. Wei, J. Yang, P. Zhou and Q. Hu, *RSC Adv.*, 2016, **6**, 481–488.
389 X. Hao, Q. Zhang, L. Li and L. Zhou, *Mater. Lett.*, 2018, **227**, 165–168.
390 S. Xu, S. Che, P. Ma, F. Zhang, L. Xu, X. Liu, X. Wang, D. Song and Y. Sun, *Talanta*, 2019, **197**, 548–552.
391 N. Wang, M. Wang, Y. Yu, G. Yang and X. Su, *New J. Chem.*, 2020, **44**, 2350–2356.
392 J. Wang, L. Zhao and B. Yan, *ACS Appl. Mater. Interfaces*, 2020, **12**, 12990–12997.
393 H. Yu, Y. Li and A. Huang, *Talanta*, 2021, **232**, 122434.
394 Y. Zhang, H. Lu and B. Yan, *Sens. Actuators, B*, 2021, **349**, 130736.
395 D. E. Wang, J. Yan, J. Jiang, X. Liu, C. Tian, J. Xu, M. Sen Yuan, X. Han and J. Wang, *Nanoscale*, 2018, **10**, 4570–4578.
396 H. Yue, J. Chen, X. Chen, X. Wang, Y. Zhang and N. Zhou, *Sens. Actuators, B*, 2021, **344**, 130270.
397 Q. Lu, M. Zhan, L. Deng, G. Qing and T. Sun, *Analyst*, 2017, **142**, 3564–3568.
398 X. Wang, S. Qian, D. Wang, C. Wang, H. Qin, L. Peng, W. Lu, Y. Zhang and G. Qing, *J. Mater. Chem. B*, 2021, **9**, 4690–4699.
399 K. Ouchi, C. L. Colyer, M. Sebaiy, J. Zhou, T. Maeda, H. Nakazumi, M. Shibukawa and S. Saito, *Anal. Chem.*, 2015, **87**, 1933–1940.
400 J. A. Cabezas, *Biochem. J.*, 1991, **278**, 311–312.
401 S. Roseman and D. G. Comb, *J. Am. Chem. Soc.*, 1958, **80**, 3166–3167.
402 D. G. Comb and S. Roseman, *J. Am. Chem. Soc.*, 1958, **80**, 497–499.
403 D. G. Comb and S. Roseman, *J. Biol. Chem.*, 1960, **235**, 2529–2537.
404 A. D. Winer and G. W. Schwert, *Science*, 1958, **128**, 660–661.
405 O. H. Lowry, N. R. Roberts and J. I. Kapphahn, *J. Biol. Chem.*, 1957, **224**, 1047–1064.
406 P. Brunetti, A. Swanson and S. Roseman, *Methods Enzymol.*, 1963, **6**, 465–473.
407 D. G. Comb and S. Roseman, *Methods Enzymol.*, 1962, **5**, 391–394.
408 K. Sugahara, K. Sugimoto, O. Nomura and T. Usui, *Clin. Chim. Acta*, 1980, **108**, 493–498.
409 S. Teshima, K. Tamai, Y. Hayashi and S. Emi, *Clin. Chem.*, 1988, **34**, 2291–2294.
410 H. Simpson, G. D. Chusney, M. A. Crook and J. C. Pickup, *Br. J. Biomed. Sci.*, 1993, **50**, 164–167.
411 T. Horiuchi and T. Kurokawa, *Clin. Chim. Acta*, 1989, **182**, 117–121.
412 J. P. Johnston, A. G. Ogston and J. E. Stanier, *Analyst*, 1951, **76**, 88–89.
413 L. Svennerholm, *Acta Chem. Scand.*, 1958, **12**, 547–554.
414 M. J. Krantz and Y. C. Lees, *Anal. Biochem.*, 1975, **63**, 464–469.
415 D. A. Craven and C. W. Gehrke, *J. Chromatogr.*, 1968, **37**, 414–421.
416 J. Casals-Stenzel, H.-P. Buscher and R. Schauer, *Anal. Biochem.*, 1975, **65**, 507–524.
417 J. P. Kamerling, J. F. G. Vliegenthart, C. Versluis and R. Schauer, *Carbohydr. Res.*, 1975, **41**, 7–17.
418 H. K. B. Silver, K. A. Karim, M. J. Gray and F. A. Salinas, *J. Chromatogr.*, 1981, **224**, 381–388.
419 A. K. Shukla, N. Scholz, E. H. Reimerdes and R. Schauer, *Anal. Biochem.*, 1982, **123**, 78–82.
420 A. K. Shukla and R. Schauer, *J. Chromatogr.*, 1982, **244**, 81–89.
421 N. K. Karamanos, B. Wikström, C. A. Antonopoulos and A. Hjerpe, *J. Chromatogr.*, 1990, **503**, 421–429.
422 F. Unland and J. Muthing, *Biomed. Chromatogr.*, 1992, **6**, 155–159.
423 E. L. Romero, M. F. Pardo, S. Porro and S. Alonso, *J. Biochem. Biophys. Methods*, 1997, **35**, 129–134.
424 S. M. Levonis, J. Pittet, B. C. M. Pointon and S. S. Schweiker, *J. Chromatogr., B*, 2019, **1104**, 130–133.
425 K. Kobayashi, Y. Akiyama, K. Kawaguchi, T. Shinzo and T. Imanari, *Anal. Sci.*, 1985, **1**, 81–84.
426 K. Li, *J. Chromatogr.*, 1992, **579**, 209–213.
427 S. Honda, S. Iwase, S. Suzuki and K. Kakehi, *Anal. Biochem.*, 1987, **160**, 455–461.
428 K. R. Anumula, *Anal. Biochem.*, 1995, **230**, 24–30.
429 S. Hara, M. Yamaguchi, Y. Takemori and M. Nakamljra, *J. Chromatogr.*, 1986, **377**, 111–119.
430 S. Hara, Y. Takemori, M. Yamaguchi, M. Nakamura and Y. Ohkura, *Anal. Biochem.*, 1987, **164**, 138–145.
431 S. Hara, M. Yamaguchi, Y. Takemori, K. Furuhata, H. Ogura and M. Nakamura, *Anal. Biochem.*, 1989, **179**, 162–166.
432 P. G. Stanton, Z. Shen, E. A. Kecorius, P. G. Burgon, D. M. Robertson and M. T. W. Hearn, *J. Biochem. Biophys. Methods*, 1995, **30**, 37–48.
433 M. J. Martín, E. Vázquez and R. Rueda, *Anal. Bioanal. Chem.*, 2007, **387**, 2943–2949.
434 A. Kawasaki, M. Yasuda, K.-I. Mawatari, T. Fukuuchi, N. Yamaoka, K. Kaneko, R. Iijima, S. Yui, M. Satoh and K. Nakagomi, *Anal. Sci.*, 2018, **34**, 841–844.
435 T. Ota, M. Yasuda, R. Iijima, S. Yui, T. Fukuuchi, N. Yamaoka, K. Mawatari, K. Kaneko and K. Nakagomi, *J. Chromatogr., B*, 2013, **932**, 152–157.
436 D. Li, *Food Sci. Biotechnol.*, 2012, **21**, 1317–1320.
437 L. Wang, D. Wang, X. Zhou, L. Wu and X. Sun, *RSC Adv.*, 2014, **4**, 45797–45803.
438 M. I. Orozco-Solano, F. Priego-Capote and M. D. Luque de Castro, *Anal. Chim. Acta*, 2013, **766**, 69–76.
439 F. Qu, L. Xia, C. Wu, L. Liu, G. Li and J. You, *RSC Adv.*, 2016, **6**, 64895–64901.
440 A. E. Manzi, S. Diaz and A. Varki, *Anal. Biochem.*, 1990, **188**, 20–32.
441 M. R. Hardy, *Methods Enzymol.*, 1989, **179**, 76–82.
442 J. S. Rohrer, J. Thayer, M. Weitzhandler and N. Avdalovic, *Glycobiology*, 1998, **8**, 35–43.
443 R. D. Rocklin, A. P. Clarke and M. Weitzhandler, *Anal. Chem.*, 1998, **70**, 1496–1501.
444 C. J. Shaw, H. Chao and B. Xiao, *J. Chromatogr. A*, 2001, **913**, 365–370.

445 M. van der Ham, B. H. C. M. T. Prinsen, J. G. M. Huijmans, N. G. G. M. Abeling, B. Dorland, R. Berger, T. J. de Koning and M. G. M. de Sain-van der Velden, *J. Chromatogr., B*, 2007, **848**, 251–257.
446 P. Allevi, E. A. Femia, M. L. Costa, R. Cazzola and M. Anastasia, *J. Chromatogr. A*, 2008, **1212**, 98–105.
447 L. A. Hammad, D. Z. Derryberry, Y. R. Jmeian and Y. Mechref, *Rapid Commun. Mass Spectrom.*, 2010, **24**, 1565–1574.
448 Y. Shi, X. Xu, M. Fang, M. Zhang, Y. Li, B. Gillespie, S. Yorke, N. Yang, J. C. McKew, W. A. Gahl, M. Huizing, N. Carrillo-Carrasco and A. Q. Wang, *J. Chromatogr., B*, 2015, **1000**, 105–111.
449 C. Li, L. Liu, H. Xie and N. Liu, *Int. J. Dairy Technol.*, 2015, **68**, 166–173.
450 S. F. Fernando and B. W. Woonton, *J. Food Compos. Anal.*, 2010, **23**, 359–366.
451 T. Hayama, Y. Sakaguchi, H. Yoshida, M. Itoyama, K. Todoroki, M. Yamaguchi and H. Nohta, *Rapid Commun. Mass Spectrom.*, 2010, **24**, 2868–2874.
452 A. Tebani, D. Schlemmer, A. Imbard, O. Rigal, D. Porquet and J. F. Benoist, *J. Chromatogr., B*, 2011, **879**, 3694–3699.
453 D. Wang, X. Zhou, L. Wang, S. Wang and X. L. Sun, *J. Chromatogr., B*, 2014, **944**, 75–81.
454 F. Priego-Capote, M. I. Orozco-Solano, M. Calderón-Santiago and M. D. Luque de Castro, *J. Chromatogr. A*, 2014, **1346**, 88–96.
455 B. Yesilyurt, U. Sahar and R. Deveci, *Mol. Reprod. Dev.*, 2015, **82**, 115–122.
456 F. T. A. Chen, T. S. Dobashi and R. A. Evangelista, *Glycobiology*, 1998, **8**, 1045–1052.
457 F. Y. Che, X. X. Shao, K. Y. Wang and Q. C. Xia, *Electrophoresis*, 1999, **20**, 2930–2937.
458 X. Dong, X. Xu, F. Han, X. Ping, X. Yuang and B. Lin, *Electrophoresis*, 2001, **22**, 2231–2235.
459 K. Strousopoulou, M. Militsopoulou, K. Stagiannis, F. N. Lamari and N. K. Karamanos, *Biomed. Chromatogr.*, 2002, **16**, 146–150.
460 A. Taga, M. Sugimura, S. Suzuki and S. Honda, *J. Chromatogr. A*, 2002, **954**, 259–266.
461 K. Ortner and W. Buchberger, *Electrophoresis*, 2008, **29**, 2233–2237.
462 Y. Zheng, T. Wang, J. Kong, Y. Ma, Y. Heng, Y. Ren, J. Ye and Q. Chu, *Chin. J. Chem.*, 2016, **34**, 925–930.
463 Y. Wang, J. Kong, Z. Chen, D. Luo, J. Ye and Q. Chu, *Food Anal. Methods*, 2018, **11**, 1105–1112.
464 S. A. M. Marzouk, S. S. Ashraf and K. A. Al Tayyari, *Anal. Chem.*, 2007, **79**, 1668–1674.
465 S. A. M. Marzouk, J. D. Haddow and A. Amin, *Sens. Actuators, B*, 2011, **157**, 647–653.
466 A. Fatoni, A. Numnuam, P. Kanatharana, W. Limbut and P. Thavarungkul, *Electrochim. Acta*, 2014, **130**, 296–304.
467 Y. Zhou, H. Dong, L. Liu, J. Liu and M. Xu, *Biosens. Bioelectron.*, 2014, **60**, 231–236.
468 Y. Zhou, H. Huangfu, J. Yang, H. Dong, L. Liu and M. Xu, *Analyst*, 2019, **144**, 6432–6437.
469 F. Huang, B. Zhu, H. Zhang, Y. Gao, C. Ding, H. Tan and J. Li, *Microchim. Acta*, 2019, **186**, 1–11.
470 T. V. Shishkanova, G. Broncová, Z. Němečková, V. Vrkoslav, V. Král and P. Matějka, *J. Electroanal. Chem.*, 2019, **832**, 321–328.
471 T. Liu, B. Fu, J. Chen, Z. Yan and K. Li, *Electrochim. Acta*, 2018, **269**, 136–143.
472 Y. Lv, Y. Zhou, H. Dong, L. Liu, G. Mao, Y. Zhang and M. Xu, *ChemElectroChem*, 2020, **7**, 922–927.
473 W. Hai, S. Pu, X. Wang, L. Bao, N. Han, L. Duan, J. Liu, T. Goda and W. Wu, *Langmuir*, 2020, **36**, 546–553.
474 S. Ding, S. Cao, Y. Liu, Y. Lian, A. Zhu and G. Shi, *ACS Sens.*, 2017, **2**, 394–400.
475 G. Broncová, P. Matějka, Z. Němečková, V. Vrkoslav and T. V. Shishkanova, *Electroanalysis*, 2018, **30**, 672–680.
476 L. Chen, N. Wang, J. Wu, F. Yan and H. Ju, *Anal. Chim. Acta*, 2020, **1128**, 231–237.
477 J. Wang, S. Zhang, H. Dai, H. Zheng, Z. Hong and Y. Lin, *Biosens. Bioelectron.*, 2019, **142**, 111567.
478 D. Fang, S. Zhang, H. Dai, Z. Hong and Y. Lin, *Electrochim. Acta*, 2019, **326**, 134956.
479 N. Cao, F. Zhao and B. Zeng, *Sens. Actuators, B*, 2020, **313**, 128042.
480 A. Kugimiya, H. Yoneyama and T. Takeuchi, *Electroanalysis*, 2000, **12**, 1322–1326.
481 S.-J. Duan, X.-W. He, L.-X. Chen and Y.-K. Zhang, *Gaodeng Xuexiao Huaxue Xuebao*, 2012, **33**, 464–469.
482 X. Qiu, X. Y. Xu, X. Chen, Y. Wu and H. Guo, *Anal. Bioanal. Chem.*, 2018, **410**, 4387–4395.
483 A. Kugimiya and T. Takeuchi, *Biosens. Bioelectron.*, 2001, **16**, 1059–1062.
484 S. Li, J. Liu, Y. Lu, L. Zhu, C. Li, L. Hu, J. Li, J. Jiang, S. Low and Q. Liu, *Biosens. Bioelectron.*, 2018, **117**, 32–39.
485 E. Vinogradova, A. Tlahuice-Flores, J. J. Velazquez-Salazar, E. Larios-Rodriguez and M. Jose-Yacaman, *J. Raman Spectrosc.*, 2014, **45**, 730–735.
486 A. C. Hernández-Arteaga, F. C. Delgado-Nieblas, H. J. Ojeda-Galván, J. J. Velázquez-Salazar, E. Vinogradova, M. José-Yacamán, R. A. Guirado-López and H. R. Navarro-Contreras, *J. Phys. Chem. C*, 2017, **121**, 21045–21056.
487 A. Hernández-Arteaga, J. de Jesús Zermeño Nava, E. S. Kolosovas-Machuca, J. J. Velázquez-Salazar, E. Vinogradova, M. José-Yacamán and H. R. Navarro-Contreras, *Nano Res.*, 2017, **10**, 3662–3670.
488 X. Teng, F. Chen, Y. Gao, R. Meng, Y. Wu, F. Wang, Y. Ying, X. Liu, X. Guo, Y. Sun, P. Lin, Y. Wen and H. Yang, *Anal. Chem.*, 2020, **92**, 3332–3339.
489 https://www.elabscience.com/p-sialic_acid_sa_colorimetric_assay_kit-40365.html (Accessed November 2021).
490 https://www.mybiosource.com/assay-kits/sialic-acid/2540448 (Accessed November 2021).
491 https://www.mybiosource.com/general-assay-kits/sialic-acid-sa/2563693 (Accessed November 2021).
492 https://www.biovision.com/sialic-acid-nana-colorimetric-fluorometric-assay-kit.html (Accessed November 2021).
493 https://www.bioassaysys.com/Sialic-acid-Assay-Kit-(ESLA-100).html (Accessed November 2021).

494 https://www.lsbio.com/assaykits/sialic-acid-assay-kit-colorimetric-fluorometric-ls-k187/187 (Accessed November 2021).
495 https://www.promocell.com/product/sialic-acid-nana-assay-kit/ (Accessed November 2021).
496 https://www.abcam.com/sialic-acid-nana-assay-kit-ab83375.html (Accessed November 2021).
497 https://www.antibodies-online.com/kit/411705/Sialic+Acid+NANA+Colorimetric/Fluorometric+Assay+Kit/ (Accessed November 2021).
498 http://www.cohesionbio.com/goods.php?id=127272 (Accessed November 2021).
499 https://www.mybiosource.com/general-assay-kits/sialic-acid/8309610 (Accessed November 2021).
500 https://www.mybiosource.com/assay-kits/sialic-acid-nana/841610 (Accessed November 2021).
501 https://www.usbio.net/kits/S1013-31Q/sialic-acid-assay-kit-bioassaytrade-colorimetricfluorometric-high-sensitivity (Accessed November 2021).
502 https://www.usbio.net/kits/A0535-01A/n-acetylneuraminic-acid-nana-sialic-acid-bioassaytrade-kit (Accessed November 2021).
503 https://www.creativebiomart.net/sialic-acid-nana-colorimetricfluorometric-assay-kit-463657.htm (Accessed November 2021).
504 https://www.creativebiomart.net/sialic-acid-assay-kit-502969.htm (Accessed November 2021).
505 http://www.abnova.com/products/products_detail.asp?catalog_id=KA1655 (Accessed November 2021).
506 https://www.bioassaysys.com/Sialic-acid-Assay-Kit-(DSLA-100).html (Accessed November 2021).
507 https://www.usbio.net/kits/S1013-31P/sialic-acid-assay-kit-bioassaytrade-colorimetricfluorometric (Accessed November 2021).
508 https://www.sigmaaldrich.com/IE/en/product/sigma/mak314?context=product (Accessed November 2021).
509 https://www.creativebiomart.net/sialic-acid-assay-kit-463740.htm (Accessed November 2021).
510 https://www.assaygenie.com/sialic-acid-assay-kit-colorimetric-or-fluorometric-ba0058/ (Accessed November 2021).
511 https://www.sigmaaldrich.com/IE/en/product/sigma/sialicq?context=product (Accessed November 2021).
512 https://www.takarabio.com/products/protein-research/glycobiology/sialic-acid-kit?catalog=4400 (Accessed November 2021).
513 https://www.agilent.com/store/productDetail.jsp?catalogId=GKK-407 (Accessed November 2021).
514 https://www.ludger.com/dmb-sialic-acid-analysis/index.php (Accessed November 2021).
515 https://www.agilent.com/store/productDetail.jsp?catalogId=GS24-SAP (Accessed November 2021).
516 W. Song, L. Ding, Y. Chen and H. Ju, *Chem. Commun.*, 2016, **52**, 10640–10643.
517 T. Gong, Y. Cui, D. Goh, K. K. Voon, P. P. Shum, G. Humbert, J. L. Auguste, X. Q. Dinh, K. T. Yong and M. Olivo, *Biosens. Bioelectron.*, 2015, **64**, 227–233.
518 X. N. He, Y. N. Wang, Y. Wang and Z. R. Xu, *Talanta*, 2020, **209**, 120579.
519 L. Liang, Y. Shen, J. Zhang, S. Xu, W. Xu, C. Liang and B. Han, *Anal. Chim. Acta*, 2018, **1033**, 148–155.
520 S. Shinde, Z. El-Schich, A. Malakpour, W. Wan, N. Dizeyi, R. Mohammadi, K. Rurack, A. Gjörloff Wingren and B. Sellergren, *J. Am. Chem. Soc.*, 2015, **137**, 13908–13912.
521 N. Peng, R. Xu, M. Si, A. Victorious, E. Ha, C. Y. Chang and X. D. Xu, *RSC Adv.*, 2017, **7**, 11282–11285.
522 Y. Geng, L. Cong, Y. Tian, Z. Huo, Y. Wang, L. Xing, S. Xu, C. Liang and W. Xu, *Sens. Actuators, B*, 2019, **301**, 127074.
523 V. Almeida-Marrero, M. Mascaraque, M. Jesús Vicente-Arana, Á. Juarranz, T. Torres and A. de la Escosura, *Chem. – Eur. J.*, 2021, **27**, 9634–9642.
524 X. Yang, L. Zhou, Y. Hao, B. Zhou and P. Yang, *Analyst*, 2017, **142**, 2169–2176.
525 D. Qian, F. Han, W. Li, N. Bao, C. Yu and H. Gu, *Microchim. Acta*, 2017, **184**, 3841–3850.
526 K. Liu, Q. Sun, L. Zhu, C. Feng, J. Zhang, Y. Wang, F. Zhang, Z. Xu and W. Zhang, *Anal. Methods*, 2015, **7**, 3819–3826.
527 L. Zhang, C. Yu, R. Gao, Y. Niu, Y. Li, J. Chen and J. He, *Biosens. Bioelectron.*, 2017, **92**, 434–441.
528 A. Matsumoto, S. Osawa, T. Arai, Y. Maejima, H. Otsuka and Y. Miyahara, *Bioconjugate Chem.*, 2021, **32**, 239–244.
529 G. Landa, L. G. Miranda-Calderón, V. Sebastian, S. Irusta, G. Mendoza and M. Arruebo, *Talanta*, 2021, **234**, 122644.
530 S. Osawa, A. Matsumoto, Y. Maejima, T. Suzuki, Y. Miyahara and H. Otsuka, *Anal. Chem.*, 2020, **92**, 11714–11720.
531 D. Sui, X. Tang, J. Ding, Y. Wang, Y. Qin, N. Zhang, X. Liu, Y. Deng and Y. Song, *Int. J. Pharm.*, 2021, **602**, 120552.
532 https://www.biovision.com/ezclicktm-sialic-acid-manaz-modified-glycoprotein-assay-kit-facs-microscopy-green-fluorescence.html (Accessed November 2021).
533 https://www.sartorius.com/en/products/protein-analysis/biosensors-chips-kits/sialic-acid-glys-kit (Accessed November 2021).